

PETROCHEMISTRY AND METAMORPHISM OF THE
TALLAN LAKE SILL, BANCROFT AREA, ONTARIO

PETROCHEMISTRY AND METAMORPHISM OF THE
TALLAN LAKE SILL, BANCROFT AREA, ONTARIO

By

JACOBUS L. GRIEP, B.Sc.

A Thesis

Submitted to the School of Graduate Studies

in Partial Fulfilment of the Requirements

for the Degree

Master of Science

McMaster University

April 1975

MASTER OF SCIENCE (1975)
(Geology)

McMASTER UNIVERSITY
Hamilton, Ontario

TITLE: Petrochemistry and Metamorphism of the
Tallan Lake Sill, Bancroft Area, Ontario

AUTHOR: Jacobus L. Griep, B.Sc. (University of
Amsterdam)

SUPERVISOR: Professor Denis M. Shaw

NUMBER OF PAGES: i-xii; 1-166

SCOPE AND CONTENTS:

A geochemical and petrological study of the Precambrian Tallan Lake Sill and surrounding rocks is presented.

Evidence in favour of an inverted, differentiated sequence of gabbros and syenites is discussed.

Chemical and mineralogical modification of the igneous assemblage during diagenesis and high-grade Grenvillian metamorphism is dealt with and placed in a regional context.

ABSTRACT

The Precambrian Tallan Lake Sill is an elongate, stratiform amphibolite body, belonging to a group of differentiated gabbros emplaced around 1250 ± 25 m.y. ago in the Bancroft area of Ontario.

Although metamorphism has obliterated all but a few primary igneous textures, it is clear from major element chemistry that the sill is a differentiated ferrogabbro of tholeiitic affinity. Some critical field observations combined with model calculations make it highly probable that the syenite underlying the metagabbros is a differentiate of the latter, indicating that the stratigraphic succession in this part of the Grenville Group is overturned.

Alkali values can not be relied upon in these model calculations, and it is shown that the chemistry of many rocks in the Bancroft area shows the effects of spilitisation and other chemical alteration, presumably due to an early episode of burial metamorphism. Metamorphism in the area is of the low-pressure intermediate type and is reflected in the coexistence of garnet, cummingtonite and hornblende in many Tallan Lake samples.

A qualitative petrogenetic grid based on the rules

of Schreinemakers' has been derived for the hornblende-cumingtonite-garnet paragenesis and the importance of the coexistence of cumingtonite and garnet as a possible geobarometer is pointed out.

Assemblages in marbles surrounding the Tallan Lake Sill point to a metamorphic maximum P and T of around 4.0-6.5 kb and 625-650°C, respectively, but retrograde reactions and extensive exsolution of coexisting amphiboles suggest a gradual decline in temperature, possibly reflecting the slow cooling and unroofing of neighbouring mantled gneiss domes.

The differentiation mechanism envisaged for the Tallan Lake Sill, involving mechanical separation of a residual, interstitial syenite liquid may have wider application, and it is suggested that the chemical discontinuity known as the Daly Gap might be so explained.

ACKNOWLEDGEMENTS

I am greatly indebted to Dr. D.M. Shaw, who initiated and supervised this work, for his guidance and endless patience, without which this work might never have been completed. Conversations and critical discussions with Drs. B.J. Burley, H.D. Grundy and R.H. McNutt and many fellow students over the past six years are gratefully acknowledged, and I wish to thank Frank Hawthorne in particular for introducing me to the secrets of crystallography and for many pointed discussions.

Conversations under varying conditions of $\text{C}_2\text{H}_5\text{OH}$ with Messrs. Fred Breaks, Bob Dalrymple, Ian Davies, Jarda Dostal, Walter Gibbins, Jan Helsen, Dick Hyde, Michael Marchand, Colin Turner and many others helped to preserve the presumed sanity of the author and will always be fondly remembered.

Mr. J.R. Muysson, who provided the chemical analyses and Mr. J. Whorwood who reproduced the illustrations are thanked for their assistance, and special thanks are extended to Helen Elliott who decoded and typed the script.

The financial assistance through grants from the

National Research Council of Canada and the Department of
Geology, McMaster University, and the recreational facilities
provided by various soccer teams kept me alive and kicking,
respectively, and are therefore thanked as well.

TABLE OF CONTENTS

	Page	
CHAPTER 1	INTRODUCTION	1
	1.1 Statement of Problem	1
	1.2 Previous Work	3
CHAPTER 2	FIELD RELATIONS AND GEOLOGY OF THE TALLAN LAKE SILL	5
	2.1 Lithology	8
	2.2 Structural Geology	14
CHAPTER 3	PETROCHEMISTRY OF THE TALLAN LAKE SUITE	19
	3.1 General Considerations	19
	3.2 Differentiation	27
	3.2.1 Mineralogical and chemical effects of differentiation	27
	3.2.2 Model calculations	36
	3.3 Chemical Alteration During Diagenesis and Low Grade Metamorphism	51
	3.4 Summary	56
CHAPTER 4	PETROGRAPHY	59
	4.1 Relict Igneous Mineralogy	59
	4.2 Metamorphic Assemblages	65
	4.2.1 Primitive metamorphic assemblage	65
	4.2.2 Main metamorphic assemblage	66
	4.2.3 Very late retrograde textures	83
	4.2.4 Other assemblages, country rocks	85
	4.3 Metamorphic Reactions	93
	4.3.1 Assemblages	93
	4.3.2 Reaction relations between cummingtonite and hornblende	96
	4.3.3 Reactions in other assemblages	108
	4.4 Si	116

	Page
CHAPTER 5 REGIONAL ASPECTS, SUMMARY AND CONCLUSIONS	121
REFERENCES	131
APPENDIX 1 CHEMICAL COMPARISON OF TALLAN LAKE ROCKS WITH OTHER SERIES	141
APPENDIX 2 ALTERATION OF IGNEOUS ROCKS, COMPARED WITH THE CHEMISTRY OF ROCKS FROM THE BANCROFT AREA	148
APPENDIX 3 PLAGIOCLASE COMPOSITIONS	152
APPENDIX 4 THERMODYNAMIC DATA FOR UNIVARIANT REACTIONS INVOLVING THE PHASES HORNBLÉNDE-CUMMINGTONITE-HEDENBERGITE-ALMANDINE-ANORTHITE-QUARTZ-CALCITE-WATER+CARBON DIOXIDE AT AN ASSUMED PRESSURE AND TEMPERATURE OF 5 kb AND 627°C	157
APPENDIX 5 CRYSTALLOGRAPHY OF SOME AMPHIBOLES AND ONE CLINOPYROXENE	161
APPENDIX 6 SAMPLE PREPARATION AND CHEMICAL ANALYTICAL PROCEDURE	163

LIST OF TABLES

		Page
Table 3A	Chemical analyses of Tallan Lake suite	20
Table 3B	Chemical analyses of Tallan Lake suite (Shaw and Kudo, 1965)	22
Table 3C	Chemistry of sediments that might be mixed in order to obtain analyses similar to Tallan Lake amphibolite	23
Table 3D	Mineral analyses used in model calculations	44
Table 3E	Least-squares estimate of parent liquid composition (420) by combining presumed differentiates with mineral analyses of Table 3D	46
Table 3F	Proportions of liquid and mineral- residue required to obtain parent liquid composition (420) and the composition of that mineral residue	49
Table 3G	Least-squares estimate of 420, by combining U.S.G.S. standards with mineral analyses of Table 3D	52
Table 4A	Modal analyses	70
Table 4B	Some parageneses in the system K-Na-Ca-Fe-Mg-Al-Ti-Si-O-H-C	95
Table 4C	Summary of symbols and minerals used in mineral reactions	97
Table 4D	Chemistry of amphiboles and whole rock containing 3-amphibole assemblage	114

LIST OF FIGURES

		Page
Figure 1.1	Location of study area	2
Figure 1.2	Geology of the Tallan Lake sill	in pocket
Figure 1.3	Distribution of gabbroic rocks in the Bancroft area	in pocket
Figure 2.1	Tectonic framework of the Grenvillian orogenic belt in Canada	6
Figure 2.2	Structural framework of the Tallan Lake sill and surrounding area	in pocket
Figure 3.1	(a) MgO vs. FeO _{tot} for some differentiated volcanic suites	25
	(b) MgO vs. FeO _{tot} for Tallan Lake rocks, compared with Skaergaard liquids	26
Figure 3.2	AFM plot for Tallan Lake analyses, compared with other differentiated suites	32
Figure 3.3	Relations between fo-content and an-content of coexisting olivines and plagioclases in two differentiated suites	38
Figure 3.4	(a) Flowchart of the operation of computer program LSPX	41
	(b) Typical output of LSPX	42
Figure 4.1	Stratigraphy (lithological, mineralogical, chemical) of the Tallan Lake sill	68
Figure 4.2	Petrogenetic grid involving the phases (ferrotremolite-ferrotschermakite)-cummingtonite-hedenbergite-almandine-anorthite-quartz-water	98
Figure 4.3	Suggested disposition of invariant points involving magnesium-free and iron-free compositions in the petrogenetic grid of Figure 4.2	102

	Page
Figure 4.4	Net involving invariant points (cpx, hb ₂ , hb ₃) and cc, CO ₂ , hb ₂ , hb ₃) of Appendix 4. 106
Figure 4.5	Isobars for the reaction 5 phlogopite + 6 calcite + 24 quartz \rightleftharpoons 3 tremolite + 5 orthoclase + 2H ₂ O + 6CO ₂ 109
Figure 4.6	Isobars for the reactions (1) 2 zoisite + CO ₂ \rightleftharpoons 3 anorthite + calcite + H ₂ O 111 (2) K-feldspar + anorthite + H ₂ O + CO ₂ \rightleftharpoons muscovite + calcite + 2 quartz (3) 2 zoisite + 3 K-feldspar + 4CO ₂ + 2H ₂ O \rightleftharpoons 3 muscovite + 4 calcite
Figure 4.7	Summary of reactions relevant to Tallan Lake assemblages 118
Figure 5.1	FeO _{tot} vs. MgO for Tudor metavolcanics 122

LIST OF PLATES

		Page
Plate I	Possible ilmenite-sphene pseudomorph after ulvöspinel	74
Plate II	New growth of hornblende in large grain belonging to primitive assemblage	74
Plate III	Textures suggestive of the reaction $hb + qz \rightleftharpoons cm + plag$	74
Plate IV	Discontinuous zoning in plagioclase	80
Plate V	Euhedral atoll garnet, with quartz and calcite	80
Plate VI	Peristerite exsolution in plagioclase	80
Plate VII	Muscovite-calcite intergrowth, suggestive of the reaction $An + kfsp + CO_2 \rightleftharpoons Ms + cc + qz$	84
Plate VIII	Micro-mylonite zone with sheared biotite	84
Plate IX	Epidote coexisting with calcite, albite and tremolite	84
Plate X	Relict forsterite in grossular skarn	89
Plate XI	Homoaxial intergrowth of gedrite, cunningtonite and hornblende in single amphibole grain	89
Plate XII	Gedrite, cunningtonite, hornblende, crossed nicols	89
Plate XIII	Poikiloblastic diopside embedded in scapolite	92
Plate XIV	Poikiloblastic cunningtonite, calcite with hornblende	92
Plate XV	Biotite-quartz-calcite symplectites formed from hornblende	92

CHAPTER 1

INTRODUCTION

1.1 Statement of Problem

In the course of fieldwork, carried out for the Ontario Department of Mines, an extensive stratiform body of amphibolite, apparently of igneous derivation, was mapped in Chandos Township, Peterborough County by Shaw (1962). This body, named the Tallan Lake Sill by Shaw is underlain by syenite gneiss, with apparent continuous gradation into the overlying amphibolite.

The occurrence of this syenite below the amphibolite was puzzling, because, although it was tempting to interpret the syenite mass as the product of differentiation of a gabbroic sill, no evidence was available to indicate the tectonic inversion of strata as seemed required by such a hypothesis.

The present work has been undertaken to examine the differentiation hypothesis on its merits and to provide a general description of the rocks comprising the Tallan Lake Sill and underlying syenites.

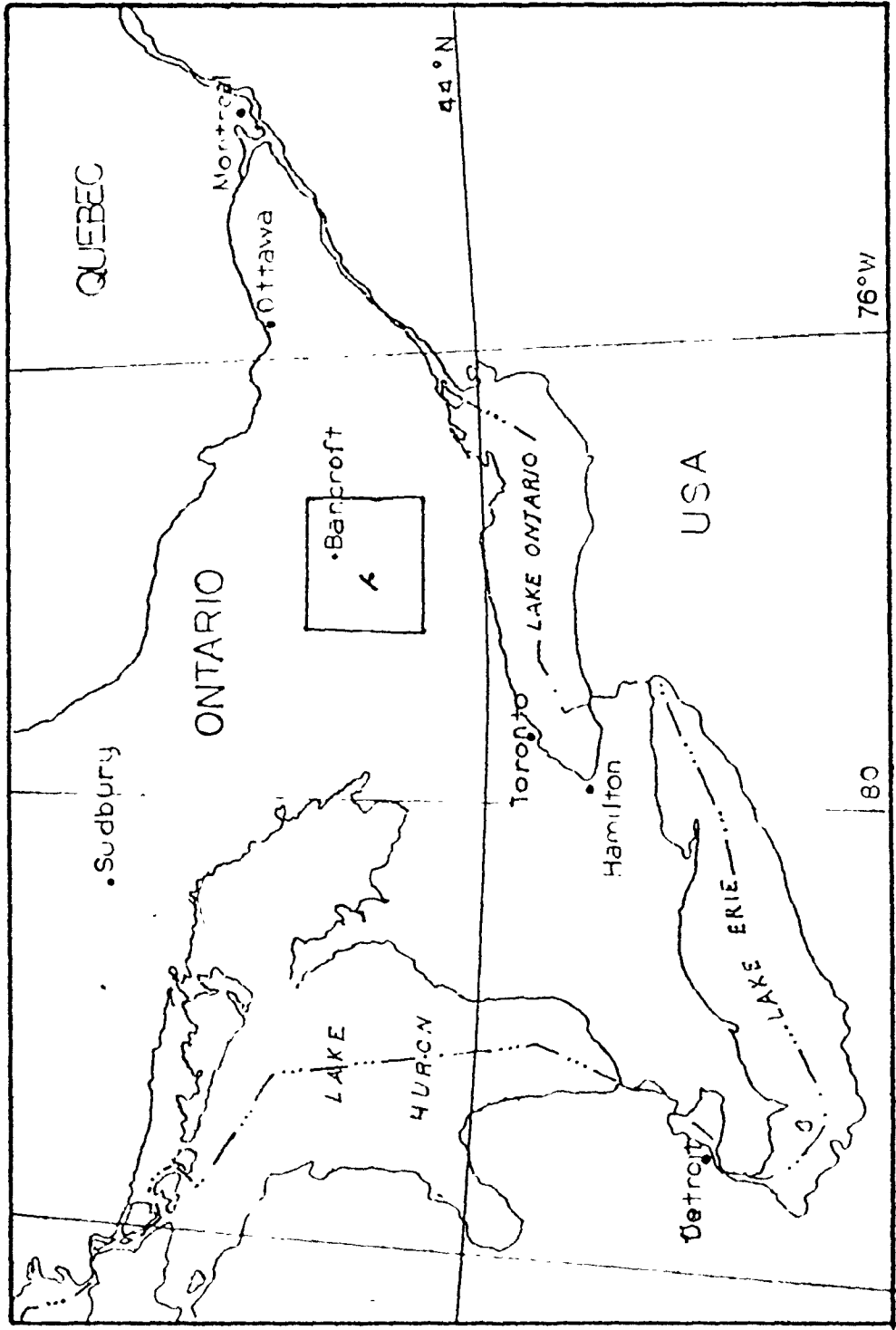


Figure 1.1 Location of study area. The area of Figure 1.3 is outlined

1.2 Previous Work

Probably the first reference to the occurrence of amphibolites, representing the metamorphosed product of igneous rocks, in Chandos Township, has been made in the classic work by Adams and Barlow (1910) dealing with the geology of the Haliburton and Bancroft areas. These authors further noted the presence of amphibolite in a quaquaversally dipping dome around Duck Lake (since renamed Clydesdale Lake), which they thought to be due to the intrusion of an (invisible) underlying granite batholith. The similarity of this Duck Lake Sill to the Tallan Lake Sill has since been noted by Shaw (1962) and particularly impressive is the fact that the former is underlain by a syenite gneiss similar to the one in the vicinity of Tallan Lake.

Shaw pointed to the fact that the Duck Lake Sill formed the logical extension of the Tallan Lake Sill on an anticlinal crest (the Rose Island Dome), southeast of the Chandos Syncline of which the Tallan Lake Sill forms the northwest limb (Figure 1.2).

○ The chemistry of some Tallan Lake amphibolites formed part of a study by Shaw and Kudo (1965), designed to discriminate between amphibolites of igneous derivation and para-amphibolites in the region. It was concluded there that the Tallan Lake rocks had by far the most igneous

chemistry of all samples investigated.

Jennings (1969) mapped the southwest termination of the Tallan Lake Sill in Anstruther Township and also outlined the existence of several lenticular gabbro bodies northeast of Tallan Lake, in Cardiff and Faraday Townships, which form the logical extension of the Tallan Lake Sill to the northeast (Figure 1.3). The bodies have not been subjected to the complete recrystallization of their original igneous mineralogy as is the case in the Tallan Lake Sill, but have in common with the latter the occurrence of a syenite or granophyre at the structural base of the bodies. No evidence in favour of a tectonic inversion of the succession was uncovered by Jennings.

CHAPTER 2

FIELD RELATIONS AND GEOLOGY OF THE TALLAN LAKE SILL

The Tallan Lake Sill is situated on the northwestern edge of what has been termed the Grenville Group Terrain of the Grenville Province by Wynne-Edwards (1972) (Figure 2.1). As indicated in the Introduction the sill is exposed in two separate outcrop areas. The Tallan Lake Sill proper is exposed as a narrow elongate band, approximately 300 to 350 meters wide, which can be followed uninterruptedly for more than 12 km (8 miles). Where foliation is well developed, it can be seen to dip uniformly to the southeast, a common dip being 60 to 70 degrees. The sill thus conforms to the northwest limb of a northeast-trending syncline, named the Chandos Syncline by Shaw (1962). Along its entire length the Tallan Lake Sill straddles a major fault in the area, the Pratt's Creek Fault. As indicated by the absence of the lower part of the section of the sill, and the occurrence of a tectonic breccia composed of blocks of marble and amphibolite in a marble matrix, this fault intersects the sill in a roadcut along Highway 28 in Anstruther Township. Southwest of its intersection with Highway 28 the sill can be followed

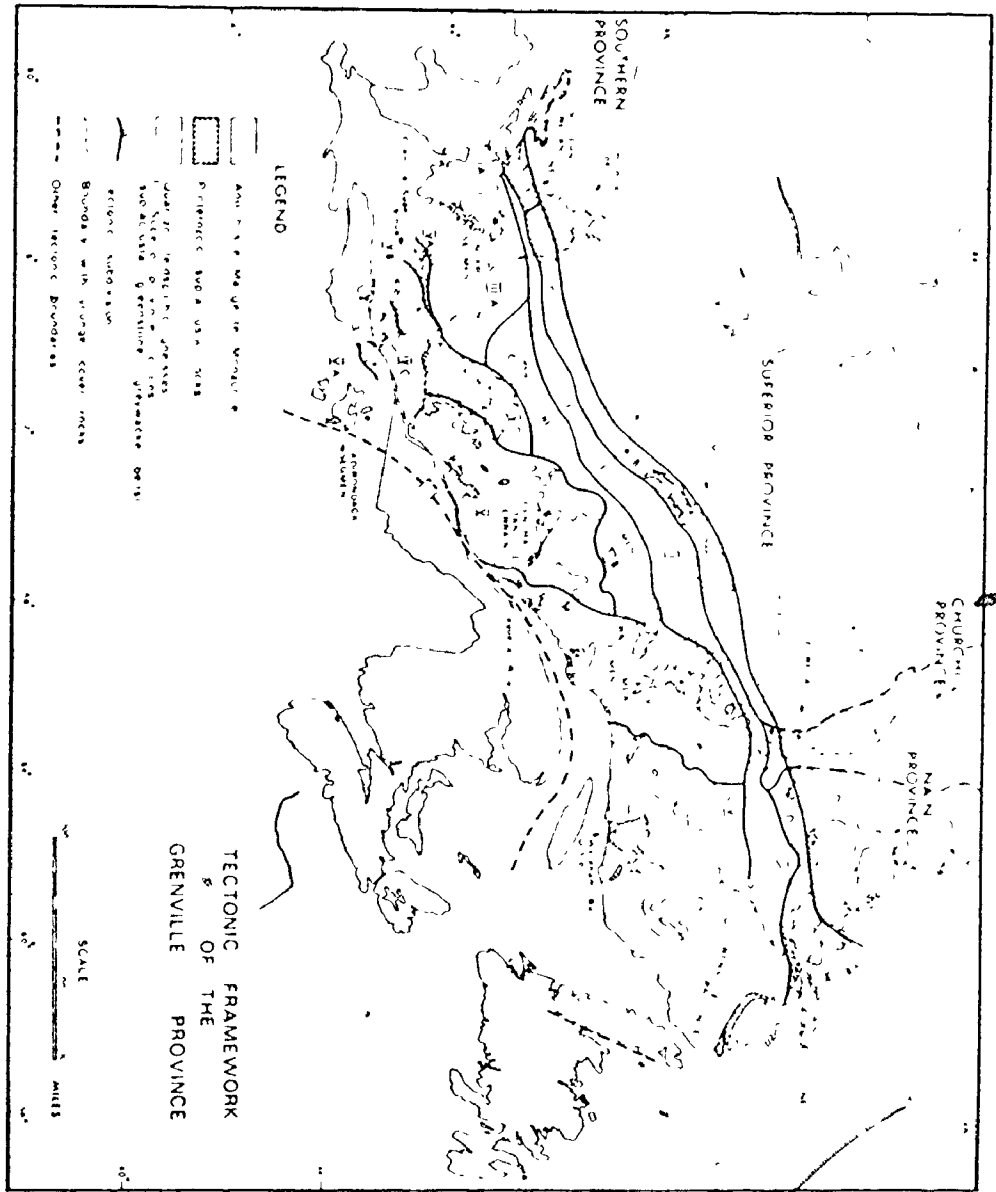


Figure 2.1 Tectonic Framework of the Grenvillian Orogenic Belt in Canada (Wynne-Edwards, 1972)

for another 2 km, but outcrop in this area is very poor and it is not known whether the sill extends much further beyond this, into the granite gneiss body of the Anstruther Dome for example, or if it terminates before reaching this body.

The second outcrop area of the sill is found around Clydesdale Lake, Chandos Township, and was named the Duck Lake Sill (Shaw, 1962), because its relationship with the Tallan Lake Sill was not definitively established. The Duck Lake Sill is exposed as a quaquaversally outward-dipping dome, the origin of which has been the subject of discussion. As mentioned previously, Adams and Barlow (1910) suggested that a batholith underneath the sill might account for the dome structure. Although this suggestion may have some merit, it is contended here that the structure is primarily due to a complex pattern of interfering folds, as will be shown in the section on Structural Geology.

Although not included in this study, it should be mentioned that a number of lenticular bodies in northeastern Chandos Township and adjacent parts of Cardiff and Faraday Townships form the logical extension of the Tallan Lake Sill to the northeast (Figure 1.3), and it is speculated here that the sill could possibly be linked with the Faraday and Mallard Lake gabbro bodies.

2.1 Lithology

The lithology of the sill can best be described as consisting of three separable units. The upper 80 or 90 meters consist of a massive greenish-black amphibole-plagioclase gneiss. Foliation is usually poorly developed and not easily distinguished in hand specimens, except for those cases in which plagioclase is a major constituent. The rocks within 1 meter of the contact are extremely fine-grained (grain size less than 0.5 mm) and display no foliation whatsoever. The fining in grain size toward the contact is conspicuous, and it is probable that it represents the originally chilled margin of the sill.

The next 100 meters lower down in the sequence is characterised by a gradual increase in feldspathic pods and laminae in the rocks, combined with the appearance of small (usually not more than 1 mm across) dark red grains of garnet. In thin section these rocks are seen to contain cummingtonite as well, but this mineral is not easily recognised in hand specimen. Mafic stringers, often very contorted, are found interspersed with the feldspathic lenses, and on the whole the rocks retain a mafic character. An interesting feature of these mafic bands is the concentration of fairly large, up to 1 cm in length, apatite needles within them.

These upper 180 meters of amphibolites, which can

best be described as hornblende-plagioclase gneisses, are to be found in all relatively well-exposed traverses made across the sill and the different units are of uniform thickness. This is in contrast to the syenite gneiss which usually is found to underlie these units and which ranges in thickness from 0 to 80 meters. The syenite gneiss is distinguished from the overlying rocks by its abundance of plagioclase feldspar. The texture of interlocking hornblende grains, characteristic for the amphibole gneisses, is replaced by one wherein poikiloblasts of amphibole are suspended in a feldspar matrix. The transition from amphibole gneiss into syenite gneiss, where exposed, is always seen to be smooth and gradational so that a boundary cannot be easily drawn. Characteristic, though not always present, for the syenite is the blue iridescence of its plagioclases, which is ascribed to peristerite exsolution in the feldspars. Mention should be made of the fact that the transition from hornblende gneiss to syenite gneiss in the Clydesdale Lake area is often marked by an abundance of marble and country rock amphibolite screens. These screens are particularly well developed in a newly (1971) blasted roadcut along Highway 620, south of Clydesdale Lake, but are also found elsewhere. The marble has in part reacted with the basic magma, as witnessed by the development of coarse-grained andradite-diopside skarn selvages surrounding the lumps of marble. Although these

marble screens play a key role in the petrogenetic model to be developed, it will suffice here to say that they occur only at this particular stratigraphic level, are up to 10 meters thick and have obviously undergone the effects of contact metamorphism by the sill.

Garnet persists in the upper 40 meters of syenite gneiss and the syenite is best described as a mafic syenite here, but lower down in the sequence gradually a more leucocratic syenite gneiss appears with amphibole and biotite as principal mafic constituents. The most leucocratic syenites are found where the syenites are thickest, i.e. along a line running west of Clydesdale Lake through Tallan Lake, and here quartz-syenites form the lowest member of the syenite unit.

Going from west to east in the Tallan Lake Sill the following situation is encountered with respect to the syenites: At the intersection with Highway 28 (Anstruther Township) no syenite is present, but some may have been cut off by the Pratt's Creek Fault. The lowest member of the sequence at Jeff Road (Anstruther Township) is a mafic, garnet-bearing syenite. Where the sill enters Chandos Township a leucosyenite is observed at the bottom of the succession, and north of Tallan Lake quartz-syenite is the lowest member. Total thickness of the syenite unit increases from 0 through 30 and 40 to 80 meters, respectively, at the

different sites (Figure 4.1). Thickness decreases toward the east of Tallan Lake and no syenite was observed at the eastern termination of the sill. Similar syenites have been found in the lenticular bodies to the northeast, also at the presumed bottom of the sequence, by Jennings (1969) and attention must be drawn to the association of sodic syenite and granite with the Faraday and Mallard Lake metaqabbro bodies (e.g. Hewitt and James, 1956). It is thus apparent that a certain channelling of the late differentiates has taken place, provided of course that the hypothesis of an inverted sequence is correct.

The country rock in which the sill is injected is in the main a quartzose, impure marble belonging to the Dungannon Formation (Shaw, 1962). Foliation in the marble is stratiform, as witnessed by its parallelism with intercalations of amphibolite in the sedimentary sequence. The marble consists mainly of calcite and diopside with minor amounts of quartz, feldspar and scapolite in places, although bands of pure calcite marble are frequently found. Intercalated with this calc-silicate sequence are bands of feather amphibolite of variable thickness, characterised by the occurrence of large amphibole aggregates with a typical feather shaped outline, lying in the plane of foliation. Such a unit of feather amphibolite, approximately 20 meters thick, is found adjacent to the sill at Highway 28, and a

similar unit is exposed near the upper contact west of Clydesdale Lake. It is possible that these two exposures are part of the same stratigraphic unit, since the sill is largely stratiform, as seen from the parallelism of the contact with the stratiform foliation. Local contact metamorphic effects on the country rock attendant upon intrusion of the sill were sought for, as they form the only means of establishing the true intrusive nature of the sill. It appears that regional metamorphic events have erased much of the original contact effects and a further complication is introduced by the uncertainty inherent in recognition of such a metamorphism. Andradite-diopside skarns are taken to be representative of such a contact metamorphism, since they were never observed outside contact areas. Such skarns are typically found in contact with the sill in the marble screens previously discussed, and one such skarn was also encountered at the lower contact of the sill, adjacent to leucosyenite, south of Clydesdale Lake. This skarn (sample 69-29-2) contains relicts of forsterite, and fresh axinite, besides diopside and andradite, a mineral paragenesis generally acknowledged distinctive as a contact assemblage. The lack of localities where the actual contact is exposed, undoubtedly related to the great weathering contrast of the basic rocks and the marble, is a major impediment to ascertaining the contact relations, however. The only place where the

upper contact is sufficiently exposed is found in the roadcut at Highway 28, where the possible existence of a chilled margin has already been mentioned. An extreme fining in the grain size of the country rock feather amphibolites toward the contact was also observed here. Within a distance of 5 meters the grain size of the rocks decreases from 2.5 mm to 0.25 mm, coupled with a significant change in the mineralogy of the rocks. A detailed account of the petrographic significance of these changes is given in the section on Petrography, where a further description of the skarn assemblage is to be found as well. Although the evidence for the intrusive nature is inadequately established, the contrast with rocks of known or supposed extrusive nature is more conclusive. The latter are always very schistose and markedly greenish in colour and never attain the same uninterrupted thickness found for the Tallan Lake rocks. Moreover, where extrusive rocks are associated with intrusive rocks, the latter are very similar to the rocks under discussion here, without distinct foliation, black in colour. We can thus be reasonably assured that the gabbroic rocks are intrusive, an assumption upon which the whole discussion to be presented hinges.

2.2 Structural Geology

The structural pattern as depicted in Figure 2.2 is relatively simple. The gross structure can be represented as a series of interfering crossfolds, one set trending northwest and another northeast. The set of folds trending N20E is represented by the Chandos syncline, the northwest limb of which is formed by the outcrop area of the Tallan Lake Sill, and the Rose Island Dome, the crest of which is occupied by the Duck Lake Sill. Further to the southeast, the northeast trending folds are obscured by the intrusion of the Loon Lake Pluton, which must have been emplaced after the major episode of folding. Southeast of the Loon Lake Pluton, the northeasterly trend of folding is found in the Methuen granite and, more to the east, in the Ridge Dome.

The northwesterly folds are more erratically disposed throughout Chandos Township. In the southwest corner of the township the Wolfe Hill anticline (Shaw, 1962) forms a member of this group, and east of the Loon Lake Pluton the Owenbrook anticline and the Glen Alda syncline are constituent members. A well defined syncline between the Wolfe Hill and Owenbrook anticlines is not present. An anticlinal axis running parallel to the northwest fold trend connects the dome structure of the Duck Lake Sill with the northern lobe of the Methuen granite. It is not clear whether this anticline is

equivalent with the Owenbrook anticline, the latter being displaced by intrusion of the Loon Lake Pluton, or if this fold is independent, being representative of the structures in the basement (see Adams and Barlow's suggestion of a batholith beneath the Duck Lake Sill).

It is clear that a third fold system must be present to allow for the postulated inversion of the Tallan Lake Sill. The northwest and northeast trending folds are relatively open, as shown by the low and intermediate dips commonly present, and have steeply dipping axial planes. Obviously an initial period of deformation must have produced isoclinal folds of considerable amplitude with subhorizontal or moderately dipping axial planes. In the absence of structural fieldwork in critical areas by the author, inferences must be made from existing geological maps and aerial photographs and the evidence remains largely circumstantial. Some observations of interest are:

(a) From aerial photographs it appears that the Chandos Syncline just west of Chandos Township is a refolded fold (see Figure 1.2). A distinct convergence and closing of beds in the limbs of the fold results in the formation of a crescent-shaped outcrop of Apsley paragneisses. The counterpart of this structure can possibly be found as a similar crescent of paragneiss found in the nose of the Rose

Island anticline. These two structures would then define a northwest trending isoclinal fold.

(b) Similar crescent and mushroom-shaped structures, indicative of refolded folds (Ramsay, 1967), are fairly common in Wollaston, Lake and Limerick Townships and lead to the general deduction of a pre-existing northwesterly trending set of isoclinal folds of large amplitude.

In view of the common occurrence of these interference patterns it is somewhat surprising that hardly any reference has been made to these structures. Undoubtedly this is to a large extent due to the complexity of the stratigraphy and the gross structural pattern in the area. The author has come across only one reference (Carmichael, 1967) in which allusion is made to a pre-existing episode of isoclinal folding. Carmichael is, however, very emphatic about his findings in Wollaston and Lake Townships: "Two important structural episodes have been distinguished. During the first structural episode, the rocks were folded isoclinally at a relatively low temperature. Deformed pebbles indicate that the rocks were greatly foreshortened perpendicular to the axial planes of these folds, and elongated parallel to the fold axes, but primary bedding is generally well preserved. At a later time, a new set of folds developed on steeply dipping, northeast-trending axial planes, and the temperature

rose to a maximum. All of the plutonic rocks had been emplaced by this time. The orientation of the early fold axes was modified both by the later folding and by the emplacement of the plutonic rocks, so that the initial orientation of the early folds cannot be determined with certainty. ... The metamorphic grade ranges from the garnet zone in the southeast to sillimanite zone in the northwest. The isograds are straight and they trend northeastward, parallel to the axial traces of the late folds, and transverse to the early folds".

The early folds might trend northwesterly then. We read further on: "The question of whether the two geometrically distinct structural episodes represent two separate orogenies, or merely two pulses of the same orogeny, cannot be answered decisively. Certainly, all the rocks of the area were involved in both structural episodes".

From the information provided above and the evidence to be presented in favour of an inverted Tallan Lake Sill, it seems evident that previous structural interpretations of the Bancroft area are in need of complete revision to allow for duplication of stratigraphic sections due to isoclinal folding. A re-examination of the stratigraphy would be most helpful in this respect, particularly because it is becoming increasingly clear that the volcanic component of the sequence, especially that of acid tuffs, has been much

underestimated before (e.g. Shaw, 1972; Van de Kamp, 1968; Carmichael, 1967). These undertakings are clearly beyond the scope of the present work, and all that can be concluded from this brief review of the structure is that an inversion of the succession, if not probable, is at least a good possibility.

CHAPTER 3

PETROCHEMISTRY OF THE TALLAN LAKE SUITE3.1 General Considerations

Two fundamental problems concerning the chemistry of the Tallan Lake Sill will be discussed with the aid of the chemical analyses presented in Tables 3A and 3B:

- (1) whether the rocks are indeed the metamorphosed equivalent of an igneous product as indicated by the field relations;
- (2) if so, the question of their chemical affinity (tholeiitic, alkalic or calc-alkaline) can be answered and the concept of a differentiated, inverted sequence may be discussed.

A comparison of Tallan Lake rocks with analyses of both sedimentary and igneous rocks is clearly in favour of an igneous derivation of the Tallan Lake Sill. Certain chemical sediments such as iron formation (Table 3C) may be similar in Fe-content, but are characteristically low in titania and alumina. Particularly if the close correspondence with analyses of igneous rocks (Appendix 1) is considered, the issue appears to be settled in favour of an igneous parentage of the Tallan Lake Sill.

Table 3A. Chemical analyses of Tallan Lake Suite*

	120	605A	420	303	309	606	207	105	310	210	110
SiO ₂	48.48	42.05	46.34	43.72	51.95	56.37	53.76	62.13	68.31	64.30	69.73
TiO ₂	2.84	4.12	3.52	4.08	1.84	1.20	1.31	0.85	0.45	0.41	0.36
Al ₂ O ₃	12.87	13.44	11.12	10.05	13.24	16.44	13.51	13.10	13.73	17.06	13.23
Fe ₂ O ₃	3.36	4.07	3.19	3.59	3.63	2.96	4.20	2.38	2.67	1.50	1.05
FeO	10.45	14.87	14.66	19.25	13.86	8.13	12.99	7.59	3.86	4.05	4.00
MnO	0.23	0.41	0.33	0.61	0.37	0.26	0.41	0.17	0.10	0.07	0.06
MgO	5.68	4.28	4.13	3.41	1.83	0.96	0.72	0.56	0.11	0.17	0.21
CaO	9.36	9.61	8.41	8.15	5.99	3.91	5.87	3.05	2.00	1.66	1.85
Na ₂ O	4.55	2.94	3.61	2.49	4.54	6.37	4.09	5.01	5.95	8.01	5.66
K ₂ O	0.38	0.42	0.54	0.42	0.45	1.09	0.98	2.07	1.67	1.83	2.12
P ₂ O ₅	0.44	1.64	2.28	1.83	0.66	0.28	0.26	0.19	0.01	0.02	0.01
H ₂ O+	1.32	1.30	1.07	1.20	0.85	0.83	0.75	0.97	0.30	0.32	0.54
H ₂ O-	0.15	0.15	0.09	0.11	0.06	0.08	0.12	0.09	0.08	0.10	0.05
CO ₂	0.42	0.27	0.15	0.59	0.37	1.49	0.30	1.73	0.20	0.13	0.80
Sum	100.53	99.57	99.44	99.50	99.64	100.37	99.27	99.89	99.44	99.63	99.67
Rb (ppm)	4.8	-	7.5	4.2	-	30	-	54	-	-	-
Distance from top (m)	60	165	180	185	195	210	225	235	260	265	270
femg	0.575	.713	.708	.839	.843	.866	.931	.908	.970	.948	.930
K/Rb	660	-	600	830	-	300	-	320	-	-	-

Table 3A/continued

Norms (wt.%)	120	605A	420	303	309	606	207	105	310	210	110
or	2.25	2.48	3.19	2.48	2.66	6.44	5.79	12.61	9.87	10.81	12.5
ab	34.08	24.88	3.55	21.07	38.42	53.90	34.61	43.65	50.35	67.78	47.8
an	13.57	22.24	12.54	15.01	14.42	13.05	15.61	7.35	5.83	5.19	4.4
q	-	-	-	0.93	3.33	2.09	7.20	15.11	21.79	5.00	22.7
ne	2.40	-	-	-	-	-	-	-	-	-	-
ol	10.36	11.72	0.32	-	-	-	-	-	-	-	-
opx	-	6.54	22.77	29.28	19.72	11.34	15.31	9.40	2.72	4.72	4.
cpx	24.71	12.49	12.19	11.67	9.55	3.93	10.40	6.20	3.56	2.57	4.
mt	4.87	5.90	4.63	5.21	5.26	4.29	6.09	3.55	3.87	2.17	1.5
il	5.39	7.82	6.69	7.75	3.49	2.28	2.49	1.66	0.85	0.78	0.6
ap	1.02	3.81	5.30	4.25	1.53	0.65	0.60	0.43	0.02	0.05	0.0

*For chemical procedure see Appendix 6

femq - Fe+Mn/Fe+Mn+Mg

120	Hornblende-plagioclase amphibolite. Assemblage 1
605A	Hornblende-cummingtonite-garnet-apatite-oxide amphibolite. Assemblage 2
420	Hornblende-cummingtonite-garnet-apatite-oxide amphibolite. Assemblage 2
303	Hornblende-cummingtonite-garnet-apatite-oxide amphibolite. Assemblage 2
309	Fe-hastingsite-cummingtonite-garnet mafic syenite. Assemblage 2
606	Fe-hastingsite-cummingtonite-garnet mafic syenite. Assemblage 2
207	Fe-hastingsite-garnet mafic syenite. Assemblage 3
105	Plagioclase-biotite syenite. Assemblage 4
310	Fe-hastingsite-plagioclase-K-feldspar quartz syenite. Assemblage 4
210	Fe-hastingsite-plagioclase-K-feldspar syenite. Assemblage 4
110	Fe-hastingsite-biotite-plagioclase-K-feldspar quartz syenite. Assemblage 4

Table 3B. Chemical analyses of Tallan Lake Suite (Shaw and Kudo, 1965)

	TL-61-65	TL-61-75	TL-61-45	TL-61-35	69-29-6	69-28-2	69-30-2
SiO ₂	47.50	46.10	46.00	47.10	42.00	50.50	53.30
TiO ₂	5.04	5.21	4.36	2.75	4.88	3.03	1.92
Al ₂ O ₃	13.60	14.20	13.00	13.00	13.00	14.50	13.80
Fe ₂ O ₃	3.50	3.80	3.90	3.80	3.50	3.00	3.00
FeO	13.68	13.88	14.15	16.18	16.54	13.85	12.10
MnO	0.29	0.32	0.32	0.37	0.38	0.32	0.29
MgO	5.20	4.80	4.30	3.30	4.80	2.60	3.60
CaO	7.80	7.90	8.60	6.40	8.60	6.30	6.60
Na ₂ O	2.82	2.96	3.10	2.92	2.71	4.58	3.44
K ₂ O	0.71	0.51	0.50	1.43	0.52	0.44	0.40
P ₂ O ₅	0.54	0.39	2.33	1.52	2.43	1.31	0.43
H ₂ O	1.19	0.70	1.20	1.36	1.53	0.88	0.97
CO ₂	0.75	0.00	0.04	0.00	0.96	0.06	0.74
Sum	102.60	100.80	101.80	100.10	101.90	101.50	100.60
femg (Fe+Mn/Fe+Mn+Mg)	.809	.826	.843	.886	.843	.893	.844
<u>Norms (wt.%)</u>							
or	4.20	3.01	2.95	8.45	3.07	2.60	2.36
ab	23.86	25.05	26.23	24.71	22.93	38.76	29.11
an	22.36	23.95	20.08	18.14	21.77	17.71	21.03
q	1.62	0.15	1.99	0.72	-	1.11	7.59
ne	-	-	-	-	-	-	-
ol	-	-	-	-	7.62	-	-
opx	22.09	21.02	23.70	29.28	19.67	22.80	22.25
cpx	10.67	10.59	6.30	3.23	4.36	4.34	7.55
mt	5.07	5.51	5.65	5.51	5.07	4.34	4.35
il	9.57	9.90	8.28	5.22	9.27	5.75	3.65
ap	1.25	0.91	5.41	3.53	5.65	3.04	1.00

Table 3C. Chemistry of sediments that might be mixed in order to obtain analyses similar to Tallan Lake amphibolite

	1	2	3	4	5
SiO ₂	51.18	39.26	36.65	24.92	63.09
TiO ₂	0.51	0.07	0.16	0.18	0.99
Al ₂ O ₃	11.95	2.88	1.02	1.82	18.58
Fe ₂ O ₃	8.09	0.63	1.77	0.66	2.17
FeO	12.15	24.94		0.40	2.73
MnO	2.71	1.23	0.04	0.11	0.22
MgO	2.42	4.62	0.50	19.70	2.67
CaO	1.12	4.62	29.43	22.32	1.11
Na ₂ O	2.12	0.00	1.01	0.03	4.54
K ₂ O	1.86	0.00	0.47	0.04	0.54
P ₂ O ₅	0.54	0.11	17.14	0.01	0.12
H ₂ O+	1.19	1.23		0.42	
H ₂ O-	0.07	0.11	3.14	0.36	2.69
CO ₂	3.70	20.46	5.19	33.82	-
S	n.d.	0.04	-	-	-
C	n.d.	0.07	0.58	0.08	-
Sum	99.61	100.27	99.25	100.04	99.45
Less O		0.02			
		100.25			

- 1 Chlorite-siderite-magnetite-quartz rock, Iron River district, Michigan. Table 14, anal. D (James, 1966)
- 2 Banded chert-carbonate rock, Gogebic district, Wisconsin. Table 17, anal. D (James, 1966)
- 3 Upper phosphorite stratum, Briansk, USSR. Total includes 0.05% FeS₂; 1.48% SO₃; 2.08% F. Table 86, anal. C (Pettijohn, 1957)
- 4 Cherty dolomite, Highland Co., Ohio. Total includes 0.15% FeS₂. Table 81, anal. E (Pettijohn, 1957)
- 5 Nonesuch shale (Keweenawan), Michigan. Table 70, anal. E (Pettijohn, 1957)

In deciding the kinship of the Tallan Lake suite we may as a first guide use the CIPW-norms. If the conventions outlined by Yoder and Tilley (1962) are employed, 15 of the 19 analyses may be classed as quartz-tholeiite, 3 as olivine tholeiite, and 1 as alkali-gabbro. Since continuous fractionation of a nepheline-normative liquid into a silica saturated one appears impossible at pressures lower than 7 kb (Yoder and Tilley, 1962), a considerable depth of emplacement of the sill would be implied.

The nepheline-normative character of sample 120 (Table 3A) is largely due to its high soda content, however, and the analysis is otherwise comparable to modern tholeiites (Appendix 1). In this connection we may mention the observations made by Van de Kamp (1968) who, comparing some sodic, nepheline-normative metavolcanics from the Bancroft area with bonafide alkalic volcanics, concludes that the former are of probable tholeiitic origin and have acquired their alkalic character through post-depositional alteration. This hypothesis will be closely examined in a further section of this chapter, where it is also concluded that alteration is the cause of the sodic nature of many rocks in the Bancroft area, including our sample 120.

Accepting silica saturation of the entire Tallan Lake suite as a fact, it is still to be decided whether the suite is tholeiitic or calc-alkaline.

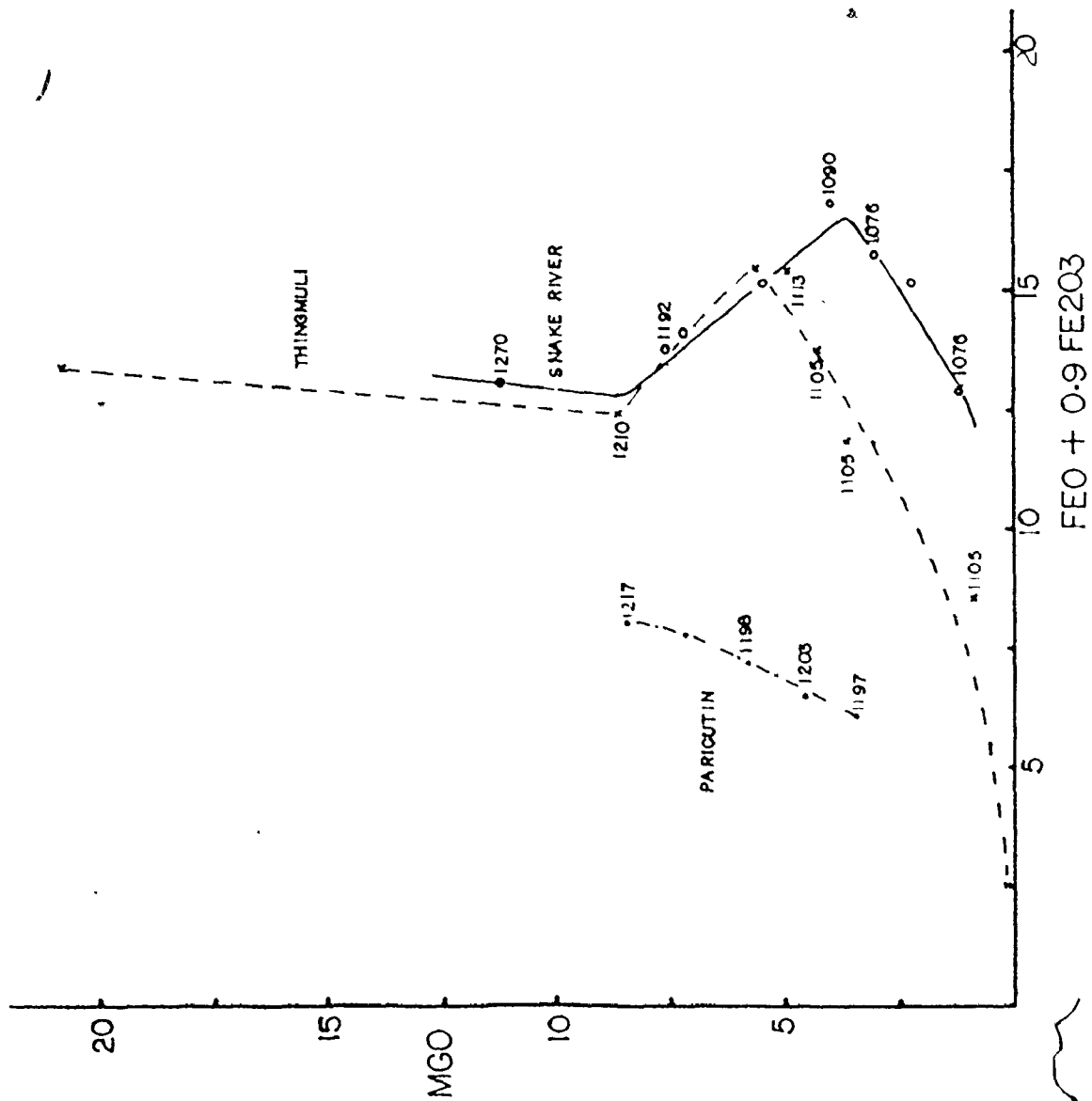
Figure 3.1 (a) MgO vs. FeO_{tot} for some differentiated volcanic suites.

Thingmuli (tholeiitic; Tilley et al., 1968), crosses

Snake River (tholeiitic; Tilley and Thompson, 1970), open circles

Paricutin (calc-alkaline; Tilley et al., 1968), dots

Figures refer to the liquidus temperatures of the different rocks at atmospheric pressure



FE0 + 0.9 FE2O3

MGO

THINGMULI

SNAKE RIVER

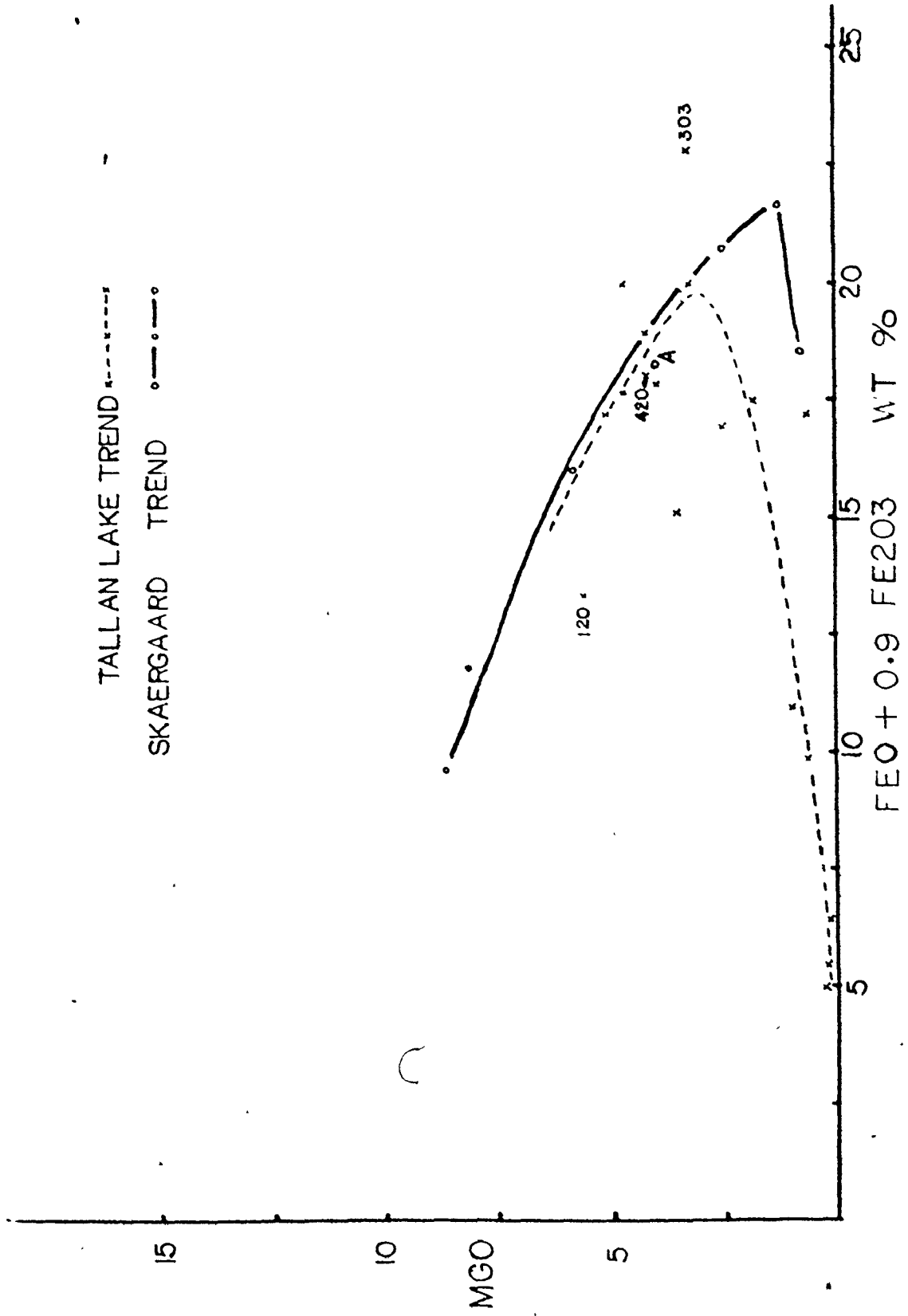
PARICUTIN

Figure 3.1 (b) MgO vs. FeO_{tot} for Tallan Lake rocks,
compared with Skaergaard liquids.

Open circles - Wager and Brown, 1967

Crosses - Tallan Lake analyses (Tables 3A
and 3B)

TALLAN LAKE TREND - - - - -
SKAERGAARD TREND ○ - - - - -



The tholeiitic nature of the rocks is perhaps best brought out in Figure 3.1 in which total iron is plotted against magnesia. The strong iron-enrichment is in clear contrast to calc-alkaline suites, in which magnetite is an early precipitate, leading to a gradual depletion in iron with differentiation (Osborn, 1959; Schairer and co-workers at the Carnegie Institution, 1963-1966).

Although comparison of the Tallan Lake trend with the tholeiitic differentiation series of Thingmuli and the Snake River Plateau (Figures 3.1a and 3.1b) offers the suggestion of a single, differentiated suite, it would be unwise to accept this without careful consideration, for it is clear that, as soon as differentiation in situ of the sill is firmly established, the concept of an inverted sequence will be virtually unassailable.

Consequently the differentiation of similar rock suites must be closely examined, and a brief summary of the main aspects of such differentiated sequences is given in the following section.

3.2 Differentiation

3.2.1 Mineralogical and chemical effects of differentiation

In order to compare the differentiation trends

observed in some tholeiitic rock series with analyses from the Tallan Lake Sill, the following procedure was used: Analyses showing less than 50% SiO_2 and in major element chemistry closely comparable to the basic members of the Tallan Lake Sill were initially looked for. If a similar satisfactory correspondence between intermediate and acid members of the same differentiation series, on the one hand, and Tallan Lake rocks, on the other, is found, a reasonable case for continuous differentiation of the sill can then be made. The rock suites which emerge as suitable chemical analogues of the Tallan Lake series are all of typically anorogenic environment (e.g. Iceland, East Pacific Rise, Snake River Plateau), with the possible exception of rocks associated with anorthosites (Adirondack Massif, Michikamau Anorthosite), which are partly of disputed origin and environment (Kranck, 1966; Michot, 1966).

It is noteworthy that the Tallan Lake analyses do not compare exclusively with either intrusive (cumulate) or extrusive (essentially liquid) compositions. As can be seen in Appendix 1, most analyses resemble lavas and dyke rocks, although some (e.g. samples 303, 309, 207) have a distinctively "intrusive" (i.e. cumulate) chemical character.

The intrusive tholeiitic differentiation series is exemplified by large layered intrusions, of which the Skaergaard Intrusion and the Michikamau Intrusion are examples,

and by the rocks associated with the anorthosite massifs of Eastern Canada and adjoining parts of the U.S.A. It is to be noted that, whereas silicic differentiates are virtually absent in the layered intrusives, such rocks are conspicuous members of the anorthosite suite (e.g. mangerite, charnockite). A fairly typical differentiation pattern is displayed by the Skaergaard Intrusion in E. Greenland. The layered gabbros can be divided in three parts (Wager and Brown, 1967): a lower zone in which magnesian olivine, clinopyroxene and plagioclase are the main constituents; a middle zone in which olivine is absent and clinopyroxene and plagioclase predominate; and an upper zone characterised by the coexistence of (iron-rich) olivine and quartz, again with plagioclase and clinopyroxene. Differentiation of the Michikamau Intrusion is completely analogous to that of the Skaergaard, although plagioclase is the predominant cumulate mineral here. Extremely iron-rich rocks are only found as dykes (Emslie, 1966) and not in the layered zones as with the Skaergaard.

Early magnesian differentiates belonging to the anorthosite suite are unknown, and the least evolved members of the suite are the vast accumulations of plagioclase, which form the bulk of the massifs. Norites and other, more iron-rich rocks containing orthopyroxene in addition to clinopyroxene and plagioclase, grade into silicic mangerite

and charnockite, where fayalite again is present, at the periphery of the anorthosite massifs (e.g. de Waard, 1970).

The extrusive tholeiitic differentiation series is complementary to the intrusive series, with respect to the fact that liquid compositions are better studied here. One of the best documented sequences is that of the Galapagos Archipelago (McBirney and Williams, 1969), where a central volcanic complex developed upon a basement of oceanic tholeiites, possibly due to mantle plume activity at a triple junction of oceanic plates (e.g. Morgan, 1971).

Feldspar-phyric lavas attest to the importance of plagioclase precipitation in the early development of the central volcanoes and these are followed by iron-rich titaniferous lavas, the ferrobasalts, which carry plagioclase and clinopyroxene as phenocrysts. Fayalite appears in tholeiitic andesites (Icelandites) which are locally present. Even more silicic rocks are present in small parasitic cindercones and spattercones, but these are separated from the Icelandites by a chemical discontinuity, the Daly Gap, which spans a range from 53-57% SiO_2 (see also Chayes, 1963), for which no volcanic compositions are known from the Galapagos Islands. Interesting is also the presence of many inclusions of plutonic rock fragments, presumably from subvolcanic magma chambers, in many lavas and cindercones.

These inclusions range in composition from eucrite (plagioclase-clinopyroxene cumulate) to quartz-syenite.

The differentiation pattern of Thingmuli volcano in Iceland and the volcanoes of the Snake River Plateau in the Western U.S.A., is very similar to that of the Galapagos Islands, except for the absence of silicic trachytes on the Snake River plains, where the most silicic differentiates consist of tholeiitic andesites.

In all fundamental aspects these differentiated suites are similar to the Tallan Lake Sill, for the trend towards extreme iron enrichment is accompanied by an increase in titania and particularly phosphorus, coupled with a decrease in silica. Only when the trend toward iron enrichment ceases does differentiation toward silicic members take place, presumably through precipitation of ulvöspinel or magnetite.

Notably different from the Tallan Lake series are the alkali values of some suites, particularly the Snake River basalts and Adirondack anorthosite suite, which yield highly potassic differentiates. The possibility of deep crustal contamination has been raised for both series, however (Tilley and Thompson, 1970; Anderson and Morin, 1966). The possibility of significant additions of soda to Tallan Lake syenites must also be entertained (see Chapter 3.3).

Figure 3.2 AFM plot for Tallan Lake analyses (crosses),
compared with other differentiated suites.

Solid line - Tallan Lake trend

Heavy dashed line - Skaergaard and
Michikamau trend (identical)

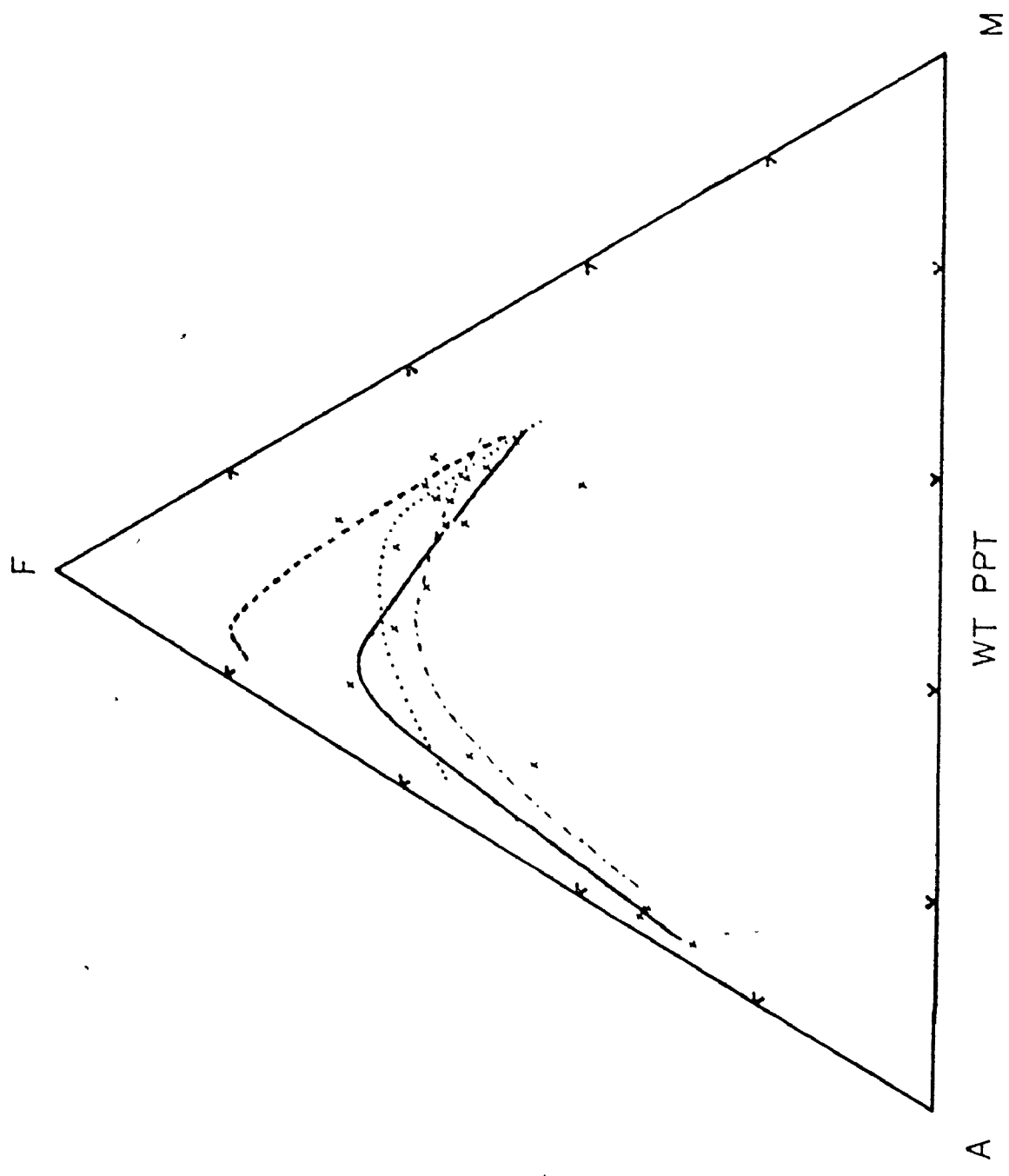
Dash-dot line - Galapagos trend

Stippled line - Snake River trend

A - $\text{Na}_2\text{O} + \text{K}_2\text{O}$

F - $\text{FeO} + .9\text{Fe}_2\text{O}_3$

M - MgO



Hence, although the AFM-diagram of Figure 3.2 is suggestive in depicting the similarity to various differentiated sequences, it may not be too reliable, especially with regard to the more silicic differentiates.

As far as the mineralogy of the differentiation series is concerned, the conclusions based on the study of cumulate rocks, which are supported by melting experiments on volcanic rocks (e.g. Tilley et al., 1968) are the following:

(1) Initially large quantities of magnesian minerals such as orthopyroxene, clinopyroxene and particularly olivine are precipitated, which in the course of fractional crystallisation are accompanied by gradually increasing amounts of plagioclase. Work on the Skaergaard Intrusion (Wager and Brown, 1967) has shown that when approximately 60% of the original magma had solidified, plagioclase was the predominant cumulate mineral.

Due to a low initial f_{O_2} of the magma (e.g. Yoder and Tilley, 1962) no magnetite is precipitated and the liquid is depleted in MgO (see Figure 3.1a) and, to a lesser extent, SiO_2 .

(2) Due to a reaction relation with the liquid, common to all tholeiitic series (Yoder and Tilley, 1962), olivine will no longer precipitate at a certain stage of fractionation,

and clinopyroxene, sometimes accompanied by pigeonite, is the sole ferromagnesian mineral to precipitate. The liquid becomes increasingly enriched in iron due to the fact that the solid solutions are more magnesian than the magma they crystallised from. As silica is withdrawn from the liquid, Ti and Al will substitute for Si in the clinopyroxene lattice (Kushiro, 1960).

Olivine, more iron-rich than Fa_{60} , may again be found as a cumulate mineral in the late stages of fractionation.

(3) In the final stages of differentiation, a steadily rising f_{O_2} will initiate the precipitation of magnetite or ulvöspinel and the liquid will be rapidly depleted in Fe. Precipitation of apatite commonly coincides with the onset of magnetite crystallisation, and the apatite-oxide cumulates are usually the most mafic rocks encountered in differentiated complexes.

(4) After precipitation of magnetite, differentiation of the small amount of liquid left (less than 1% of the original volume of magma in the case of the Skaergaard Intrusion) proceeds to form silicic granophyres (or trachytes and rhyolites in the extrusive complexes).

It is perhaps noteworthy that, at the point of magnetite crystallisation, all liquids of both the Thingmuli

and Snake River suites remain at the same liquidus temperature (see Figure 3.1a). As solidus temperatures generally go down with increasing silica content (Tuttle and Bowen, 1958), it may be expected that such liquids will remain for a considerable period of time in a slowly cooling magma chamber, thus enhancing the possibility of being squeezed out as a separate intrusive or extrusive, as a result of tectonism. This would adequately explain the separate intrusion of the Tinden granophyre sill in the Skaergaard complex and might also provide a general explanation for the Daly Gap.

The objective of this rather lengthy exercise has been to provide us with the possible igneous mineralogy of a possibly differentiated tholeiitic sill.

The next step will be to construct a differentiation model which takes into account certain critical observations from the field and the laboratory, as well as the consistent chemical relationships between the important cumulate minerals (Figure 3.3) in other differentiated suites. The decision on whether the Tallan Lake Sill is overturned or not, must ultimately rely on the failure or success of this model, which is discussed in the following section.

3.2.2 Model calculations

The field and petrographic observations on the Tallan Lake Sill which have a bearing on the differentiation model to be adopted are the following:

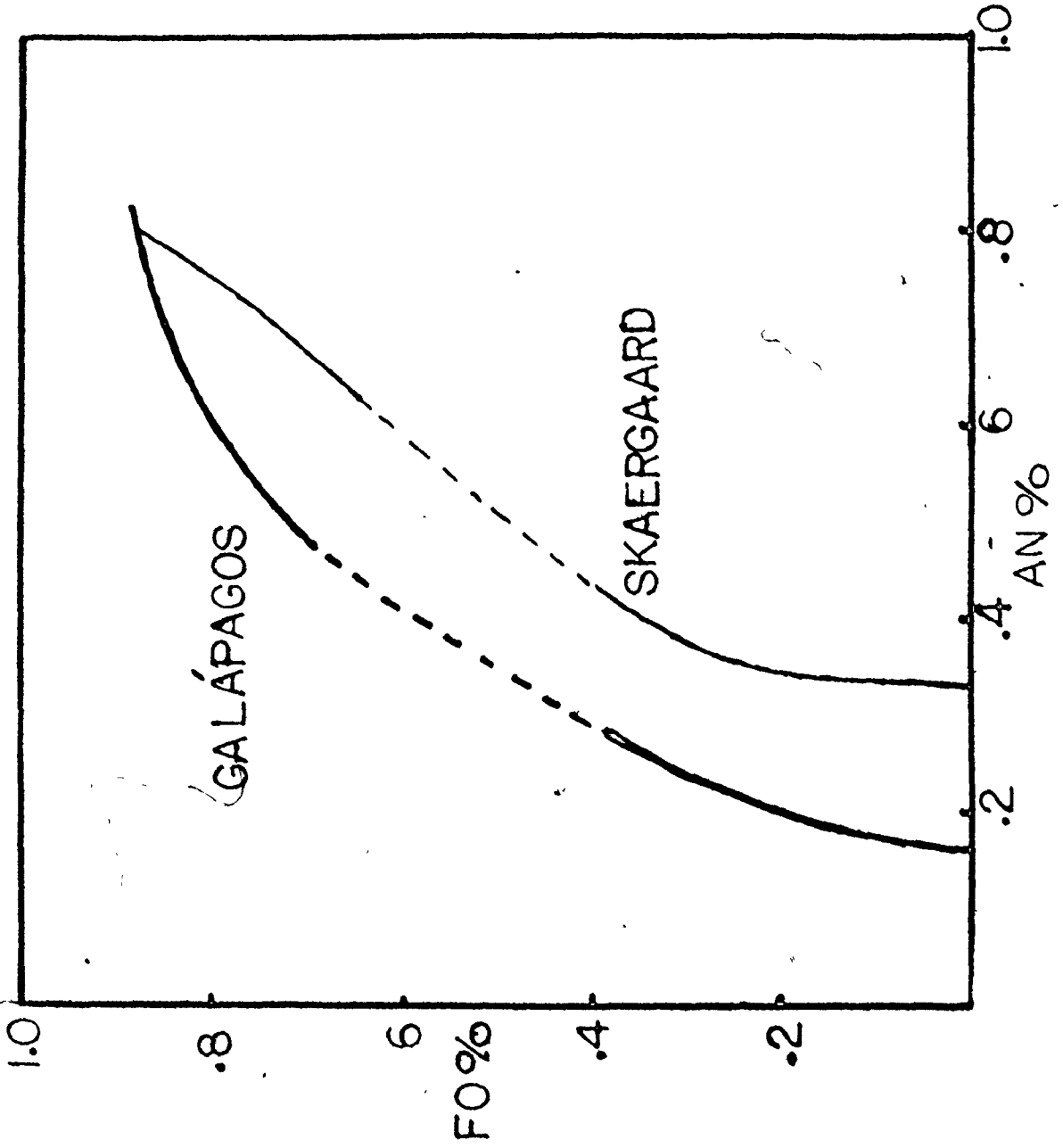
- (1) The uppermost 180 meters of the sill consist of a metagabbro, which becomes conspicuously more mafic in the bottom part of that section. Whereas in the upper part plagioclase is abundant and textures may be interpreted as metamorphosed fluxion structures, such features are lacking in the lower, more mafic portion, where apatite and oxides increase in abundance (Figure 4.1).
- (2) Although the contact with the underlying mafic syenites is gradational, the transition from oxide-rich gabbro to syenite is rapid, being accomplished over distances of less than 10 meters. The transition zone is in places marked by an abundance of marble screens in the sill, fine exposures of which can be seen in a recent (1971) roadcut along Hwy 620 near Clydesdale Lake.
- (3) The sill has the shape of an inverted saucer of which the inner portion is filled with syenite. The most leucocratic syenites are found in this central

portion and the syenites are thickest there. The syenite thins out toward the rim of the saucer and is absent in peripheral regions.

Assuming that the sill in its present tectonic position is inverted, we envisage emplacement of the sill as follows: initially a ferrobasalt liquid was intruded along a strata-bound surface, carrying with it in suspension mainly plagioclase; quiescent crystallisation and settling of the crystal mush ensued, leaving a ferrosyenite liquid in the pore spaces; subsidence in the centre of the phacolith finally caused the roof of the sill to collapse. By then a more or less rigid meshwork of crystals had been established in the sill, allowing a relatively clean separation of the interstitial syenite liquid. Local feeder dykes of syenite, such as the one seen in outcrop along Hwy 28, assured transport to the central portion of the sill. It is clear that we view the marble screens as parts of the collapsed roof. The apatite cumulates that occur above these screens (or, below before tectonic inversion) may represent the heavy residue left behind on ascent of the syenite, and thus entirely the product of crystallisation in situ.

Clean separation of a differentiated liquid from a crystal mush in such a manner has recently been advocated

Figure 3.3 Relations between fo-content and an-content of coexisting olivines and plagioclases in two differentiated suites. Dashed portions of lines represent these segments of differentiation sequence in which no olivine was precipitated



by Lindsley et al. (1971) and Thompson (1972). It is clear that the model can be put to the test by subtracting a syenite composition from a presumed, unmodified ferrobasalt composition to yield a plausible crystal cumulate. The crystal cumulate is probably quite simple mineralogically: as previously stated, the experimental evidence points to an assemblage consisting of plagioclase, clinopyroxene, olivine and magnetite; ferrobasalts from Iceland (Thingmuli; Carmichael, 1964), Snake River Plateau (Tilley and Thompson, 1970) and Galapagos Islands (McBirney and Williams, 1969) all carry these phases as phenocrysts.

Plots in which the fs-content in the clinopyroxene is related to the fa-content in the corresponding olivine show an unequivocal covariance for most differentiated sequences, and it is to be expected that if the iron content of the pyroxene is known, the olivine composition can be calculated. A less straightforward relationships between fayalite content and plagioclase composition is observed (Figure 3.3), and a range of 15% an is possible for any given olivine composition. Further chemical inferences on the original mineralogy of the sill have been made as follows: some hornblendes from the sill are laced with ilmenite inclusions. This has been interpreted (see section on Petrography) as a feature inherited from a titaniferous clinopyroxene. This checks with the common experience that

pyroxenes from ferrogabbros are titanium-rich. The presence of magnetite as a precipitate from the magma can not only be indirectly established from the shape of the FeO vs. MgO curve (Figure 3.1b), but is also made probable from the observation of certain ilmenite intergrowths in the oxide-rich gabbro and the syenites. In these, ilmenite spindles meet at angles of approximately 60° , mimicking skeletal ulvöspinel grains of the type found in many volcanic rocks, for instance the Picture Gorge basalts (see Lindsley et al., 1971, Plate 4A).

As a model for the composition of the parent magma at a certain stage of differentiation, rock composition 420 has been chosen. The sample locality of this rock lies along the periphery of the region in which abundant syenite occurs and the rock itself is underlain by less than 10 meters of syenite. The close proximity of the rock to the contact and its fine-grained nature make it probable that it underwent rapid cooling. We may point to the fact that, although the sample has the highest phosphorus content of all samples investigated, only medium-sized apatites (2-3 mm in length) are present, in sharp contrast to the oxide-rich apatite cumulate rocks in which large apatites (1-2 cm in length) can be observed.

It is clear that, for our model of the emplacement

Figure 3.4 (a) Flowchart of the operation of computer
program LSPX

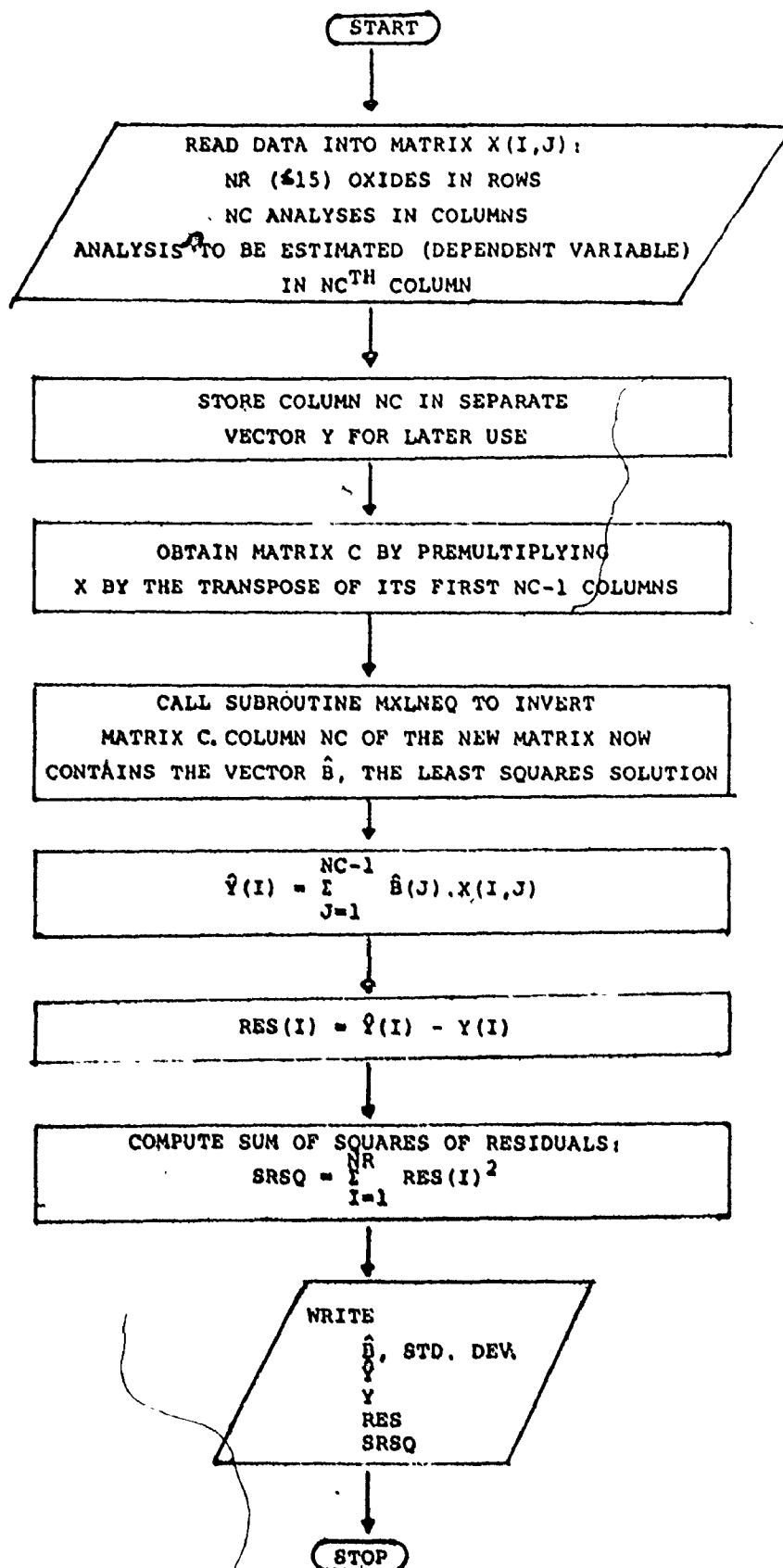


Figure 3.4 (b) Typical output of LSPX. Symbols are those used in Figure 3.4(a)

THIS IS A TEST TO CHECK FEASIBILITY OF THE PROPOSED
 PETROGENETIC MODEL. CLINOPIROXENE (AGUSR) OLIVINE (FA62), ULVOSPINEL,
 PLAGIOCLASE (AN33.7) AND APATITE (APBUSH) ARE COMBINED WITH
 PRESUMED DIFFERENTIALS TO PRODUCE PARENT LIQUID (L20).

X	J	AGUSK	FA62	AN33.7	APBUSH	ULVSO	INPUT	DATA
1	SI02	47.92	32.94	62.94	0.00	.22	42.38	38
	TI02	3.95	.11	0.00	0.00	25.60	3.97	30
	AL203	17.25	.15	22.43	0.00	10.30	17.92	34
	FCOTOT	10.29	40.73	0.00	0.00	68.30	4.22	34
	MNO	10.11	10.80	6.00	0.00	1.95	8.61	34
	CAO	10.59	6.43	7.63	53.74	0.00	3.09	34
	MA20	0.00	0.00	1.00	0.00	0.00	0.00	34
	K20	0.00	0.00	0.00	0.00	0.00	0.00	34
	P205	0.00	0.00	0.00	0.00	0.00	0.00	34

Y	ST	Y	RES
47.32	0.38	47.38	-0.06
3.32	0.37	3.64	-0.32
17.99	0.34	17.92	0.07
0.10	0.22	0.00	0.10
8.70	0.09	8.69	0.01
4.02	0.33	3.33	0.69
2.11	0.33	2.33	-0.22

RESULTS	RESIDUALS
SI02	-0.06
TI02	-0.32
AL203	0.07
FCOTOT	0.07
MNO	0.10
CAO	0.01
MA20	0.01
P205	-0.22

VARIABLE	COEFF.	STD DEV.
AGUSR	0.2163	0.938
FA62	0.2282	0.212
AN33.7	0.0572	0.205
APBUSH	0.0836	0.743
ULVSO	0.0404	0.050
	0.0823	0.088

SUM OF SQUARES OF
 RESIDUALS
 0.2594
 SRSQ

COEFF.	STD DEV
0.2163	0.938
0.2282	0.212
0.0572	0.205
0.0836	0.743
0.0404	0.050
0.0823	0.088

of the syenites to be applicable, simple addition of chemical analyses of the different syenites with analyses of minerals inferred to have been part of the original mineralogy of the sill will result in analysis 420, if the following conditions are satisfied: (1) we can make an accurate estimate of mineral compositions from analyses available in the literature; (2) the different compositions of the syenites are a result of gravitational settling of minerals rather than the product of fractionation processes due to cotectic crystallisation.

To test our model numerically, the program LSPX (Bryan et al., 1969) was employed to make the necessary calculations. The program makes use of all 10 oxides normally determined in a conventional chemical analysis, rather than the limited number used in Harker diagrams, and provides the user with a least squares estimate of the composition to be approximated (= parent rock). The operation of the program is schematically represented in Figure 3.4. Mineral analyses used are listed in Table 3D. Unfortunately no analyses of clinopyroxenes were found that corresponded favourably to the Fe/Mg ratio in 420, the parent rock. The Fe/Mg ratio of an augite from a more magnesian lava from the Snake River series (Tilley and Thompson, 1970) was therefore adjusted to conform to the formula of clinopyroxene coexisting with olivine

Table 3D. Mineral analyses used in model calculations

	1	2	3	4	5
SiO ₂	47.92	32.94	62.94	0.00	0.22
TiO ₂	3.02	0.10	0.00	0.00	25.60
Al ₂ O ₃	3.95	0.10	22.04	0.00	1.30
FeO*	17.20	48.86	0.43	0.00	68.50
MnO	0.25	0.75	0.00	0.00	0.60 ^a
MgO	10.94	16.80	0.29	0.00	1.95
CaO	16.11	0.45	6.69	53.74	0.05
Na ₂ O	0.59	0.00	7.03	0.00	0.00
K ₂ O	0.00	0.00	1.02	0.00	0.00
P ₂ O ₅	0.00	0.00	0.00	42.00	0.00
Sum ^b	99.98	100.00	100.44	95.74	98.22

* Total iron recalculated as FeO

a A value of 1.69% MnO was used in calculations involving USGS standards

b The fact that not all totals come to 100% does not affect the quality of the least-squares estimate. It does, however, result in a slight over-estimate of amounts of minerals required.

1. AGUSR. Snake River augite (62 h; Tilley and Thompson, 1970). Fe/Mg ratio adjusted to conform to composition $Wo_{36}En_{34}Fs_{30}$.
2. FA 62. Computed from olivine analyses given by Deer, Howie and Zussman (1962).
3. AN 33.7. Computed from plagioclase analyses given by Deer, Howie and Zussman (1962).
4. APBUSH. Bushveld fluor-apatite (Grobler and Whitfield, 1970).
5. ULVSO. Ulvöspinel from Socorro Island, East Pacific Rise (Bryan, 1970).

(fa_{62}) in a (hypothetical) Skaergaard liquid very similar to sample 420 (liquid A of Figure 3.1b). The anorthite content of the plagioclase was determined by trial and error runs of the program and its orthoclase content was estimated by comparison with analyses given by Lindsley et al. (1971) for the Picture Gorge basalts. There is very little to choose between the various published analyses of ulvöspinel, but a microprobe analysis is preferred here because of the difficulty in obtaining a pure sample for conventional "wet" analysis.

Although the selection of mineral analyses has admittedly been biased toward obtaining a good computer solution, the correspondence of estimates with the actual rock analysis 420 (Table 3E) must be considered excellent, especially in view of the fact that only 6 variables (analyses) were used to obtain the estimate (it is evident that as the number of variables approaches the number of equations [number of oxides] a trivial solution will be produced). One component that is consistently underestimated is MnO, however. Discrepancies in the estimated and observed value for this oxide can be easily removed if the MnO content of the ulvöspinel is adjusted to 1.69% (which appears not to be an unreasonable value).

Major differences still remain in the respective

Table 3E Least-squares estimate of parent liquid
composition (420) by combining presumed
differentiates with mineral analyses of
Table 3D

values for the alkalis and cannot be so removed (especially since the plagioclase composition chosen represents the best fit for all samples), but it is encouraging to note that the largest differences pertain to those samples which have the highest sodium values (606 and 210) and are, therefore, suspected to have undergone sodium enrichment.

Attention must be drawn to the amount of liquid subtracted from sample 420. The rock composition of 606 accounts for more than 50% of analysis 420, whereas more acid syenites account for progressively smaller proportions. This is interpreted to mean that the more acid syenites represent a cleaner liquid residue than the mafic ones. The so obtained differentiation sequence 420-606-210-105-310-110 corresponds to the height in intrusion (Table 3A) with the exception of Sample 210.

The real test concerning the validity of our differentiation model should be to inspect whether a constant mineral residue is left after subtraction of the syenite liquid. Since it is clear that ulvöspinel is the heaviest mineral in the crystalline extract, it was thought best to normalise the mineral proportions relative to ulvöspinel and investigate the results. From Table 3F it is clear that samples 105, 310 and 110 leave a very similar extract and that significant deviations are found for 606 and 210, which are presumably plagioclase-rich, possibly due to flotation of

Table 3F. Proportions of liquid and mineral-residue required to obtain parent liquid composition (420) and the composition of that mineral residue

Variable	Ppt	Variable	Ppt	Variable	Ppt	Variable	Ppt	Variable	Ppt	Variable	Ppt
110	1.336	210	2.247	310	1.501	105	1.895	606	6.519		
AN 33.7	3.220		2.426		3.160		3.238		1.016		
AGUSR	1.418		1.907		1.495		1.600		2.773		
FA 62	1.024		0.907		1.010		0.991		0.695		
APBUSH	0.467		0.478		0.473		0.479		0.564		
ULVSO	1.000		1.000		1.000		1.000		1.000		
		110 res	210 res	310 res	105 res	606 res	605A	303			
SiO ₂	42.93	41.41	42.75	43.02	36.72	43.15	44.96				
TiO ₂	4.21	4.69	4.26	4.31	6.04	4.23	4.20				
Al ₂ O ₃	10.97	9.38	10.83	10.81	5.77	13.79	10.34				
FeO*	20.34	22.14	20.36	19.97	24.97	19.02	23.12				
MnO	0.39	0.43	0.39	0.38	0.41	0.42	0.63				
MgO	4.98	5.60	5.09	5.17	7.53	4.39	3.51				
CaO	9.86	10.94	9.99	10.02	13.31	9.86	8.38				
Na ₂ O	3.30	2.20	3.20	3.30	0.79	3.02	2.56				
K ₂ O	0.25	0.11	0.31	0.14	-0.04	0.43	0.43				
P ₂ O ₅	2.77	3.11	2.82	2.89	4.42	1.68	1.88				

plagioclase. We may, however, point to the virtually constant ratio of magnetite:olivine:apatite for all samples except 606. The first two minerals have a higher density than any of the other minerals and apatite may not have escaped from the crystalline meshwork by virtue of its large size and non-equant dimensions; the needle-like prisms of apatite in the syenite contrast sharply with the stout prisms in the oxide-rich rocks (see section on Petrography).

The composition of the mineral residue left over by subtraction of 105, 110 and 310 has also been listed in Table 3F, and the similarity to analyses 303 and 605A is obvious. This again substantiates our contention that the oxide-rich gabbros represent the mineral extract left behind on ascent of the syenite and offers support for the validity of differentiation of the syenite from the gabbro.

Noteworthy is the fact that less differentiated rocks such as 120 are not easily related to 420 by the choice of minerals employed. Residuals are usually larger than 1, which tends to suggest that the validity of such a procedure is in question. Returning to Figure 3.1a and observing that the liquidus temperatures for a similar variation in the Snake River basalts encompass a range of roughly 70°C, this should not be unexpected and is rather in favour of our model in which a prolonged period of quiescent crystallisation is envisaged.

In order to ascertain that no spurious solutions were obtained due to an unfortunate choice of mineral compositions, the model was also tested against U.S.G.S. standard rocks G-2, GSP-1, AGV-1 and BCR-1 in the place of the syenites. It will be seen from Table 3G that the solutions have large residuals and are indeed inferior to the ones previously obtained, particularly when allowance is made for the fact that the MnO content of the ulvöspinel had been adjusted here to 1.69%, resulting in perfect solutions for that oxide.

With all due caution, we may conclude that the calculations support the concept of consanguinity of the syenite with the ferrogabbro. This being the case, it is difficult to envisage the syenite as a separate intrusion, in a sense other than that postulated in our model. Hence, it is assumed that the Tallan Lake Sill is a tectonically inverted, differentiated sequence.

3.3 Chemical Alteration During Diagenesis and Low Grade Metamorphism

In previous sections on the chemistry of the Tallan Lake suite, the opinion was submitted that the rocks have undergone chemical alteration which has mainly resulted in the depletion of calcium and the introduction of sodium

Table 3G Least-squares estimate of 420, by combining
U.S.G.S. standards with mineral analyses of
Table 3D

into the rocks. The remarkable similarity of sample 120 and Thingmuli basalt G101 (Carmichael, 1964; see Appendix 2a) for all oxides other than Na_2O and CaO certainly seems to bear this out, and the difficulty in reconciling alkali contents of the sodic syenites with a simple differentiation mechanism has already been noted. We are of the opinion that these changes in chemistry are to be expected during diagenesis and low grade metamorphism.

Albitisation of plagioclase feldspar causes probably the most significant change in chemistry of volcanic rocks in contact with seawater, a process usually referred to as spilitisation. A compilation of spilite analyses by Vallance (1960) seems to substantiate the selective replacement of calcium by sodium, as a result of which most spilites plot in the alkali-basalt field in the silica vs. combined alkalis plot of Macdonald and Katsura (1964; see also Yoder, 1967). Experimental confirmation of such a process due to interaction with seawater has been provided by Orville (1972).

Hydration and devitrification of volcanic glass furnishes further spectacular examples of chemical alteration as attested to by some analyses listed in Appendix 2b. Although the chemical effects of such alteration seem to be rather variable, the decrease in CaO has to be observed. Alkali contents may actually also decrease during such palagonitization, however. That chemical alteration has

played an important part in the history of the rocks in the Bancroft area is suggested by the following facts:

(1) Of 16 analyses of Hermon amphibolites listed by Jennings (1969), 5 are either nepheline- or corundum-normative.

Several more are given by Van de Kamp (1968). These rocks can by no stretch of the imagination be classified as alkaline basalts or peraluminous volcanics, as emphasized by the latter author. Leaching of CaO would adequately account for such a normative character (Vallance, 1967).

(2) Examination of chemical analyses of the Tudor volcanics from Sethuraman (1970) (see Appendix 2a) shows a remarkable inverse correlation between Na_2O and CaO contents, irrespective of bulk rock chemistry. This is expected to be a result of cation exchange on the plagioclase. The rocks can be classified as high-alumina basalts (Sethuraman, 1970), the main constituent of which must be plagioclase.

(3) Gedrite-cordierite rocks are quite common in the high grade metamorphic terrain of the Haliburton Highlands (e.g. Lal and Moorhouse, 1969). Vallance (1967) has drawn attention to the peculiar chemistry of such rocks, notable features being the lack of CaO and alkalis. Anthophyllite-cordierite assemblages are typically found in contact metamorphosed spilites, suggesting that spilitisation is a primary

requirement for the formation of such assemblages. Since the chemistry of these rocks bears the most resemblance to altered volcanic glasses (Appendix 2b), it is reasonable to assume that the progenitors of these rocks were chlorite-rich basic metatuffs. In this context we may mention the observation by Tuominen and Mikkola (1950) that anthophyllite-cordierite gneisses were only to be found in fold hinges in the Orijärvi region of Finland. The authors concluded that the high ductility contrast between pre-existing chlorite schists and more competent feldspathic beds (leptites) was the cause of such a mode of occurrence.

Since alteration must also have exerted a profound influence on the composition of more silicic rocks in the area, several analyses from the Silent Lake Pluton (Brooks, 1971) have been included in Appendix 2c for comparison with alteration products of acid volcanics from the literature.

It is obvious from Appendix 2 that many of the peculiarities in the chemistry of rocks from the Bancroft area are matched in alteration products of modern volcanic rocks. The average for a great number of analyses of the Tudor volcanics seems high in Na_2O and low in CaO , when compared with fresh oceanic tholeiites, but this discrepancy disappears when oceanic spilites are taken into account. Similarly, there is no need to resort to schemes involving removal of specific elements during anatexis (Lal and Moorhouse,

1969) when alteration of volcanic glass will adequately explain the compositional variations in anthophyllite-cordierite rocks, especially when such a mode of formation has been substantiated by field observations (Vallance, 1967).

The fact that spilitisation has seriously affected the chemistry of the Tallan Lake Sill, combined with the observation that the amphibolites in direct contact with the sill are obviously more calcium-rich (since they do not contain a calcium-poor amphibole), than the spilitic rock (sample 1317, Appendix 2a) which contains the three amphibole assemblage farther away from the contact, suggests that the alteration was mainly achieved during diagenesis and possible low-grade metamorphism. It would follow that the intrusion of the Tallan Lake Sill preceded this event, suggesting a relatively short time span between extrusion of the lavas and emplacement of the gabbroic series.

3.4 Summary

The chemistry of the Tallan Lake Sill (Tables 3A, 3B) is clearly comparable with some well known tholeiitic differentiated sequences such as the Skaergaard Intrusion in Greenland and the Thingmuli volcano in Iceland.

The chemical and mineralogical differentiation pattern of such tholeiitic series has been traced and it is found, for instance, that the chemistry of the apatite-rich

cumulates which overlie the mafic syenites of the Tallan Lake Sill, reflects the critical stage in the development of a tholeiitic series, where magnetite precipitates from the liquid, leading to silica enrichment of residual liquids (sample 303; Figure 3.1b). A petrogenetic model is developed in which the frequent occurrence of elongate marble xenoliths between apatite gabbro and mafic syenite forms a key element. These xenoliths are seen as part of the collapsed roof of the sill, forming a membrane through which a relatively clean syenite residue (previously residing in the interstices of a relatively rigid mineral meshwork) is pushed upwards as a result of tectonic forces.

Computer-generated least squares solutions of a presumed parent liquid support the concept of consanguinity of syenites and gabbro and it is concluded that the Tallan Lake suite is one single, tectonically inverted, differentiated sequence.

Attention is drawn to the sodic nature of some Tallan Lake gabbros and syenites and a comparison is made with spilitic rocks. The chemistry of the Tallan Lake suite and that of most metavolcanics in the Bancroft area, reflects the alteration that accompanies burial metamorphism and is, for instance, closely comparable with the Kowoonawan basalts (Jolly and Smith, 1972). An interesting sideline to this study is the interpretation of the rocks comprising the Silent

Lake "pluton" (Breaks, 1971) as altered silicic volcanics, with sillimanite-nodules within them as metamorphosed, silicified lithophysae.

It is conceivable that the petrogenetic model developed for the Tallan Lake Sill is not only of local significance. Assuming that the iron-rich liquids, initially intruded in the Tallan Lake area, were extrusive as well, and that a similar statement can be made about the Tallan Lake syenites, it would follow that a well-defined Daly Gap would separate syenites and ferrobasalts. The trachytes would mainly be present in small cindercones, as is commonly the case in central volcanic complexes around the world. It is further interesting to speculate on the early differentiates consanguineous with the Tallan Lake Sill, since it is clear from comparison with other suites that the Tallan Lake gabbros represent highly evolved compositions. The likely progenitors of the sill are the anorthositic, layered gabbros in the Bancroft area (such as the Mallard Lake, Umfraville, Thanet gabbro bodies), particularly since analyses of these are closely comparable with those of the Marginal Border Group of the Skaergaard Intrusion, and feldspar-phyric lavas in central volcanic complexes such as Thingmuli volcano and the Galapagos Islands.

CHAPTER 4

PETROGRAPHY

This section deals mainly with the metamorphic assemblages as they are found in the different rocks composing the sill, but an attempt will be made to reconstruct the original igneous mineralogy since this is of obvious importance to our hypothesis of an inverted, differentiated gabbro.

4.1 Relict Igneous Mineralogy

The criteria applied in this study for a mineral to qualify for the above category are as follows: (a) proven inertia during metamorphism and (b) distinctive textural features not reconcilable with a metamorphic mode of derivation.

Falling into the first group are the accessory minerals apatite, zircon and allanite. All these minerals are markedly euhedral in contrast to the anhedral and poikiloblastic textures displayed by the certifiably metamorphic minerals. In addition, these minerals have responded to deformation by granulation and do not show the annealed cracks displayed by metamorphic plagioclases and amphiboles.

The distinctions made under (b) are evidently more arbitrary than those in category (a). Belonging to this group are certain plagioclases in the syenites, which are large (3 cm), tabular crystals, often characterised by Carlsbad-albite twinning. With increasing deformation these grains become progressively granulated and resemble the ordinary metamorphic plagioclases.

In general the ilmenite and magnetite present in the rocks cannot be considered to be of igneous origin (although the original gabbro must have contained similar oxide phases), but peculiar ilmenite intergrowths observed in a number of samples (such as 303 and 109, see Plate I), where skeletal ilmenite grains meet at angles of 120° , are strongly reminiscent of the ilmenite exsolution along (111) in ulvöspinel that is often observed as a result of oxidation of the oxide phase in volcanic rocks (compare these textures, for instance, with those pictured by Lindsley et al., 1971, in their Plate 4A). The presence of so-called ilmenite domains in some hornblendes is taken to be indicative of the previous existence of a titaniferous pyroxene in these rocks, as will be explained in "Primitive Assemblage" in section 4.2. As the minerals from group (a) shed some light on the pattern of differentiation and the crystallisation sequence within the sill they will now be reviewed in some more detail.

Apatite

As can be seen from Figure 4.1 and Table 4A, apatite increases in modal abundance from the top of the sill downwards, only to decrease again in the syenites. This fact is also borne out by the chemical analyses, since a linear dependence of the modal apatite content on the P_2O_5 content of the rocks is to be expected. A general downward increase in size is also to be noted: thirty meters below the upper contact grains measuring 0.5×2.0 mm are common, whereas in the mafic pods just above the syenites (170 meters below the top) "giant" apatites more than 1 cm in length can be observed. In the syenites a marked downward decrease in both size and abundance of the apatite is apparent and the mineral disappears altogether in the leucosyenites. (With the exception of sample 210, where no apatite needles occur in the feldspar matrix, but a cluster of large, corroded apatites was seen in thin section. These grains are most reasonably interpreted as xenocrysts.)

Zircon

This mineral shows much the same distribution throughout the sill as apatite. Although far less abundant (only a few grains are generally present per thin section) in the mafic rocks, zircon attains quite respectable dimensions for rocks of such mafic character. Twenty meters from

the top of the sill sparsely distributed grains measure 0.2x0.8 mm and zircons of this size are generally present in all gabbroic facies of the sill. A general downward increase in zircon content of the rocks is to be noted, however. Especially in the mafic syenites zircon is an abundant accessory, averaging about 8 grains (0.3x1.0 mm and larger) per thin section. Towards the leucocratic syenites zircon again decreases in size, although its actual abundance (see Figure 4.1) does not change appreciably. In the quartz-bearing syenites, however, zircon is only sparingly found, in grains measuring 0.05x0.2 mm. In some samples rather large zircon grains enclosed small grains of apatite. This is taken to be indicative of the relatively late entry of zircon in the crystallisation sequence, and is in accord with our observation that the peak in modal abundance for zircon is reached when apatite abundance begins to tail off.

Allanite

Although a few small, scattered grains of allanite are present in the gabbroic rocks and the mafic syenites, this mineral is usually found as relatively large (1.0 mm in diameter) euhedral grains in the leucosyenites. Larger grains may show a fresh core and a metamict rim, but smaller grains are commonly wholly metamict. Some zircons can be found as inclusions in the allanite grains, indicating that

the latter was one of the latest phases to crystallize from the magma. Here it must be noted again that its greatest modal abundance is accordingly delayed, until the leucosyenite stage has been reached.

Sulfide minerals are nowhere very abundant, constituting only a fraction of the opaque minerals, but show a gradual increase in abundance toward the lower part of the sill and are of frequent occurrence in the mafic syenites. This would seem to corroborate Jennings' (1969) observation of sulfide-rich acid rocks associated with the lenticular gabbro bodies in southwest Faraday Township.

Relict igneous textures such as layering are obscured by gneissic metamorphic layering. It must be noted though that the mafic rocks at the top of the intrusion often display a remarkable banding (in sharp contrast with the syenites which are relatively homogeneous), with mafic and feldspar-rich laminae alternating. Where mafic and feldspathic bands are folded and contorted, often giving rise to feldspathic pods in the rock, apatite crystals are usually bent and broken in complete parallelism with the mafic stringers.

The observations presented above lead to the following synthesis, which is largely consistent with the model presented in the section on the chemistry of the rocks.

1. The gabbroic rocks consisted mainly of pyroxene, plagioclase and an oxide phase, which may have included both ilmenite and ulvöspinel. A regime of flow layering is suggested by the alignment of apatite prisms with the lithological banding. Size distribution of the accessory minerals is relatively uniform.

2. The size distribution and modal abundance of the accessory minerals are in accord with the conclusion, based on the chemistry of the suite, that the sill forms one differentiated sequence. The successive peaks in modal abundance of apatite, zircon and allanite in progressively more leucocratic rocks strongly support this conclusion, and are consistent with observations made on other differentiated suites.

3. In view of the mineralogical evidence to be presented in favour of a contact zone at the top and bottom of the sill, there can hardly be any doubt that the sill is indeed intrusive.

If, as is proposed here, the syenites are the result of in situ differentiation of a gabbroic intrusive, the conclusion is inescapable that the sill has been tectonically inverted. The writer is not aware of any mechanism of differentiation, which would result in the formation of an extensive syenitic differentiate at the bottom of a gabbroic mass.

4.2 Metamorphic Assemblages

In general three assemblages can be distinguished in any one rock. These will henceforth be designated as

- (a) the primitive assemblage;
- (b) the main metamorphic assemblage;
- (c) late metamorphic assemblages.

4.2.1 Primitive metamorphic assemblage

This assemblage, which is the earlier in terms of metamorphic evolution, is entirely distinguished on the basis of textural criteria. It is characterised, and this is its only truly distinctive feature, by stout, stumpy prisms of hornblende, which commonly show bluish-green colours and are characteristically littered with an abundance of small (0.02-0.05 mm), rounded blebs of ilmenite. These inclusions are usually aligned in irregular, linear patterns which bear no rational relationship to the amphibole lattice. Since these linear structures often intersect at right angles, the primitive hornblendes may be pseudomorphs after igneous, titaniferous clinopyroxenes.

The transition from the primitive assemblage to the main metamorphic assemblage may be summarised as follows: bluish-green colours in the hornblende give way to olivogreen colours in the rims of these grains and the slender,

small satellite prisms that usually surround or replace the large primitive grains (Plate II). Concomitant with this change in colour and size of the amphibole is a strong tendency for the ilmenite to collect into larger grains either in the quartz matrix outside, or in the amphibole grains themselves. This change is tentatively correlated with a prograde metamorphic event.

Primitive hornblende grains are present in most mafic rocks, with the exception of the syonites and the rocks occupying the upper 30 meters of the sill.

4.2.2 Main metamorphic assemblage

As outlined above, the main metamorphic assemblage is distinguished from the primitive assemblage mainly on textural grounds. This distinction is quite straightforward due to the discrepancy in size of the amphiboles characteristic for these assemblages, and the fact that the "primitive" hornblende contains ilmenite domains. The distinction from late, retrograde assemblages is much more difficult for the following reasons:

1. Detailed analysis of the phase assemblages shows that the changes from "main" to "retrograde" are continuous and gradational;

2. Partly as a result of (1), multiple generations of the same mineral, associated with different grades of

metamorphism, may be present in the same rock. A good example of this is the two generations of biotite commonly found. The later generation is usually accompanied by calcite, but not always. In the latter case it is very difficult to tell generation 1 from generation 2;

3. Since several main metamorphic assemblages are present as a result of the chemical variation in the sill and the country rock, it is very unlikely that every main metamorphic assemblage formed at the same point in time, making the term a very arbitrary one (assemblage 2 could be retrograde with respect to 1, etc.).

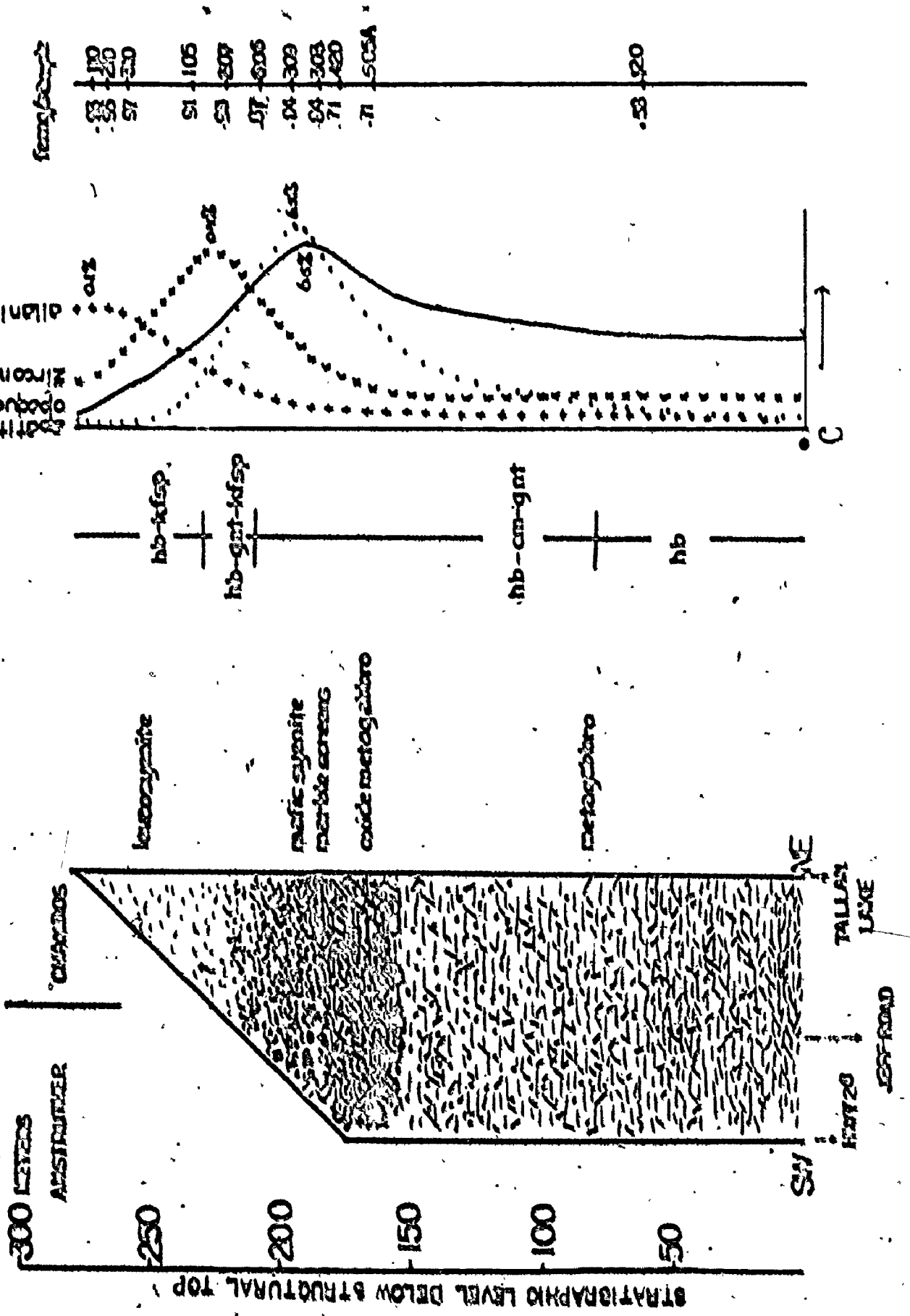
Even if it were desirable, it is clearly not possible to attempt a rigorous separation of the main assemblages and the retrograde ones. In the detailed description that follows, they are therefore treated together.

The following criteria were applied to distinguish stable coexistence of the minerals within the different multi-phase assemblages:

(a) Development of mutual, crystallographically rational, phase boundaries;

(b) Association of phases with a fixed plagioclase composition within an assemblage. Since reliable plagioclase compositions can be obtained with optical means, and such compositions, providing the bulk composition remain constant,

Figure 4.1 Stratigraphy (lithological, mineralogical, chemical) of the Tallan Lake sill.
Stratigraphic level in meters below the structural top of the sill



are generally acknowledged to reflect a certain metamorphic grade, much emphasis was placed on such associations (see Appendix 3);

(c) Textural criteria (grain size, habit, blastesis, etc.).

The following mineral associations, mainly formed in response to compositional changes within the sill (Figure 4.1), belong to the main assemblage:

- (1) Hornblende-plagioclase-ilmenite-quartz-biotite/sphene
- (2) Hornblende-plagioclase-cumingtonite-garnet-ilmenite-quartz-sphene
- (3) Hornblende-plagioclase-garnet/epidote-alkali feldspar-ilmenite-quartz-sphene
- (4) Hornblende-plagioclase-alkali feldspar-ilmenite-quartz-biotite.

In addition, magnetite is encountered in all but a few Tallan Lake samples.

4.2.2.a Assemblage 1

Hornblende-plagioclase-ilmenite-quartz-biotite/sphene

Since all assemblages seem to be mainly compositionally controlled, they form a crude means of establishing a stratigraphy within the sill (see Figure 4.1). The particular

Table 4A. Modal Analyses

	120	420	393	606	405	205	105	310	210	110	1317
Plagioclase	39.0	36.7	10.8	54.6	43.5	44.9	56.9	55.5	78.0	51.9	27.4
Hornblende	54.9	40.5	62.2	4.7	1.7	25.2	-	9.1	6.7	3.4	47.1
Cumingtonite	-	9.2	3.8	4.0	8.4	1.0	-	-	-	-	4.5
Cedrite	-	-	-	-	-	-	-	-	-	-	19.1
Garnet	-	0.1	0.9	5.5	0.1	1.0	-	-	-	-	-
Quartz	0.5	0.6	3.2	6.3	11.2	9.9	19.3	22.5	*	26.1	-
Opaque	4.2	4.5	5.7	2.5	3.8	1.8	0.6	1.6	*	*	1.9
Sphene	0.9	-	-	-	-	-	*	*	*	*	-
Calcite	*	1.0	3.2	4.0	3.3	4.2	4.7	0.6	*	1.4	-
Biotite	0.5	3.4	3.7	17.8	26.4	11.6	17.1	0.2	6.0	8.4	*
Alkali feldspar	-	-	-	-	-	-	*	10.2	8.5	8.0	-
Apatite	*	4.0	6.5	0.3	1.7	0.4	0.5	*	*	*	*
Zircon	*	*	*	0.1	*	*	0.1	*	0.2	0.2	-
Allanite	-	-	-	*	-	*	*	*	0.1	0.6	-
An & t	26/21+15	15+19/13	17/13	15+19/13/0	16/13	13+8/0	9/0	5/0	5/0	5/0	20+22
Assemblage	1	2	2	2	2	2	4	4	4	4	-
Points counted	639	859	844	870	850	850	808	834	850	859	729

- absent

* trace

† for designation of plagioclase composition see Appendix 3.

assemblage now under discussion constitutes the upper 80 meters of the sill.

As can be seen from Table 4A for specimen 120, which is more or less representative of the assemblage, hornblende is the main constituent mineral, usually accounting for 50-60% by volume of the rocks.

Hornblende is either accompanied by biotite or sphene, two minerals which display a definite antipathetic relationship toward one another (on a small scale only; they may both be present in the same hand specimen). The reason for the mutual incompatibility of sphene and biotite is not clear, although it seems that sphene appears in assemblages recrystallised under essentially isochemical conditions, whereas biotite results from the addition of potash.

Where a pre-existing hornblende contains ilmenite domains, the ilmenite inclusions are usually converted to sphene at the outer rim of the domain, and sphene clearly coexists* with the recrystallised hornblende, as is well illustrated in Plate II. The typical plagioclase composition coexisting with sphene is An_{26} - An_{28} . Of note is the reverse zoning in the plagioclase (see Appendix 3) often observed in rocks containing "primitive" hornblende.

Symplectic intergrowths of biotite and quartz are often seen in rocks not containing sphene. Biotite usually cuts across pre-existing hornblende grains and does not

*Whenever coexistence is discussed, equilibrium coexistence is implied, unless otherwise indicated.

appear to be aligned along the plane of foliation. The mineral has a distinctive "foxy" red colour suggestive of a high titanium content, an indication substantiated by its formation from ilmenite deduced from reaction textures. Plagioclase compositions coexisting with this sub-assembly vary considerably, but always the same composition is found in contact with biotite as well as hornblende, suggesting that the latter two are in equilibrium.

A second type of biotite, accompanied by calcite and little or no quartz and dull brown in colour, occurs embedded in plagioclase grains. Sharply delineated sodic rims (hereafter referred to as discontinuous zoning) surround the calcite and biotite grains, which are demonstrably later than either one of the sub-assemblages discussed above. The sodic rims are usually An_{16} in composition.

In those cases in which recrystallisation of the primitive assemblage has not been severe (e.g. 2217) plagioclase grains display well developed "triple points", indicative of a static mode of metamorphism. Plagioclase cores seem to reflect the composition attained during this event, ranging from An_{43} at the top of the sill, to around An_{20} at the base of the unit defined by assemblage 1. The lack of "primitive" hornblende with ilmenite domains at the top of the sill has already been discussed and must reflect

the absence of the phase (probably clinopyroxene) in the igneous assemblage from which this hornblende is postulated to have formed.

4:2.2.b Assemblage 2

Hornblende-cummingtonite-garnet-plagioclase-ilmenite-biotite-quartz

This assemblage underlies assemblage 1 and as a stratigraphic unit comprises approximately 130 meters of the sill. The main distinctive features are the presence of garnet and cummingtonite and the absence of aphenone, and a generally more pervasive recrystallisation relating to the main metamorphic event. The equilibrium coexistence of cummingtonite and hornblende appears to be well established. Homoaxial intergrowths of the two phases are omnipresent and the occurrence of exsolution lamellae of cummingtonite in hornblende and vice versa attest to stable coexistence over a certain range of temperature. Due to a recent upsurge in interest in coexisting amphiboles, many excellent descriptions of the textures exhibited by this amphibole pair have appeared in the literature (e.g. Ross et al., 1969; Jaffe et al., 1968). The interested reader is referred to these references for a description of textures not directly relevant to the present discussion.

Plate I

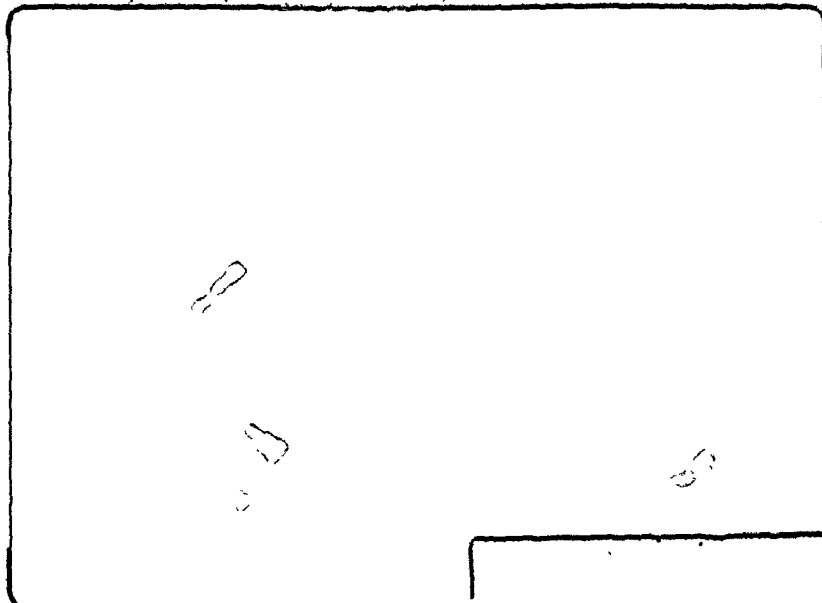
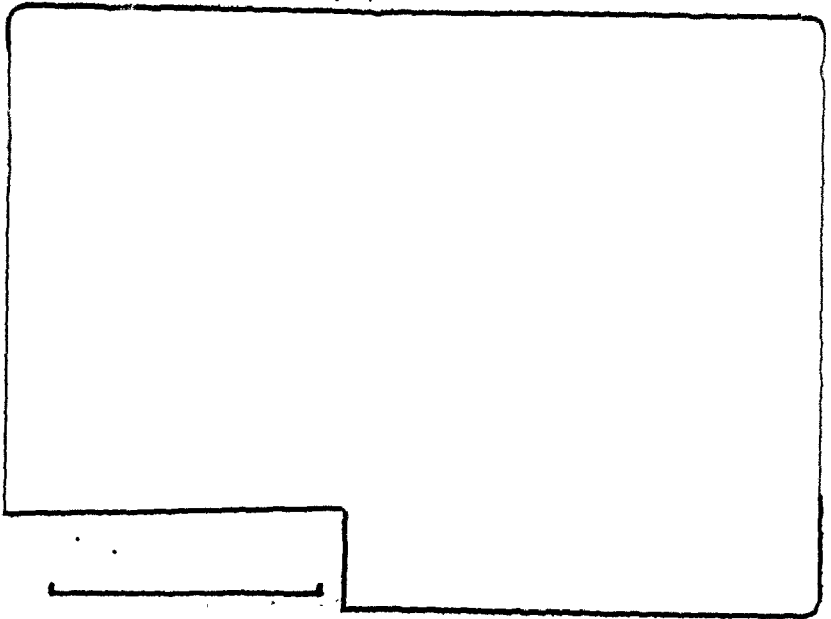
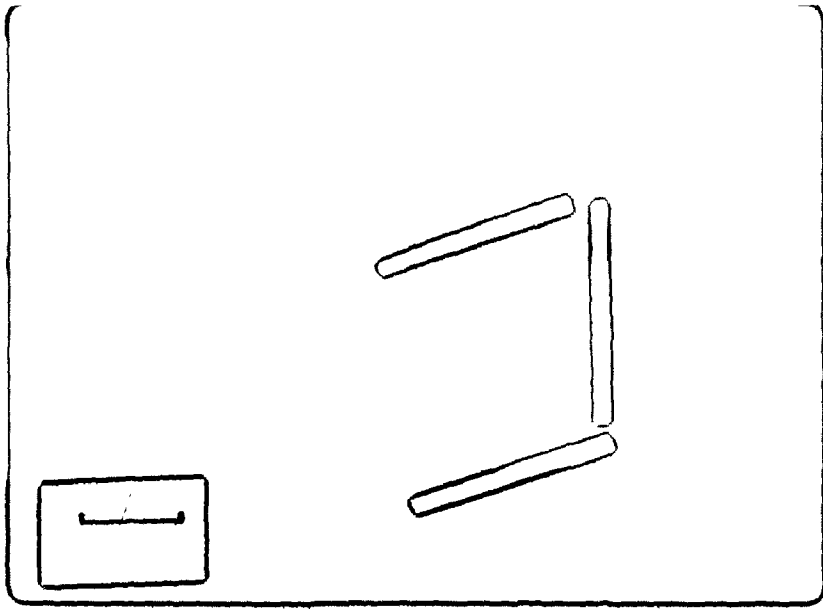
Possible ilmenite-sphene pseudomorph after ulvöspinel. Matrix consists of hornblende, plagioclase and quartz. Sample 109. Polarised light. (27.5x). In this, and all subsequent plates, the horizontal bar represents 0.5 mm.

Plate II

New growth of hornblende belonging to main metamorphic assemblage in a large grain from the primitive assemblage. Note ilmenite inclusions in latter (centre) and absence of these near new grain. Some sphene (high relief, upper and lower righthand corner) is present around new hornblende. Sample 609. Polarised light. (75x)

Plate III

Textures, suggestive of the reaction $hb + qtz \rightarrow em + plag$. Note that cummingtonite (bright green) only occurs adjacent to quartz grains, and optical continuity of quartz (white, left of centre) in three separate grains, suggesting extensive replacement. Sample 111. Crossed nicols. (75x)



Equilibration of garnet with the amphiboles is harder to demonstrate since the minerals are usually not closely associated, garnet being restricted to the more plagioclase-rich parts of the rock. The first appearance of both cummingtonite and garnet at the same stratigraphic height within the sill, about 80 meters from the top, the close association with cummingtonite in those instances where garnet has resulted from reaction with hornblende, and the lack of resorption textures, make it highly probable that garnet was indeed in equilibrium with both amphiboles. This, of course, does not imply that garnet formation might not initially have preceded cummingtonite formation or vice versa.

As with assemblage 1 several sub-assemblages can again be distinguished.

In those cases, very few in number where biotite is absent, garnet is often seen in direct contact both with ilmenite and hornblende. Cummingtonite is clearly a reaction product of the reaction with hornblende producing garnet, but also is formed by the reaction of calcic amphibole with quartz (see Plate III), suggesting the type of reaction proposed by Shido (1958). Plagioclase is invariably reversely zoned from An_{16} - An_{19} with an abundance of rounded quartz inclusions, predominantly in the sodic core. Magnetite is characteristically present in minor

amounts.

Rocks containing large amounts of biotite are mainly restricted to the western part of the area (traverses 117 - 4917, 120 - 606, 905 - 105) although a general increase in biotite content is also to be noted toward the more syenitic differentiates.

Biotite flakes, dull, dark brown in colour, are characteristically aligned along ilmenite-rich zones and display no obvious reaction relation with the poikiloblasts of hornblende surrounding these zones. In general no calcite is associated with these biotites. Quartz and reversely zoned plagioclase ($An_{16}-An_{19}$) littered with quartz inclusions beside garnet and cummingtonite complete the assemblage. As is the case with assemblage 1, no preferred orientation of the biotite is evident, although the zonal arrangement around ilmenite grains, which themselves are aligned along the foliation plane, produces the semblance of a preferred orientation in many cases. In samples untouched by the late calcite-biotite association no separate grains of cummingtonite are present, and the latter only appears as exsolution lamellae in hornblende. It would thus appear that garnet and biotite are formed at a temperature higher than that at which the coexisting hornblende intersects the hornblende-cummingtonite solvus.

Comparison of biotite-rich rocks with those from

the Duck Lake Dome which do not contain early biotite or, for that matter, any other potash-rich phase such as alkali feldspar, strongly suggests that the potash needed to form biotite was introduced through the fluid phase.

The biotite-calcite association is again of late origin and is present in most rocks comprising the assemblage. Discontinuous zoning in the plagioclase is correlated with the presence of these two minerals (as is well illustrated in Plate IV), the sodic rim being usually An_{13} - An_8 in composition, around a basic core (again An_{16} - An_{19}), although small portions of the rim may be pure albite. In the latter case very thin lamellae may be observed within the albite having a higher relief and intersecting the albite law twinning plane at approximately 14° . There is little doubt that these are peristerite lamellae along (081). Often the interface between the plagioclase core and the sodic rim is aligned along the same plane, as can be seen again in Plate IV.

Hornblende and garnet stability and growth extend part of the way into the conditions defined by the biotite-calcite association, as seen by their relation with sodic plagioclase rims. If large amounts of biotite are present, this can lead to the eventual disappearance of hornblende, the reaction products being calcite, biotite and cumingtonite. Garnet growth is in most cases enhanced by biotite

growth, depending, of course, on the availability of alumina. Large porphyroblastic garnets contain in some cases biotite flakes which are smaller than the ones occurring outside the garnets. Pre-emption of garnet growth is indicated by the occurrence of garnets, intergrown with quartz and calcite, of which only the rim is complete (see Plate V). Preliminary results from X-ray diffraction patterns indicate that the garnet is nearly pure almandine.

As is to be expected, early biotite cannot be distinguished from the biotite associated with calcite in the majority of rocks which contain a mixed biotite population. Rather, it would seem to relate to a continuous event whereby the fluid becomes increasingly impoverished in carbon dioxide. The large variations in calcite-biotite ratio observed appear to indicate that the potassium content of the fluid varied considerably from place to place, whereas the initial CO_2 content was reasonably constant (e.g. see modal analyses 105, 205 and 405 in Table 4A). An insight into the temporal relationships between assemblages 1 and 2 is afforded by sample 605B. "Primitive" hornblende grains are present in which the inclusions associated with the ilmenite domains have largely been converted to sphene. Rather small, compact satellite grains of hornblende can in all probability be correlated with the development of sphene. These grains in turn are surrounded by larger, distinctly

poikiloblastic amphibole grains which contain exsolved cummingtonite lamellae. Separate grains of cummingtonite are always found to be associated with biotite, calcite and albite. It would thus appear again that the development of biotite and hornblende, on the one hand, and sphene and hornblende, on the other, are mutually exclusive. In many cases the hornblende-cummingtonite association must be retrograde with respect to assemblage 1.

4.2.2.c Assemblage 3

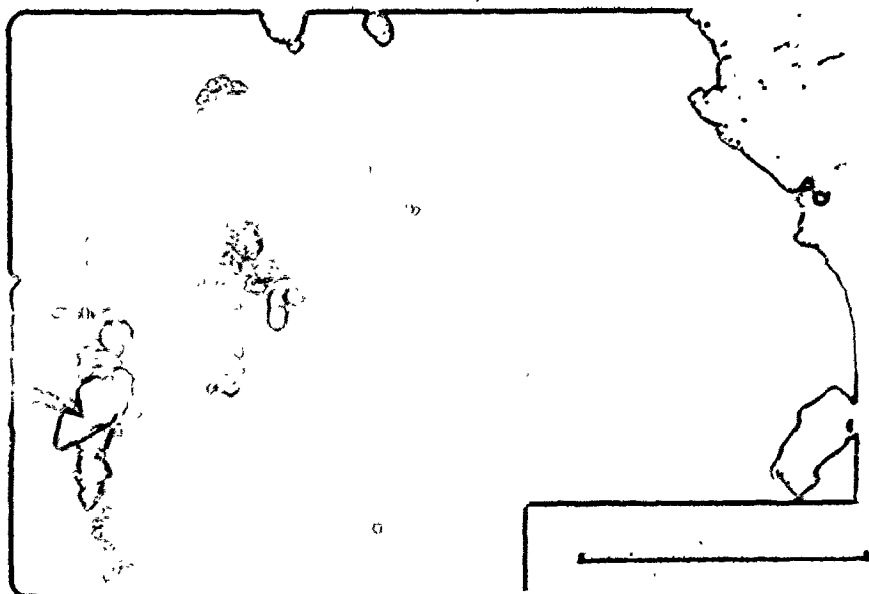
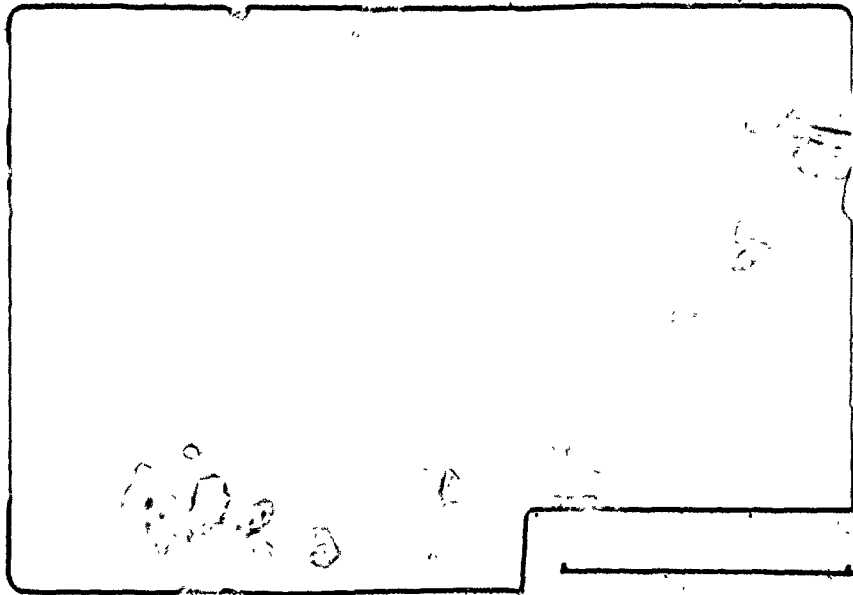
Ferrohastingsite - garnet - plagioclase- alkali feldspar - ilmenite - quartz (-epidote)

This assemblage is restricted only to the intermediate syenites and the stratigraphic unit reaches a maximum thickness of 30 meters in the Duck Lake Dome. The assemblage is absent in the western part of the Tallan Lake Sill proper, because of the absence of intermediate syenitic differentiates. Directly adjacent to the country rock marbles at the lower contact is a thin zone, underlying leucosyenites, in which assemblage 3 reappears as indicated by samples 109 and 69-29-3. This may be due to the fact that some marble was assimilated at the lower contact, or that the original roof rocks, (of an inverted sill) were somewhat more mafic than the syenites they envelop. Since the plagioclase is

Plate IV Discontinuous zoning in plagioclase, against biotite. Note the straight boundary, separating An₁₆ (black, right centre) from An₁₃ (dark grey, left of centre), which follows the peristerite exsolution plane (081). Sample 209. Crossed nicols. (75x)

Plate V Euhedral atoll garnet (black, with hexagonal outline), the core of which is filled with quartz and calcite. Sample 205. Crossed nicols. (75x)

Plate VI Peristerite exsolution in plagioclase. Note the opposite orientation in albite twins, and the fact that alteration zones around K-feldspar, consisting of pure albite, are free of peristerite lamellae. Garnet (black, directly below K-feldspar) is probably being resorbed and epidote (high relief, pink, centre photo) is being formed. Sample 69-29-3. Crossed nicols. (75x)



very sodic in all cases the latter interpretation is favoured.

The pleochroism of the amphibole (X - light green; Y - dark olive-green; Z - nearly opaque, dark blue-green), its $2V$ ($2V_x = 40^\circ - 20^\circ$), and its large b-spacing (see Appendix 5) all indicate that we are dealing with ferro-hastingsite. Grains may be compact or poikiloblastic, the former being texturally early grains.

Garnet is usually present as compact, small grains, quite often along alteration zones in plagioclase. These alteration zones normally contain albite, but sometimes alkali feldspar is present as well. In cases where moderate amounts of alkali feldspar are present, this mineral always replaces plagioclase (Plate VI), and alteration zones always seem to emanate from the alkali feldspar centre. In some instances epidote is present in these alteration zones as well, and may therefore be included in the assemblage.

An interesting aspect of the alteration induced by the introduction of alkali feldspar is the development of a "herringbone" structure in adjacent albite twins of the plagioclase (Plate VI), identical to textures described by Appleyard (1969). In sections cut perpendicular to the a-axis, lamellae intersect the (010) plane at 14° . It is clear that the alteration has served to emphasize the peristerite exsolution.

In the western part of the region, alkali feldspar and epidote have never been observed and biotite is abundant. It is probable that hornblende and K-feldspar reacted to form biotite and calcite. Late biotite and calcite with associated sodic plagioclase rims are best observed in the eastern part of the region, whereas a mixed biotite population is present in the western part. Again, sphene may be present when early biotite is lacking (e.g. 109), although this is not common. Reappearance of sphene seems indicated in those (retrograded) rocks where all hornblende has been replaced by biotite and garnet is absent (e.g. 105). It is accompanied by magnetite in this case.

4.2.2.d Assemblage 4

Ferrohastingsite - plagioclase - alkali feldspar - sphene - magnetite - quartz

Rocks comprising this assemblage include the leucosyenites and quartz-syenites around Clydesdale Lake and Tallan Lake. The thickness of the assemblage never exceeds 50 meters. Biotite is always associated with calcite and, when present, amphibole is no longer stable. Late biotite is green in colour (possibly rich in ferric iron) and associated with muscovite and calcite (Plate VII).

Plagioclase is very sodic (An_9), but attains pure albite composition when associated with muscovite. Alkali feldspar often replaces plagioclase, but is not necessarily introduced through the fluid phase, although remobilisation appears evident.

Sphene and magnetite are stable throughout the various retrograde assemblages.

4.2.3 Very late retrograde textures

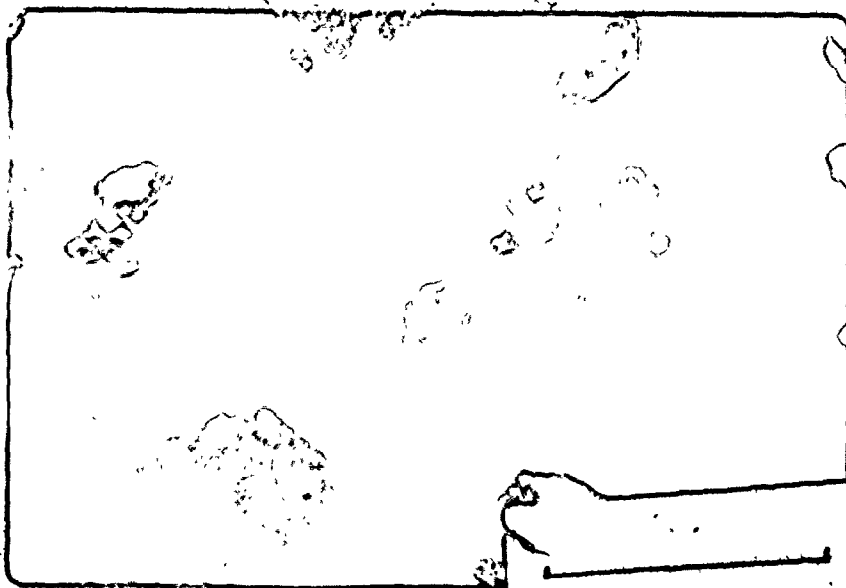
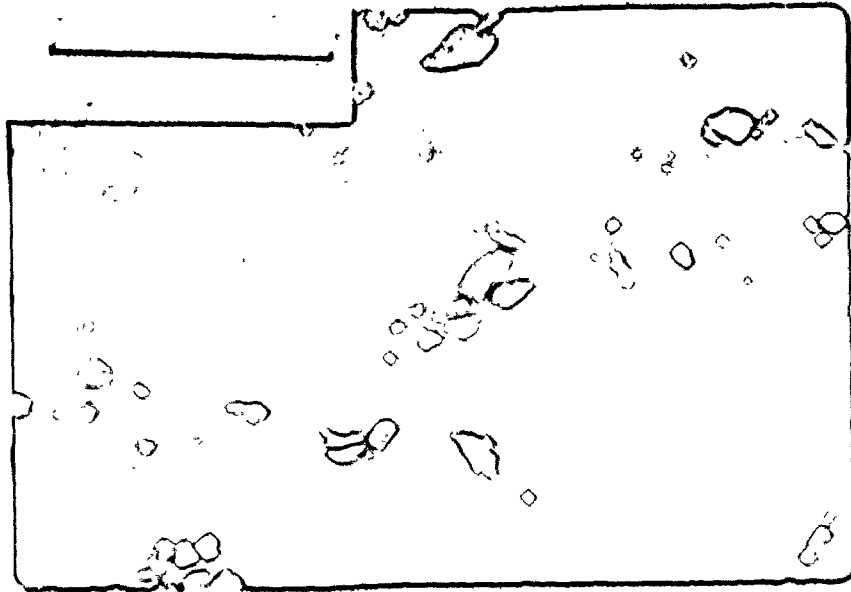
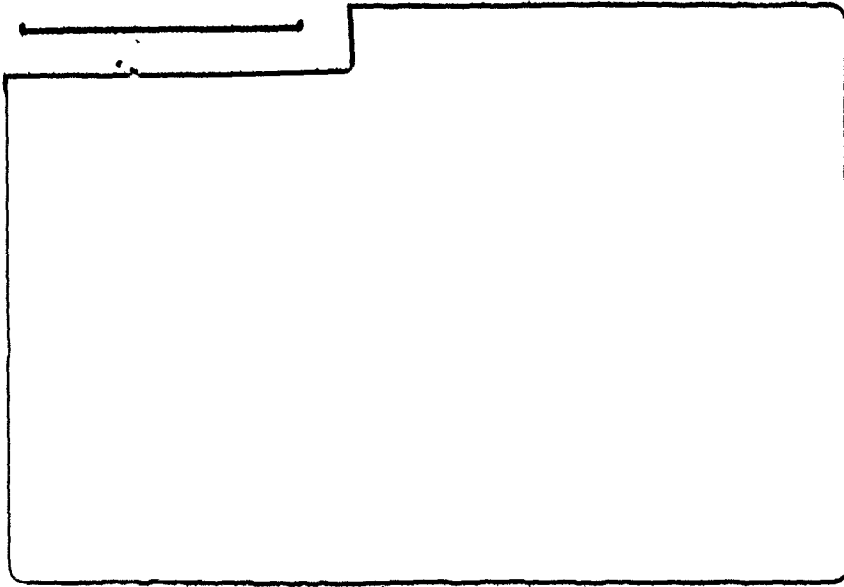
In many samples micro-fractures cutting all metamorphic minerals can be found. Often these fractures are filled with calcite. In sample 105 one such fracture cuts all minerals except for quartz and late albite. This, in the writer's opinion, indicates that the metamorphic fluid contained appreciable amounts of silica and alkalis, besides CO_2 , and is the principal reason why such reliance was placed on the plagioclase composition associated with certain metamorphic minerals in constructing the various assemblages, and why the mantling of ilmenite with silica in assemblage 1 (also a common feature in the other assemblages) was considered a sign of relative reactivity.

Although granulation is mainly related to the stratiform foliation in the rocks, and in other cases to the growth of garnet, some mylonite zones in rocks collected

Plate VII Muscovite-calcite intergrowth suggestive of the reaction $An + Kfs + CO_2 \rightleftharpoons Ms + cc + qtz$. Note how calcite replaces former plagioclase (below centre). Sample 219. Crossed nicols. (75x)

Plate VIII Micro-mylonite zone with sheared biotite. Sample 719A. Crossed nicols. (75x)

Plate IX Epidote (dark green, left of centre and blue-green, upper right corner) coexisting with calcite, sodic plagioclase (rims around more calcic cores) and tremolite (brighter coloured parts of basal sections, left centre) in leucodiorite dyke. Sample 2617. Crossed nicols. (75x)



north of Tallan Lake are clearly younger (since they cut the foliation), and are undoubtedly related to the Pratt's Creek Fault. Extreme granulation of plagioclase and quartz is evident along these zones and some grains of biotite are cut and displaced relative to each other, as is well illustrated in Plate VIII.

4.2.4 Other assemblages, country rocks

No meaningful correlation of the metamorphic relations established for the ortho-amphibolites with those for the country rocks appears possible at present, due to the paucity of the latter in the writer's collection. They will, therefore, only be discussed briefly.

Mention should be made of the assemblages present in a leucodiorite dyke which cuts the sill (at a very low angle) in the roadcut at Highway 28. Relict igneous clinopyroxene is present, and although it is tempting to correlate this dyke with the leucosyenites with which it has several features in common, its relation to the sill is uncertain.

Hornblende (after pyroxene), plagioclase and sphene are early, whereas a late association of epidote, plagioclase (more sodic), alkali feldspar, calcite, tremolite, magnetite and quartz, is also present. Hornblende appears to be

unstable with respect to tremolite (Plate IX). Assemblages in the country rock can be divided into two: (a) calc-silicate assemblages and (b) amphibolite assemblages.

(a) calc-silicate assemblages

The dominant assemblage is diopside-calcite-plagioclase-quartz-sphene. Retrograde with respect to the dominant assemblage is the assemblage calcite-tremolite/actinolite-plagioclase-quartz. In some instances late talc fibres surround the diopside grains. Careful optical study seems to indicate the complete absence of dolomite.

In more pelitic compositions the assemblage calcite-quartz-alkali feldspar-plagioclase-biotite-sphene is present. This assemblage is apparently time-equivalent to the tremolite-bearing one in the subalkaline calc-silicate rocks.

Calc-silicate skarns associated with the sill around Clydesdale Lake provide quite a different metamorphic record. Skarns of this type are nearly completely silicated, although obviously derived from marbles: this is a compelling argument to ascribe them to contact effects related to the intrusion of the sill. One such skarn (69-29-2) was found to contain diopside and the alteration products of forsterite (Plate X), and a mineral that fills the interstices between these two and was identified as axinite, as

the principal minerals that can be attributed to the contact metamorphism. Grossularite, calcite, sphene and anorthitic plagioclase complete this contact assemblage.

(b) amphibolite assemblages

Descriptions of these assemblages all relate to a 20 meter thick sequence of so-called feather amphibolites which are found adjacent to the upper contact of the sill in the roadcut at Highway 28.

The simple assemblage plagioclase-hornblende-ilmenite-sphene-quartz is present in most of these rocks, although the introduction of potash leads to the development of biotite, calcite and cummingtonite, as is the case with the ortho-amphibolites, with the difference that garnet is nowhere observed.

In close proximity to the sill the following rapid succession of assemblages is observed:

- (1) plagioclase - quartz - hornblende - cummingtonite -
ilmenite - biotite - calcite (1217)
- (2) plagioclase - hornblende - cummingtonite - gedrite -
ilmenite - biotite (1317)
- (3) plagioclase - hornblende - gedrite - ilmenite -
biotite (1417)
- (4) plagioclase - hornblende - ilmenite (1517)

In addition to the tremendous reduction in the number of phases from 7 to 3, a decrease in the size of the amphiboles from more than 3 mm in sample 1217 to less than 0.4 mm in sample 1517, is to be noted. Sample 1517, which is less than 1 meter removed from the contact with the sill, also has a distinct hornfelsic texture and the rock displays irregular cracks, filled with plagioclase and apatite, much the same as dessication cracks in mud. All the changes from a normal, porphyroblastic feather amphibolite to the dense hornfels occur within 5 meters from the contact with the sill.

The three amphibole assemblage, gedrite/anthophyllite-hornblende-cummingtonite, has only recently been described in the literature (e.g. Robinson et al., 1969) and it is therefore important to investigate whether equilibrium coexistence is indicated in this case.

Results from Buerger precession photographs summarised in Appendix 5 indicate that the optical identification of the dark tan ortho-amphibole as gedrite is warranted. Gedrite often enclosed cummingtonite, a texture that is apparently often observed whenever these two coexist (e.g. Robinson and Jaffe, 1969), although the enclosures are typically "open ended", and both phases are in contact with plagioclase. Two-phase grains of hornblende and cummingtonite, both displaying mutual exsolution, are also common, and grains

Plate X.

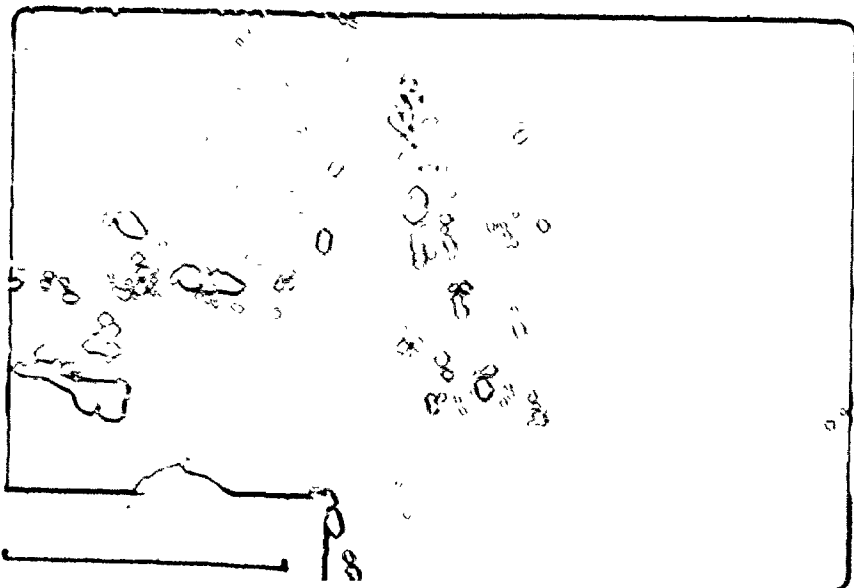
Relict forsterite (brownish areas) in grossular (black, euhedral outlines) - diopside (bright coloured) skarn. Some axinite (medium grey, lower relief than diopside, above centre), plagioclase and quartz form the matrix of the skarn. Sample 69-29-2. Crossed nicols. (75x)

Plate XI

Homoaxial intergrowth along c-axis of gedrite (tan coloured, 2 areas surrounding cummingtonite), cummingtonite (colourless) and hornblende (green) in a single amphibole grain. Note the exsolution of cummingtonite, visible as very fine lamination, along $(\bar{1}01)$ in hornblende. Sample 1317. Polarised light. (75x)

Plate XII

The same grain as in Plate XI. Note the straight extinction of gedrite. Sample 1317. Crossed nicols. (75x)



containing hornblende and gedrite, although least common, have also been observed. The case for equilibrium coexistence of the three amphiboles is made virtually complete by the observation of three-phase grains, a fine example of which is pictured in Plate XI.

The decrease in the number of phases and corresponding decrease in grain size toward the contact are interpreted to mean that the dry rocks close to the contact were less accessible to the metamorphic fluid than rocks at a certain distance.

(c) assemblages containing scapolite

Scapolite is of common occurrence in the country rock marbles and amphibolites, and was also observed in several samples from the sill. The mineral invariably replaces plagioclase and usually islands of plagioclase with the same crystallographic orientation can be observed in the scapolite mass. In one instance (717) distinctly porphyroblastic scapolite was observed in a silicate marble, closely associated with large porphyroblastic diopside (Plate XIII). In all marbles tremolite appears to postdate the introduction of scapolite. In samples from the sill (assemblage 1) scapolite is associated with biotite (with foxy-red colour) and sphene. Its introduction appears to postdate the mineral foliation.

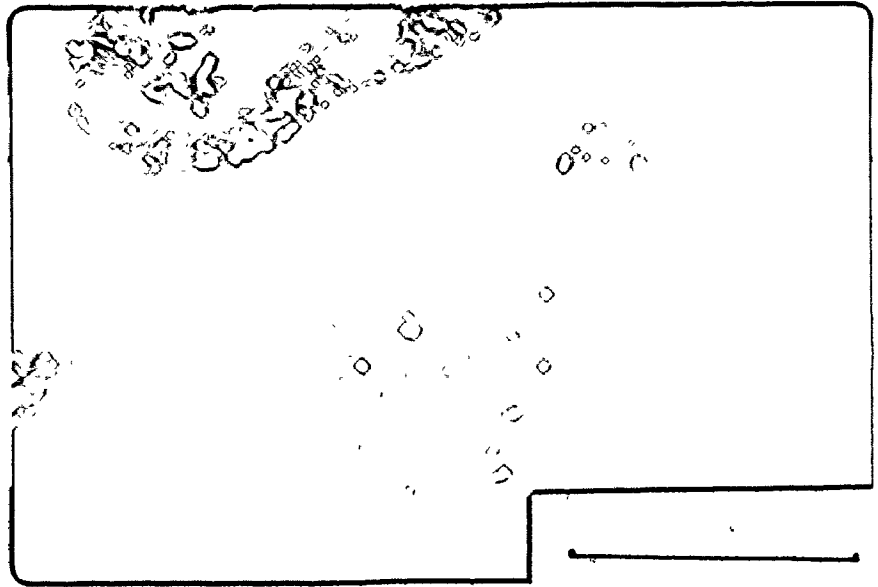
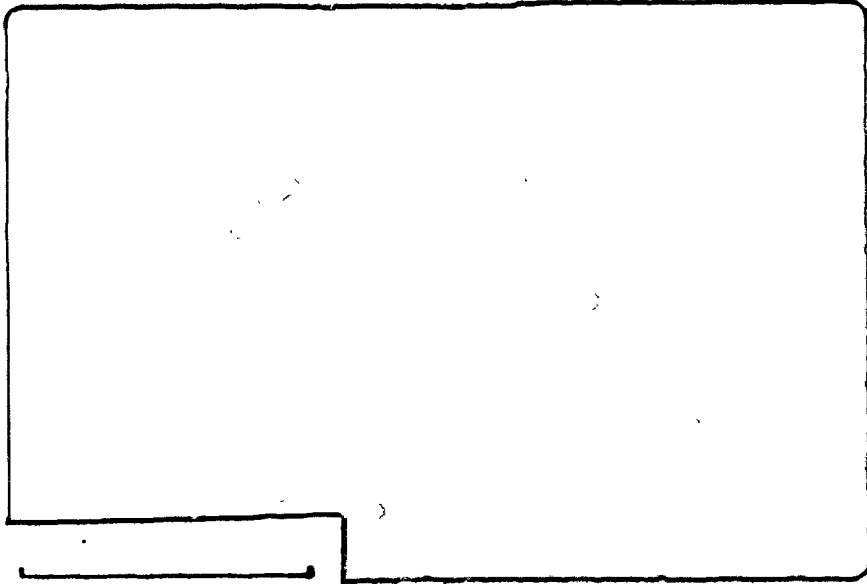
(d) assemblages in granitic dykes

Granitic dykes are frequent in the western part of the area, but are present in other parts of the area as well. They are non-foliate in nature and in places distinctly pegmatitic. Their main constituents are plagioclase and quartz. Alkali feldspar may be abundant or entirely lacking. Although the number of samples is too limited to be definite, the abundance of alkali feldspar seems to be related to the thickness of the dyke, small dykes containing no K-feldspar. The contact between rocks from the sill and the granitic dykes is always marked by a thin zone (about 1 cm thick) in which hornblende is completely converted to biotite. For some distance biotite is still very abundant in the amphibolite, with the mineral displaying the same characteristic colour as the early biotite typical for that assemblage (red in assemblage 1, dull brown in assemblages 2 and 3). Furthermore, it appears that the more alkali feldspar is present in the dyke, the less biotite is present in the surrounding rock. It is, therefore, concluded that the intrusion of granitic dykes (which cut the foliation) was coincident with the development of the early biotite in the main metamorphic assemblages. Retrograde metamorphism in the dykes is essentially the same as that observed in assemblage 4. Biotite breaks down to muscovite and magnetite, which are

Plate XIII Poikiloblastic development of diopside (high relief, centre, left and righthand side of photo) embedded in scapolite (yellowish and blue-green colours) in a matrix of quartz and plagioclase. Sample 717. Crossed nicols. (75x)

Plate XIV Poikiloblast of cummingtonite, enclosing quartz grains, and calcite grain (upper left corner), embedded in hornblende (dark), suggestive of the reaction $hb+CO_2 \rightleftharpoons cm+qz+cc+H_2O$. Note the density of hornblende exsolution lamellae (lamination) in cummingtonite. Sample 305. Crossed nicols. (75x)

Plate XV Biotite-quartz-calcite symplectites formed through the breakdown of hornblende (inclusions in central biotite grain). Note the general absence of K-feldspar adjacent to biotite, suggesting the reaction $Kfsp+hbl+CO_2 \rightleftharpoons bi+cc+qz$. Sample 110. Crossed nicols. (27.5x)



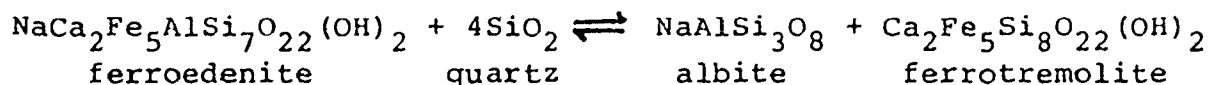
often accompanied by calcite. Late calcite and quartz veins, as in sample 105, are present, while chlorite was also observed. Typical for the pegmatitic phases of the granite dykes is the occurrence of large, dark greenish-brown tourmaline crystals, probably similar to the ones associated with the Silent Lake Pluton reported by Breaks (1971). Tourmalines occurring as an indigenous phase in the leucosyenites are always very small and have a characteristic blue colour. Tourmalinisation of some sill rock with large brown tourmalines is, therefore, probably related to the granite dykes, whereas the occurrence of axinite in skarns may have been the product of boron metasomatism from within the sill. Whether scapolitisation can be attributed to the intrusion of the granite dykes is uncertain, but remains a possibility.

4.3 Metamorphic Reactions

4.3.1 Assemblages

Assemblages contained in the Tallan Lake Sill that are believed to be equilibrium assemblages, are listed in Table 4B, in approximate order of iron enrichment. A broad distinction can be made between biotite-bearing assemblages and those that do not contain this mineral. This is believed to be due to introduction of potassic fluids from

granitic dykes into some parts of the Tallan Lake Sill, as explained in an earlier section. If we also take into account the late metamorphic, carbonate-bearing assemblages, it may be concluded that all assemblages encountered can be represented in the 11-component system K-Na-Ca-Fe-Mg-Al-Ti-Si-O-H-C. It is probable, however, that the component Na may be neglected in the presence of quartz. Noting that edenite substitution in the hornblende can be represented as



it is apparent that elimination of Na as a component only leads to elimination of the activity of albite in the system as a variable. With the removal of Na, we are left with 10 components in a system in which P, T, f_{O_2} , $f_{\text{H}_2\text{O}}$, f_{CO_2} and the activity of the soluble potash component (a_K) must be rated as important variables. It can be seen from Table 4B that in only one assemblage are all these variables independently variable. In terms of the Gibbs Phase Rule it may be noted that no assemblage is less than divariant, i.e. P and T are independently variable, which in itself is good evidence that equilibrium was maintained throughout the metamorphic episode. Data on mineral compositions are needed, however, for a rigorous demonstration of equilibrium.

Table 4B. Some Parageneses in the System K-Na-Ca-Fe-Mg-Al-Ti-Si-O-H-C

Assemblage	Solid Phases	Probable Independent Variables
Assemblage 1	hb-plag-qtz-ilm-mt	$a_{K^+}, f_{O_2}, f_{H_2O}, f_{CO_2}, P, T$
	hb-plag-qtz-ilm-mt-sph	$a_{K^+}, f_{H_2O}, f_{CO_2}, P, T$
	hb-plag-qtz-ilm-mt-bi	$f_{O_2}, f_{H_2O}, f_{CO_2}, P, T$
Assemblage 2	hb-plag-qtz-ilm-mt-bi-cq	f_{O_2}, f_{H_2O}, P, T
	hb-cm-gnt-plag-qtz-ilm-mt	a_{K^+}, f_{CO_2}, P, T
	hb-cm-gnt-plag-qtz-ilm-mt-bi	f_{CO_2}, P, T
Assemblage 3	hb-cm-gnt-plag-qtz-ilm-mt-bi-cc	P, T
	hb-gnt/ep-plag-kfsp-qtz-ilm-mt-sph	f_{CO_2}, P, T
	hb-gnt-plag-qtz-ilm-mt-bi-cc	f_{H_2O}, P, T
Assemblage 4	hb-plag-kfsp-qtz-ilm-mt-bi	f_{CO_2}, f_{H_2O}, P, T
	plag-kfsp-qtz-ilm-mt-sph-bi-cc	f_{H_2O}, P, T
	plag-qtz-ilm-mt-sph-bi-ms-cc	f_{H_2O}, P, T

It is also useful to remark on the limitations imposed upon the assemblages by the Gibbs Phase Rule. It can be seen (Table 4B) that both f_{O_2} and f_{H_2O} in the assemblage hornblende-cummingtonite-garnet-plagioclase-quartz are apparently buffered. The regular variation in the extinction angle γ/c of cummingtonite with chemical variation in the sill, is probably a direct result of the limited variance of this assemblage.

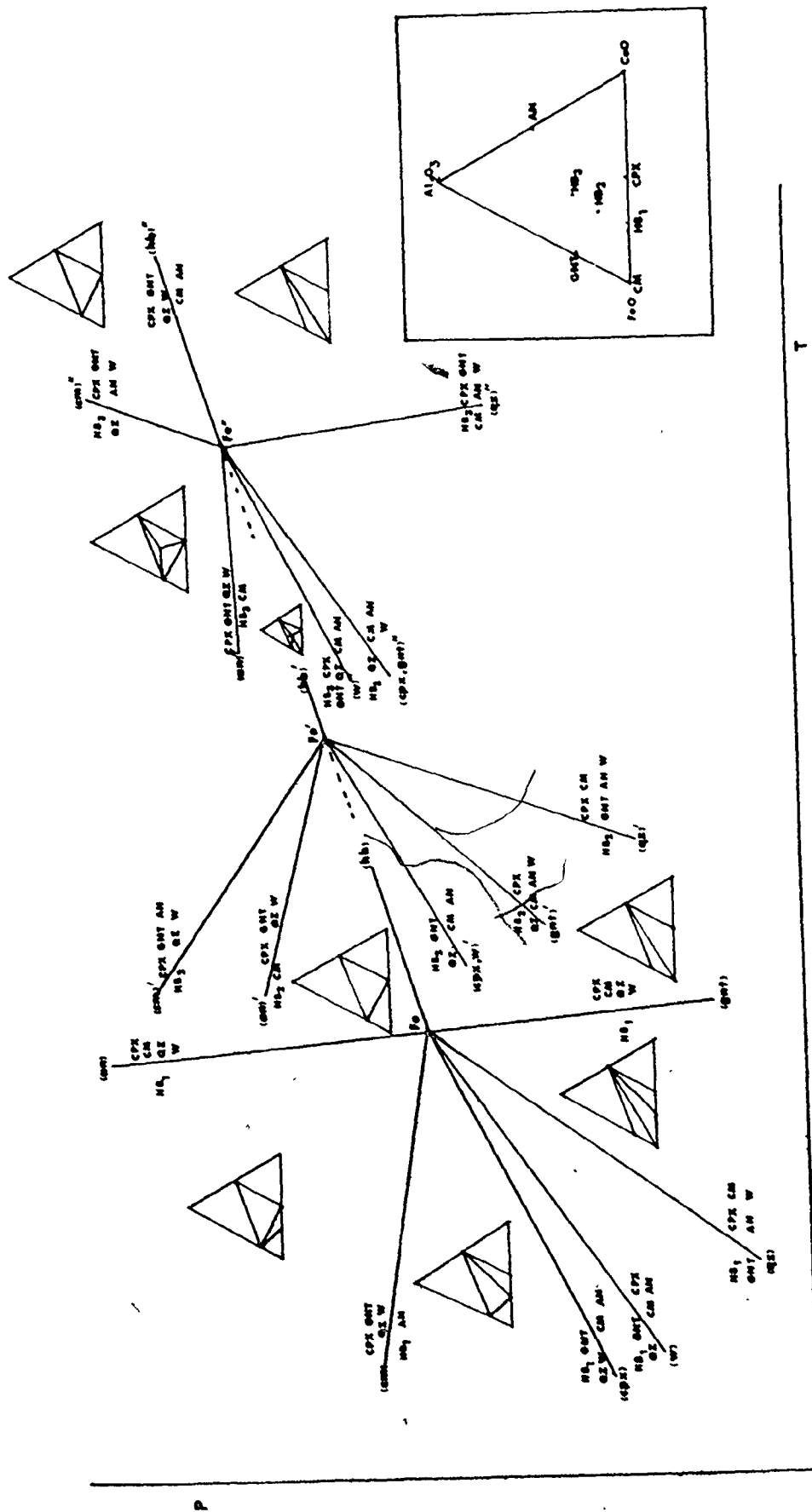
4.3.2 Reaction relations between cummingtonite and hornblende

In order to make a qualitative assessment of the significance of the garnet-hornblende-cummingtonite paragenesis from the Tallan Lake Sill, a petrogenetic grid for part of the system $CaO-FeO-Al_2O_3-SiO_2-H_2O$, involving the phases (ferrotremolite-ferrotschermakite)-hedenbergite-grunerite-almandine-anorthite-quartz-water was prepared. The choice of these minerals stems from the fact that clinopyroxene is the dominant ferromagnesian mineral accompanying cummingtonite and hornblende in low-pressure metamorphic terrains, such as the Abukuma Plateau, while garnet is prominent in intermediate-pressure environments (e.g. Ernst, 1968; Robinson and Jaffe, 1969; Hietanen, 1973). Due to the limited amount of thermodynamic data on these

Table 4C. Summary of symbols and minerals used in mineral reactions

hb ₁	ferrotremolite	$\text{Ca}_2\text{Fe}_5\text{Si}_8\text{O}_{22}(\text{OH})_2$
hb ₂	ferrohornblende	$\text{Ca}_2\text{Fe}_4\text{Al}_2\text{Si}_7\text{O}_{22}(\text{OH})_2$
hb ₃	ferrotschermakite	$\text{Ca}_2\text{Fe}_3\text{Al}_4\text{Si}_6\text{O}_{22}(\text{OH})_2$
cm	cummingtonite	$\text{Fe}_7\text{Si}_8\text{O}_{22}(\text{OH})_2$
cpx	hedenbergite	$\text{CaFeSi}_2\text{O}_6$
gnt	almandine	$\text{Fe}_3\text{Al}_2\text{Si}_3\text{O}_{12}$
an	anorthite	$\text{CaAl}_2\text{Si}_2\text{O}_8$
kfsp	K-feldspar	KAlSi_3O_8
bi	annite	$\text{KFe}_3\text{AlSi}_3\text{O}_{10}(\text{OH})_2$
sph	sphene	CaTiSiO_5
ilm	ilmenite	FeTiO_3
mt	magnetite	Fe_3O_4
qz	quartz	SiO_2
w	water	H_2O
cc	calcite	CaCO_3
ms	muscovite	$\text{KAl}_3\text{Si}_3\text{O}_{10}(\text{OH})_2$
ep	epidote	$\text{Ca}_2\text{FeAl}_2\text{Si}_3\text{O}_{12}(\text{OH})$

Figure 4.2 Petrogenetic grid involving the phases (ferrotremolite-ferrotschermakite)-cummingtonite-hedenbergite-almandine-anorthite-quartz-water. Mineral parageneses are projected through SiO_2 onto the Al_2O_3 -CaO-FeO plane (see inset) and apply only to quartz-bearing assemblages. Invariant points Fe, Fe' and Fe" are $(\text{cc}, \text{CO}_2, \text{hb}_2, \text{hb}_3)$, $(\text{cc}, \text{CO}_2, \text{hb}_1, \text{hb}_3)$ and $(\text{cc}, \text{CO}_2, \text{hb}_1', \text{hb}_2)$ of Appendix 4(b) respectively. PT coordinates are arbitrary, but 25° on the horizontal scale equals 1 kb on the vertical scale. Slopes of reactions calculated for assumed P and T of 5 kb and 625°C (see Appendix 4).



minerals, the petrogenetic grid was constructed using the geometric approach of Schreinemaker's (cf. Zen, 1966). Hence, the resulting diagram is entirely qualitative and not fixed in P-T space. It is to be noted, for instance that, as only the slopes for the reactions are correct, units along the P and T axes of Figure 4.2 are arbitrary, with the only requirement that 25°C along the T-axis equals 1 kb along the P-axis.

All univariant reactions, together with values for their P-T slopes are listed in Appendix 4. Slopes for these reactions were computed from the relation $dP/dT = \Delta S/\Delta V$, using entropies calculated for an assumed pressure and temperature of 5 kb and 900°K (=627°C), respectively.

Entropies for the various minerals are also given in Appendix 4 and were calculated as follows:

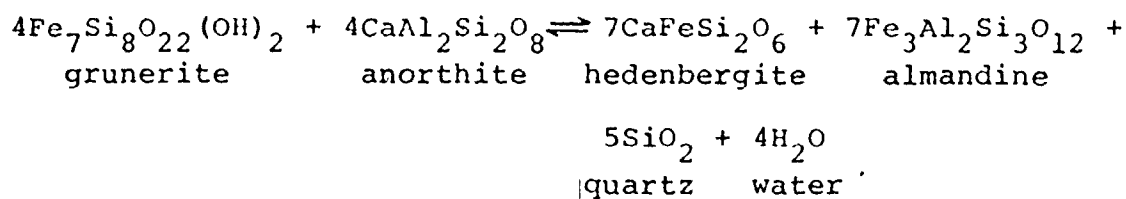
1. Assume that the difference in entropy between $\text{CaAl}_2\text{SiO}_6$ and $\text{CaMgSi}_2\text{O}_6$ represents a fair estimate for the substitution $\text{Al}^{\text{VI}}\text{Al}^{\text{IV}} \rightleftharpoons \text{MgSi}$ in the amphiboles;
2. Assume that the difference in entropy between forsterite and fayalite represents a typical value for the substitution $\text{Mg} \rightleftharpoons \text{Fe}$;
3. Assume that the difference in entropy between Ca-olivine and fayalite represents the difference $2/3 \cdot (S_{\text{grossular}} - S_{\text{almandine}})$.

It is evident that the scheme proposed here is similar to the additivity model by Fyfe et al. (1958, since the majority of the substitutions ($\text{Mg} \rightleftharpoons \text{Fe}$, $\text{Al}^{\text{VI}} \text{Al}^{\text{IV}} \rightleftharpoons \text{MgSi}$) involve only minor volume changes. Support for the essential correctness of our procedure can be found in the calculations for $S_{\text{almandine}}^{298}$ by Zen (1973), which differs only by 0.6 cal/deg gfw from our value, well within the experimental uncertainty of 1.3 cal/deg gfw stated for $S_{\text{grossular}}^{298}$ by Robie and Waldbaum (1968). It may also be observed that no conflict arises in the sequence of the univariant lines around the invariant points, which is in further support of the correctness of the thermodynamic data (see Zen, 1966).

The petrogenetic grid resulting from the calculations is presented in Figure 4.2. The lack of experimental data on the various reactions places a considerable uncertainty on the position of the different invariant points, but the configuration chosen here, implying a higher thermal stability for aluminous iron-rich amphiboles, results from the observation that in thermally metamorphosed iron-formations only tschermakitic hornblendes are found in association with cummingtonite (Bonnichsen, 1969).

Of primary significance appears to be the observation that the diagram (Figure 4.2) is essentially divided in two parts, separated by the reaction (hbl)*:

*The common usage of parenthesizing that phase which does not participate in a univariant reaction is employed here. The reactions involving the iron endmembers of the minerals are designated as follows: (cpx). Generalised reactions involving intermediate (Mg-Fe) compositions are designated thus: (cpx)

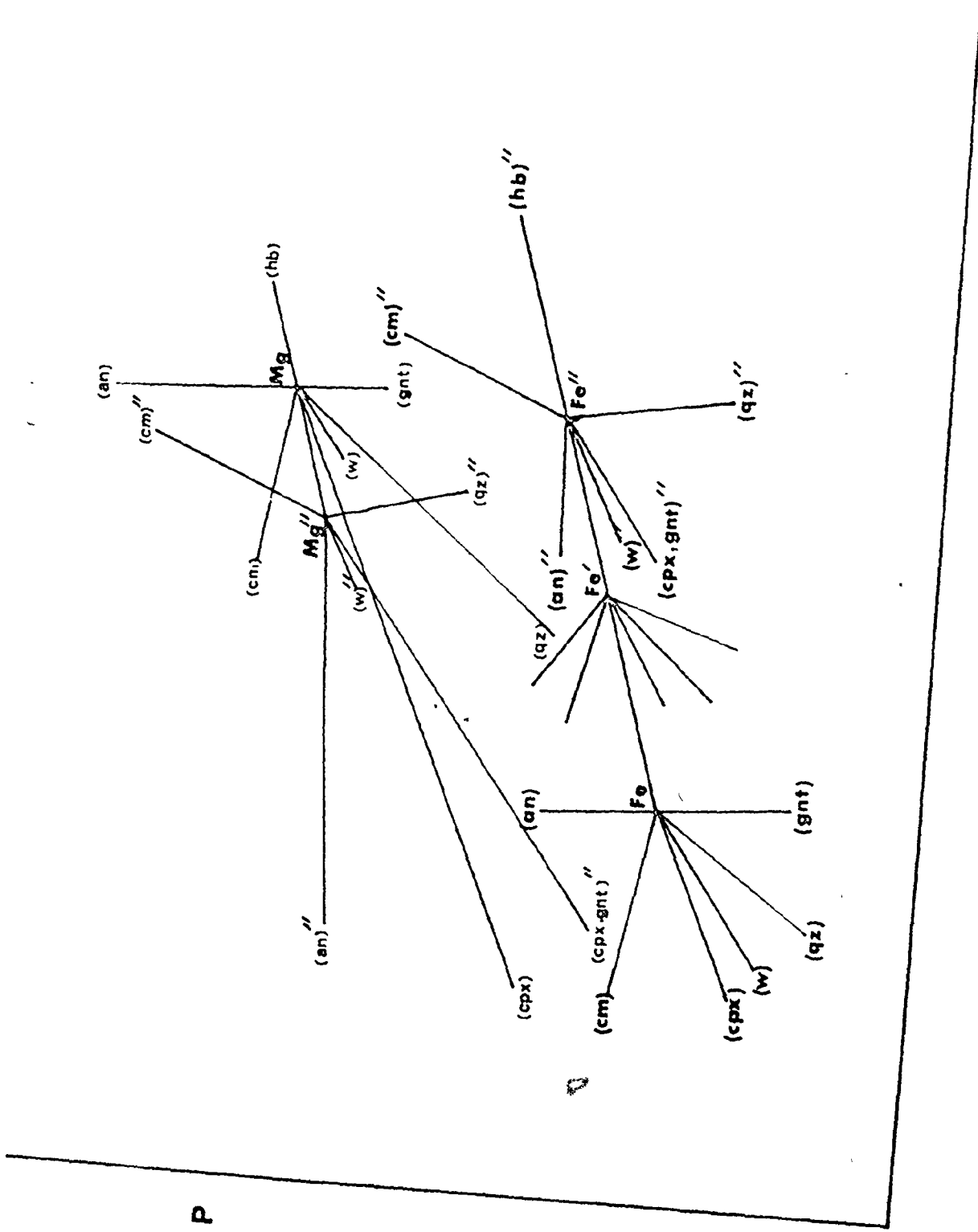


and the analogous reactions (cpx), (cpx)', and (cpx)", which have slopes very similar to (hbl). At the high-pressure side of the reaction the assemblage gnt-cm-an is no longer stable and is replaced either by the assemblage cpx (or hbl)-cm-gnt or by cpx (hbl)-gnt-an, i.e. leading to the disappearance of cummingtonite in plagioclase-bearing assemblages.

Since such a disappearance of cummingtonite in the presence of plagioclase and garnet is found in high-pressure metamorphic terrains (Barrovian facies), where cummingtonite may only be found in iron-formations in the absence of plagioclase (Klein, 1964), we may assume that the reaction (hbl) will take place at pressures around 7 kb (Winkler, 1967).

It is clear that the diagram can only be realistically evaluated if magnesium is added as another component. Addition of magnesium will not drastically alter the slopes of the different reactions (compare, for instance, the slope of 35°C/kb for decomposition of both tremolite and ferro-tremolite; Ernst, 1966), but the invariant points, particularly the one involving tremolite, will be displaced toward higher temperatures and pressures, relative to the magnesium-free reactions. It is also to be anticipated from the work by

Figure 4.3 Suggested disposition of invariant points involving magnesium-free and iron-free compositions in the petrogenetic grid of Figure 4.2



Jasmund and Schaefer (1972) that the invariant point involving magnesiotschermakite, if stable at all, will be located at a lower temperature than the tremolite point.

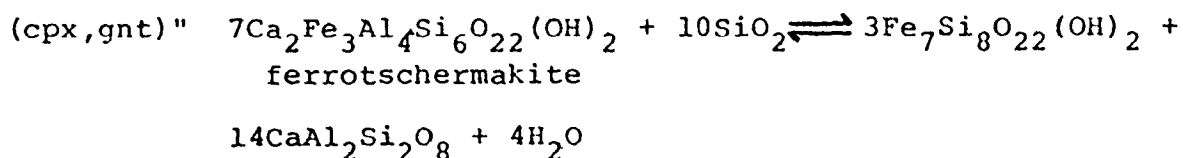
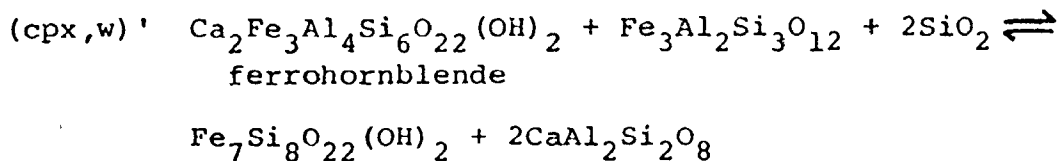
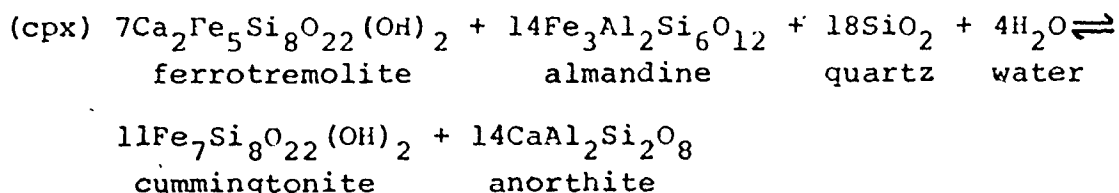
It is probably safe to assume that the reaction (HBI) of iron-free compositions will be located at considerably higher pressures than its iron-rich equivalent. A similar relationship holds, for instance, for the reaction $3 \text{ cordierite} \rightleftharpoons 2 \text{ garnet} + 3\text{Al}_2\text{SiO}_5 + 9 \text{ quartz}$, where the magnesian reaction is located some 8-10 kb above its ferrous equivalent at the same temperature (Weisbrod, 1973; Schreyer and Seifert, 1969). A curious result of this arrangement of invariant points is, that for a given pressure, the magnesian equivalents of the reactions (cpx), (cpx)', (cpx)'' occur at lower temperatures than the ferrous ones (Figure 4.3). This is probably the principal reason why, in aluminous rocks (those lying in the vicinity of the join $\text{CaAl}_2\text{Si}_2\text{O}_8 - (\text{Mg,Fe})_7\text{Si}_8\text{O}_{22}(\text{OH})_2$) of coexisting hornblende-cummingtonite pairs, the latter is the more magnesian (Klein, 1968), whereas in metamorphosed iron-formations (sub-aluminous) cummingtonite is the more iron-rich amphibole (Cameron, 1971).

It is probable that in parts of the P-T range covered by Figure 4.2, reactions involving other phases will be more stable than the ones chosen, and a complex topology for natural assemblages will result from the introduction of

other minerals such as chlorite, gedrite, cordierite, orthopyroxene, fayalite and magnetite. Gedrite and cordierite will, for instance, appear at Fe/Mg ratios for which garnet is no longer stable at low pressures, as shown by the work of Hsu and Burnham (1969).

The petrogenetic grid confirms the conclusion drawn from many textures (e.g. Plate III), that cummingtonite formation takes place through reaction of hornblende with quartz, occasionally in the presence of garnet.

Prograde cummingtonite formation is due to the following reactions:



The reaction (cpx,gnt)" has previously been proposed by Shido (1958) to account for the formation of cummingtonite

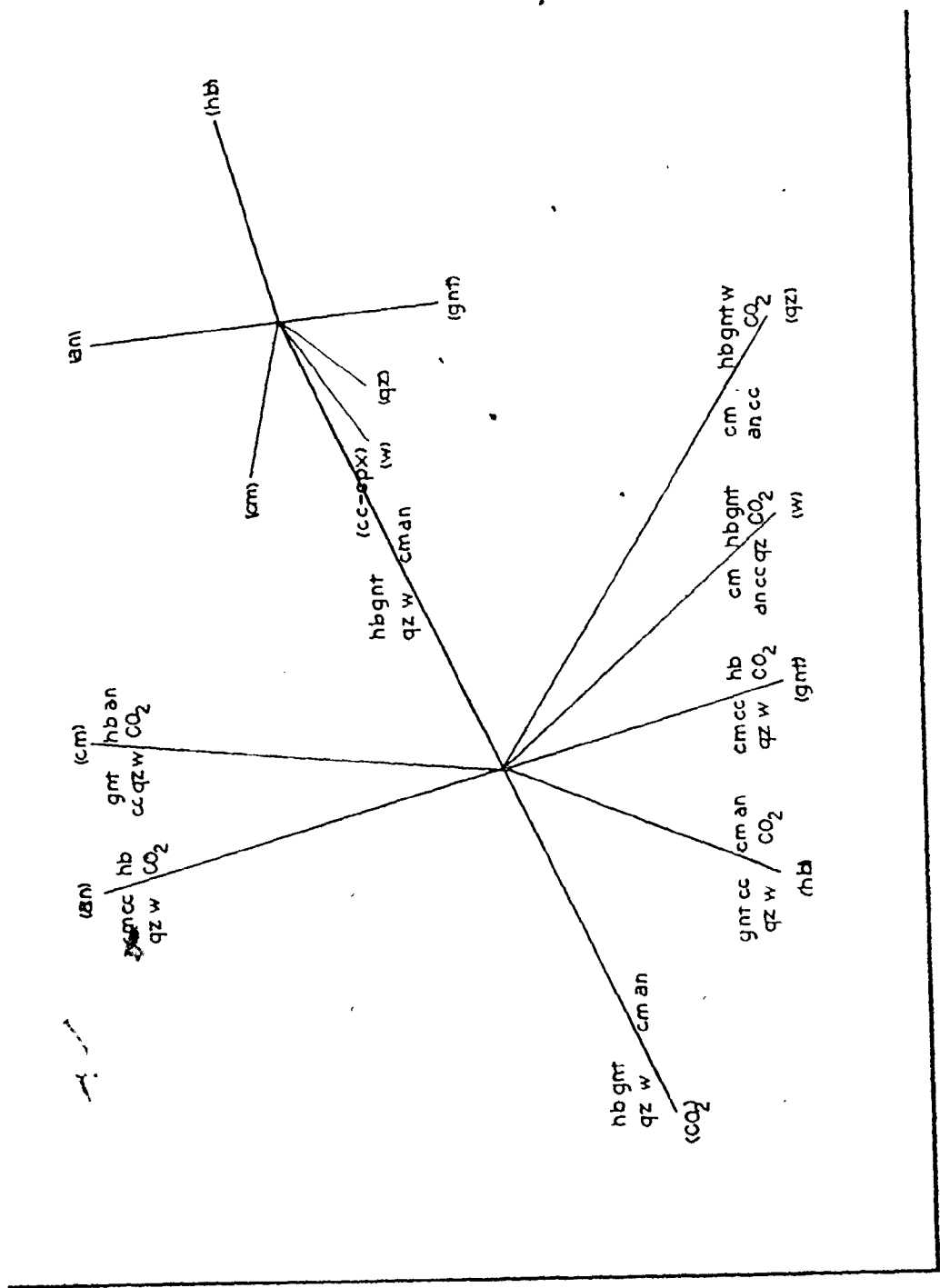
in rocks from the Abukuma Plateau in Japan.

As most cummingtonite-bearing rocks from the Tallan Lake Sill contain biotite and ilmenite a more complex reaction than $(\overline{\text{cpx}})$, $(\overline{\text{cpx}})'$ and $(\overline{\text{cpx}})''$ must be written. Mineral textures suggest a reaction of the type hornblende + garnet + ilmenite + quartz + $\text{K}^+ \rightleftharpoons$ biotite + cummingtonite + plagioclase, but detailed chemical information on the different phases would be indispensable to write a balanced reaction.

Retrogression of the prograde assemblages is usually realised through the entry of biotite and calcite in the assemblage.

Another feature that accompanies the introduction of calcite, is the renewed growth of garnet in ferrosyenites. This is clear from the poikiloblastic, euhedral habit of these garnets (e.g. Plate V), which contrasts strongly with the rounded forms found in more magnesian compositions. It is evident from the relation $G = G^\circ + RT \ln f/f^\circ$ that a lowering of the fugacity of water will result in a decrease of its free energy, thus causing dehydration reactions to be displaced toward lower temperatures. It is clear then, that with increasing CO_2 -content of the fluid phase the invariant points in Figure 4.2 will all descend along the P-T paths for the reactions (w), the only reactions which are not influenced by a lowering of $f_{\text{H}_2\text{O}}$. Such behaviour

Figure 4.4 Net involving invariant points (cpx, hb₂, hb₃) and (cc, CO₂, hb₂, hb₃) of Appendix 4. This net applies mainly to retrograde assemblages (see text)

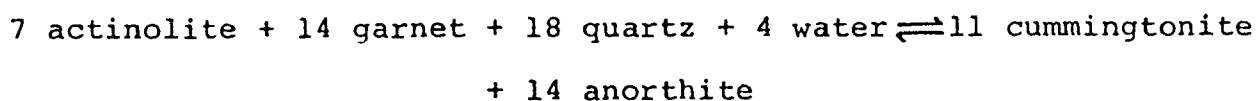


P

T

will affect the two cummingtonite producing reactions ($\overline{\text{cpx}}$) and ($\overline{\text{cpx}}$)" in different ways: at constant temperature, ($\overline{\text{cpx}}$) will be displaced toward lower pressures, while ($\overline{\text{cpx}}$)" will be shifted toward higher pressures. Since in iron-rich compositions ΔG for the latter reaction is probably positive, the effect on ($\overline{\text{cpx}}$) should be most apparent in these rocks. We have indeed found textures (newly formed garnet, hornblende porphyroblasts overgrowing an older hornblende phase and associated with some calcite) in support of the reaction $\text{cm} + \text{an} \rightleftharpoons \text{gnt} + \text{hbl} + \text{qtz}$, in sample 708, which is located some 20 meters higher in the stratigraphic section (and therefore less magnesian) than sample 508, which (still) contains cummingtonite in addition to garnet and hornblende.

As soon as calcite appears we may consider the reaction ($\overline{\text{cpx}}$):



to be the reaction (cc, CO_2) of the net involving the phases $\text{gnt-act-cm-an-cc-qz-fl}(\text{CO}_2 + \text{H}_2\text{O})$ (Figure 4.4). It will be observed from this diagram that with falling temperature (or increase in $\text{CO}_2/\text{H}_2\text{O}$ of the fluid) also the reactions ($\overline{\text{cm}}$) $3\text{hb}_1 + 5\text{an} + 11\text{CO}_2 \rightleftharpoons 5\text{gnt} + 19\text{qz} + 11\text{cc} + 3\text{w}$ and

(gnt, an) $7\text{Hb}_1 + 14\text{CO}_2 \rightleftharpoons 5\text{cm} + 16\text{qz} + 14\text{cc} + 2\text{w}$ will be crossed in rapid succession. The latter reaction has almost certainly taken place in a garnet deficient rock such as 305 (Plate XIV), in which no previous exsolution of cummingtonite was recorded, while the former may be responsible for the formation of "atoll-garnets" embedded in calcite (Plate V), which are fairly common in retrograded ferrosyenites of the Tallan Lake Sill. Here, the tschermakite component of the hornblende has probably reacted with potassium and CO_2 of the fluid phase to produce biotite, garnet and calcite. Thus, most mineral textures lend support to the conclusions drawn from a simple, theoretically derived petrogenetic grid.

4.3.3 Reactions in other assemblages

4.3.3.a Leucosyenites

It might be expected from Figure 4.4 that cummingtonite should be a ubiquitous phase in the iron-rich syenites, when calcite is present. That it is lacking altogether is the result of the incompatibility of cummingtonite and alkali feldspar (which is invariably present), which can be expressed as follows:

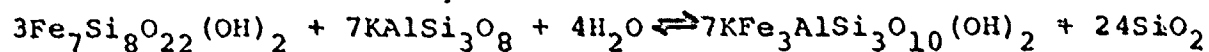
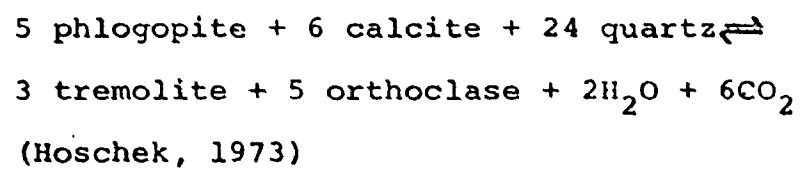
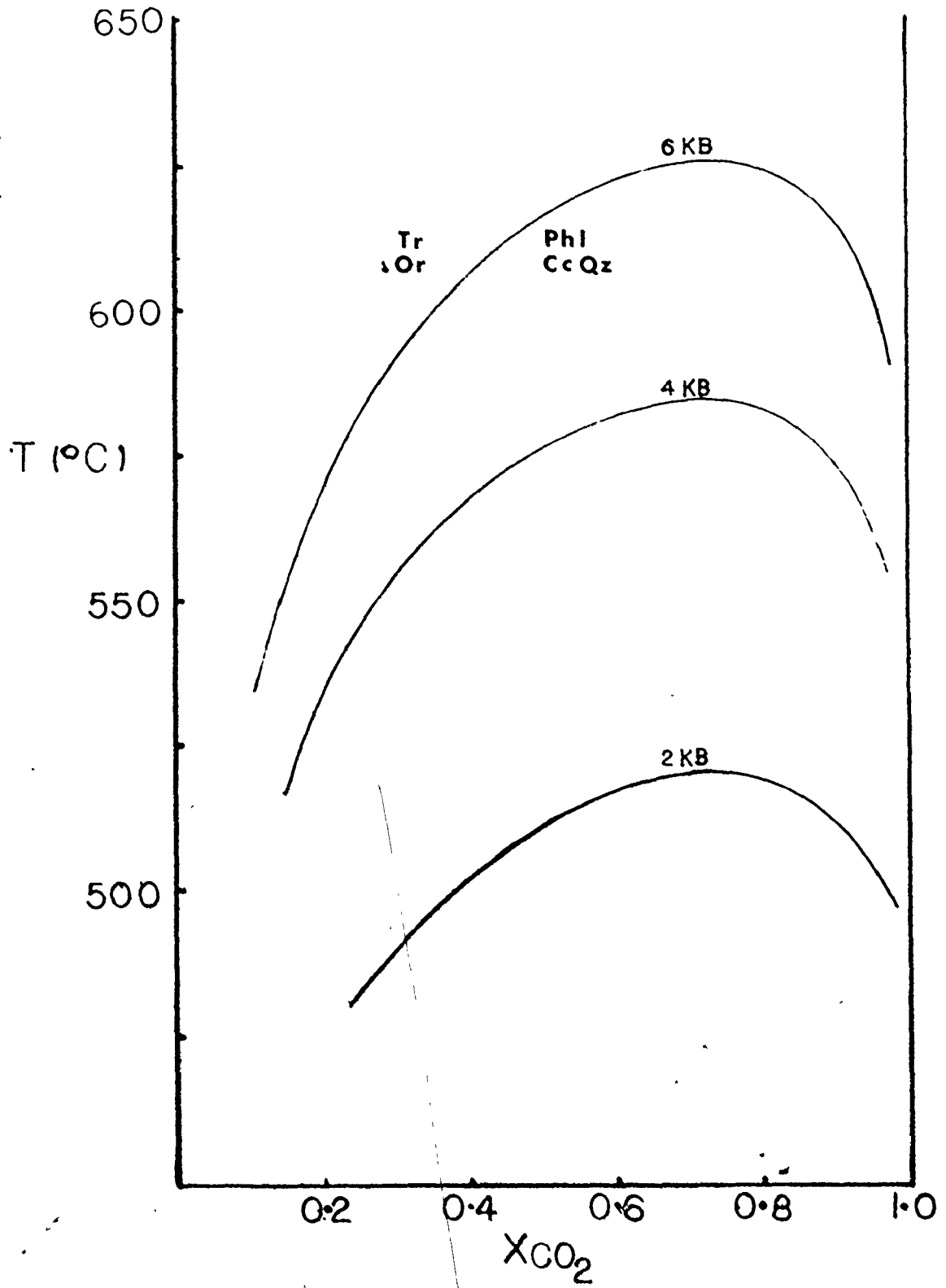
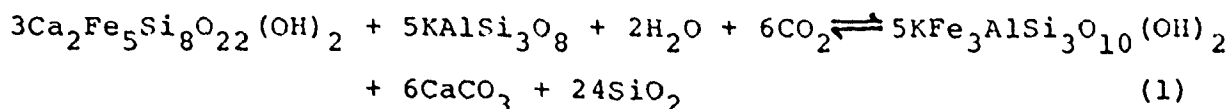


Figure 4.5 Isobars for the reaction





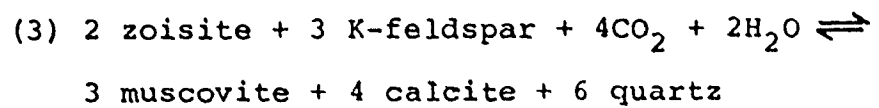
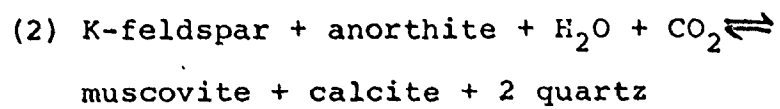
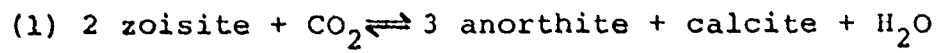
The reaction (gnt,an) from Appendix 4 can, therefore, be restated in the presence of K-feldspar as:



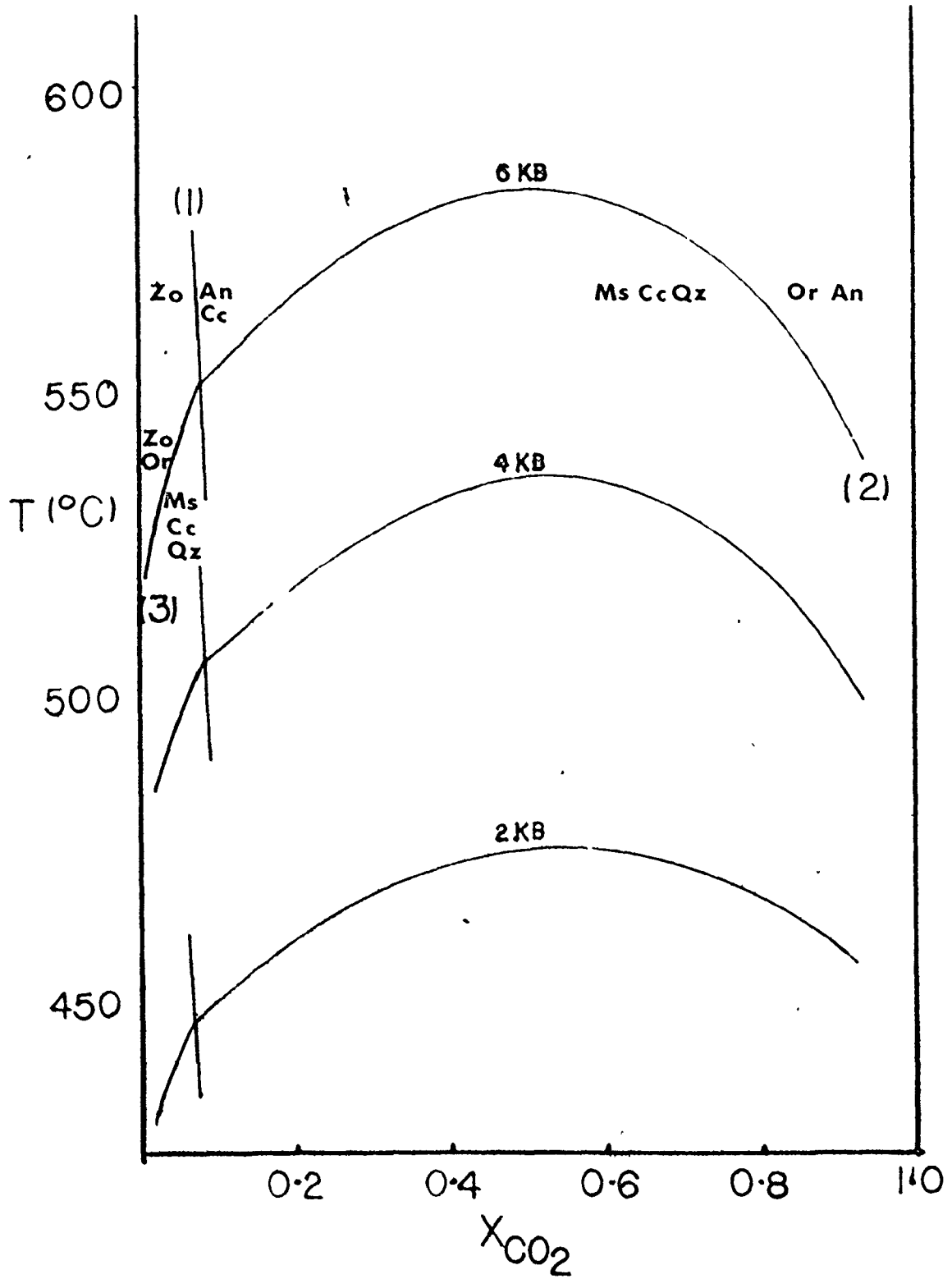
Textures, affirming that the reaction proceeds to the right, are widespread and, for example, are illustrated in Plate XV. The magnesian equivalent of this reaction (involving tremolite and phlogopite) has been experimentally studied by Hoschek (1973) (Figure 4.5), but may be more relevant to the discussion of magnesian marbles than the iron-rich compositions envisaged here. Note may be taken of the fact, however, that Carmichael (1970) has delineated a biotite isograd, based on this reaction, around the Copeway Pluton, southeast of the Tallan Lake area, which apparently transects different lithologies, and it is possible that the reaction temperature is largely independent of Fe/Mg ratio, but more responsive to changes in $\text{H}_2\text{O}/\text{CO}_2$ of the fluid phase.

It may be argued, however, that since the reaction (cpx) of Figure 4.2 will be displaced toward lower temperatures in more magnesian compositions, and following the reasoning applied in the preceding section, reaction (1) will be similarly affected. The coexistence of tremolite and alkali feldspar in magnesian marbles certainly corroborates

Figure 4.6 Isobars for the reactions

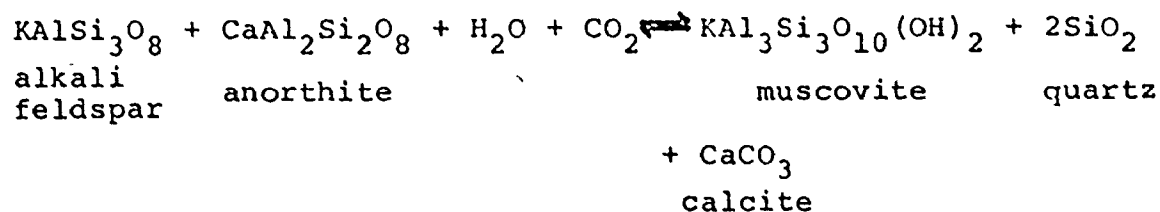


(Hewitt, 1973).



such an argument, especially in view of the higher $\text{CO}_2/\text{H}_2\text{O}$ ratio to be expected in such rocks (Figure 4.5).

In some syenites (e.g. 219, Plate VII) biotite has broken down to form a green mica, probably akin to ferriannite (Eugster and Wones, 1962), and muscovite, which coexist with plagioclase, quartz and calcite. This assemblage is of interest, not only because it is indicative of the oxidising potential of the CO_2 -bearing fluid, but also because the coexistence of muscovite, K-feldspar, plagioclase, quartz and calcite can be related to the following reaction:



which has been experimentally studied by Hewitt (1973) (Figure 4.6).

Closely related to this assemblage is the association tremolite-epidote-plagioclase-K-feldspar-calcite-quartz-sphene-magnetite in sample 2617 from a leucosyenite dyke. The fact that alkali-feldspar and magnetite coexist here points, as Eugster and Wones (1962) have shown, to a relatively high f_{O_2} (in the order of 10^{-16} or 10^{-17} bars or higher, at a total pressure of 2070 bars). This is entirely consistent with the coexistence of epidote and quartz, the lower stability of which lies in the same range of oxygen fugacities

(Holdaway, 1972). Although calcite is fairly abundant, it is clear from the data by Hewitt (1973) that X_{CO_2} of the fluid phase must have been fairly low (Figure 4.6). X_{CO_2} is of necessity lower than in the leucosyenites (ms-cc-qz stable), but the temperatures of formation of both assemblages may have been very similar. We may also point to the fact that from Moschek's (1973) data the stability of tremolite and alkali feldspar is to be expected in 2617, indicating good agreement between the various experimental procedures and natural rock systems. Almandine garnet is probably unstable relative to epidote at high f_{O_2} , and the occurrence of the latter in veinlets of K-feldspar, which in addition carry hematite (sample 69-29-3; Plate X), probably represents the most oxidised assemblage encountered. We must also point to the preponderance of sphene in this sample, a mineral that apparently always has formed in response to elevated f_{O_2} .

4.3.3.b Three amphibole assemblage

The assemblage gedrite-hornblende-cummingtonite-plagioclase-ilmenite-magnetite of sample 1317 (Plate XII), is interesting in view of the apparent rare occurrence of multi-amphibole assemblages. Three reports on the coexistence of three and even four amphiboles (always involving the phases

Table 4D. Chemistry of amphiboles and whole rock containing 3-amphibole assemblage

	1317 ¹	Hornblende ²	Gedrite ²	Cummingtonite ²
SiO ₂	47.90	43.26	43.61	54.54
TiO ₂	1.68	0.84	0.47	0.18
Al ₂ O ₃	15.18	14.19	14.26	2.07
Fe ₂ O ₃	3.94	-	-	-
FeO	8.80	14.93*	20.56*	20.23*
MnO	0.29	0.27	0.48	0.46
MgO	9.20	12.38	15.55	19.28
CaO	6.08	9.08	0.82	1.06
Na ₂ O	4.52	2.18	1.96	0.13
K ₂ O	0.08	0.12	<0.01	0.03
P ₂ O ₅	0.29	n.d.	n.d.	n.d.
H ₂ O	1.60	2.03 [†]	2.06 [†]	2.09 [†]
CO ₂	0.13	-	-	-
Sum	99.69	99.28	99.62	100.07

* Total Fe as FeO

† Calculated from structural formula

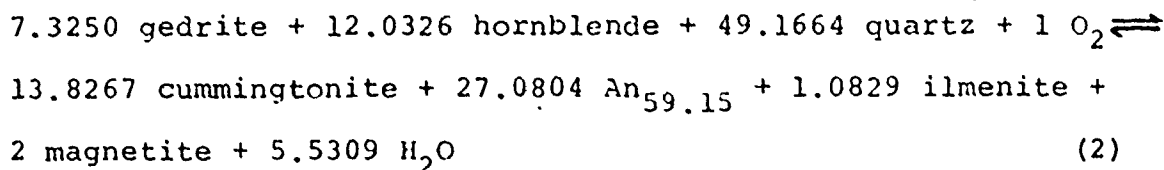
Hornblende: Na_{.65}Ca_{1.44}Fe_{1.84}Mn_{.03}Mg_{2.72}Ti_{.09}Al^{VI}_{.85}Al^{IV}_{1.62}Si_{6.38}O₂₂(OH)₂

Gedrite: Na_{.52}Ca_{.13}Fe_{2.53}Mn_{.06}Mg_{3.41}Ti_{.05}Al^{VI}_{.88}Al^{IV}_{1.59}Si_{6.41}O₂₂(OH)₂

Cummingtonite: Na_{.01}Ca_{.16}Fe_{2.43}Mn_{.06}Mg_{4.12}Ti_{.02}Al_{.17}Al_{.18}Si_{7.82}O₂₂(OH)₂

¹K. Ramlal, University of Manitoba, analyst²L. Curtis, University of Toronto, electron probe analysis

cummingtonite, hornblende, gedrite and anthophyllite) have so far appeared in the literature (Goroshnikov and Yur'yev, 1965; Robinson et al., 1969; Stout, 1972), and the present work offers the first description of the assemblage gedrite-hornblende-cummingtonite. Microprobe analyses of the minerals were obtained through the courtesy of Mr. L. Curtis at the University of Toronto, and are listed in Table 4D. An "instantaneous" reaction (assuming analysed minerals to be present among reactants and products, and probably only valid for a small increment dPT) can be written using these compositions and other phases present with the addition of quartz:



In view of the staggering consumption of quartz, it is evident why this mineral is absent in the assemblage.

The similarity of reaction (2) to the reaction ($\overline{\text{cpx}}$): $7\text{hbl} + 14\text{gnt} + 18\text{qz} + 4\text{H}_2\text{O} \rightleftharpoons 11\text{cm} + 14\text{an}$, is fairly obvious and it probably replaces the latter at lower Fe-values. It is therefore not clear why three amphibole assemblages are not more common, especially since the whole rock analysis yields a composition similar to the average spilite (Vallance, 1960) (see Appendix 2a).

4.3.3.c Calc-silicate assemblages

In magnesian calc-silicate marbles, the assemblage tremolite-calcite-quartz is predominantly found and it replaces, as many textures suggest, the mineral diopside. Some calc-silicate bands contain large amounts of biotite, however, and here diopside, not tremolite, is usually present. Since alkali feldspar is common in both assemblages, we may interpret these assemblages as follows:

- (1) X_{CO_2} in these bands was lower than in the marbles, decreasing the temperature of the reaction $5 \text{ diopside} + 3\text{CO}_2 + \text{H}_2\text{O} \rightleftharpoons \text{tremolite} + 3 \text{ calcite} + 2 \text{ quartz}$ (Metz, 1970);
- (2) As observed before, the reaction $3 \text{ actinolite} + 5 \text{ K-feldspar} + 6\text{CO}_2 + 2\text{H}_2\text{O} \rightleftharpoons 5 \text{ biotite} + 6 \text{ calcite} + 24 \text{ quartz}$ is, with increasing Fe, displaced toward higher temperatures at the prevailing pressure of metamorphism.

4.4 Summary

Although the distribution of a few accessory minerals such as apatite, zircon and allanite reflects an original, igneous stratigraphy within the Tallan Lake Sill, it is clear that the majority of the minerals present have formed during metamorphism of the sill. Four different assemblages, which are the result of chemical variation within the sill, have been distinguished, but the combined effects of retrogression

and granitisation have led to the distinction of 13 sub-assemblages (Table 4B).

These parageneses form part of an 11-component chemical system, in which a divariant assemblage consists of 9 solid phases. Since laboratory systems are not usually concerned with such complex chemical systems, a theoretical approach using the Schreinemaker's method of phase analysis (cf. Zen, 1966) was employed to study reaction relations in the assemblage hornblende-cummingtonite-garnet-plagioclase-quartz.

The petrogenetic grid thus derived offers support for a number of reactions postulated earlier on the basis of mineral textures (Figures 4.2 and 4.4).

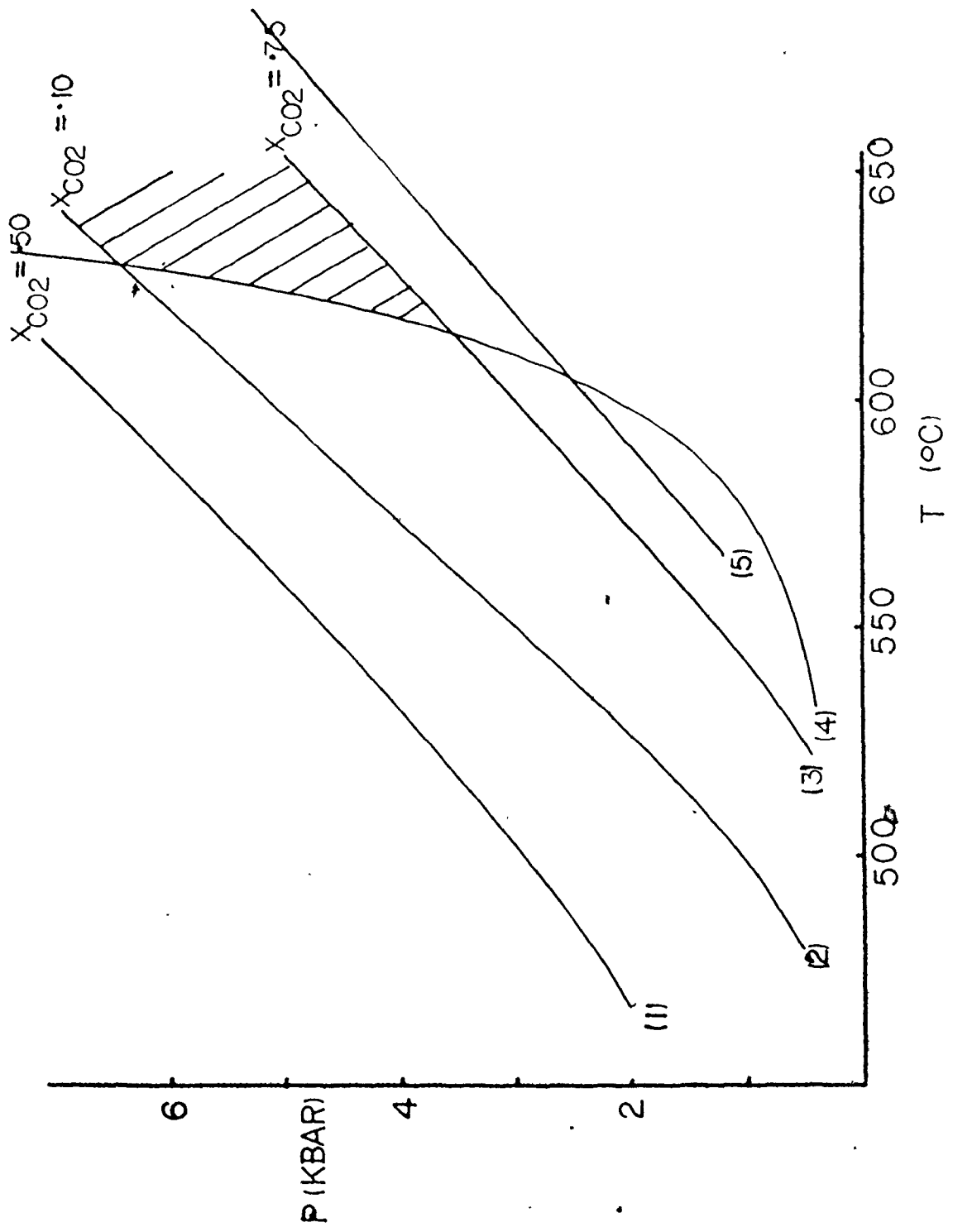
It is clear, for instance, that most cummingtonite has resulted from reaction of hornblende with quartz, which is a prograde reaction, although some has formed in the presence of calcite during retrogression of the assemblages, when metamorphic temperatures declined, accompanied with an increase in X_{CO_2} of the fluid phase. Although conclusions drawn from the petrogenetic grid are only qualitatively correct, they are supported by mineral reactions in other assemblages which are amenable to a quantitative approach. Four such reactions are collected in Figure 4.7. Of these, reactions (2,3) and (4) define the metamorphic peak, since almandine-rich garnet is present in Tallan Lake amphibolites



Figure 4.7 Summary of reactions relevant to Tallan Lake assemblages.

The hatched area indicates the maximum PT conditions attained during metamorphism of the sill.

- (1) $ms + cc + 2qz \rightleftharpoons kfsp + an + CO_2 + H_2O$ at $X_{CO_2} = .5$
(Hewitt, 1973)
- (2)&(3) $trem + 3cc + 2qz \rightleftharpoons 5di + 3CO_2 + H_2O$ at $X_{CO_2} = .1$
and $.75$ (Metz, 1970)
- (4) $chlorite + quartz \rightleftharpoons almandine + H_2O$ (Hsu, 1968)
- (5) $epidote + quartz \rightleftharpoons epidote + grossular_{ss} +$
 $anorthite + H_2O$ (Holdaway, 1972)




and diopside is an ubiquitous phase in the surrounding marbles. The minimum pressure and temperature so defined lies at 3.5 kb and 615°C, so that a reasonable guess would be 4-6 kb and 625-650°C for the maximum pressure and temperature attained, which is in complete accord with previous estimates (Jennings, 1969; Dostal, 1973). Retrogression was caused by a decrease in temperature, as is clear from intersection with reaction (1): $Kfsp + an + CO_2 + H_2O \rightleftharpoons ms + cc + 2qz$. Intersection at 560°C and 5 kb is possible when the participating plagioclase is close to An_{100} in composition, but for compositions of An_{10} , as is the case for many Tallan Lake syenites, a temperature around 500°C (Hewitt, 1973) seems more realistic.

The fact that almandine garnet is formed during retrogression may be related to a significant lowering of f_{H_2O} during that event. The temperature of 500°C for peristerite exsolution, calculated from the structural state of coexisting feldspars (Viswanathan and Eberhard, 1968) is also in agreement with conclusions reached here.

It can further be seen from reaction (5) that grossular garnet is not to be expected in the regionally metamorphosed rocks of the area. This agrees with the observation that grossular skarns are only found at the contact with the Tallan Lake Sill.

It is to be hoped that future experimental work will



outline such important reactions as (cpx) and (hb) in Figure 4.2. Only then, and in combination with chemical data on the minerals, can a precise estimate of metamorphic conditions in this area be realised.

CHAPTER 5

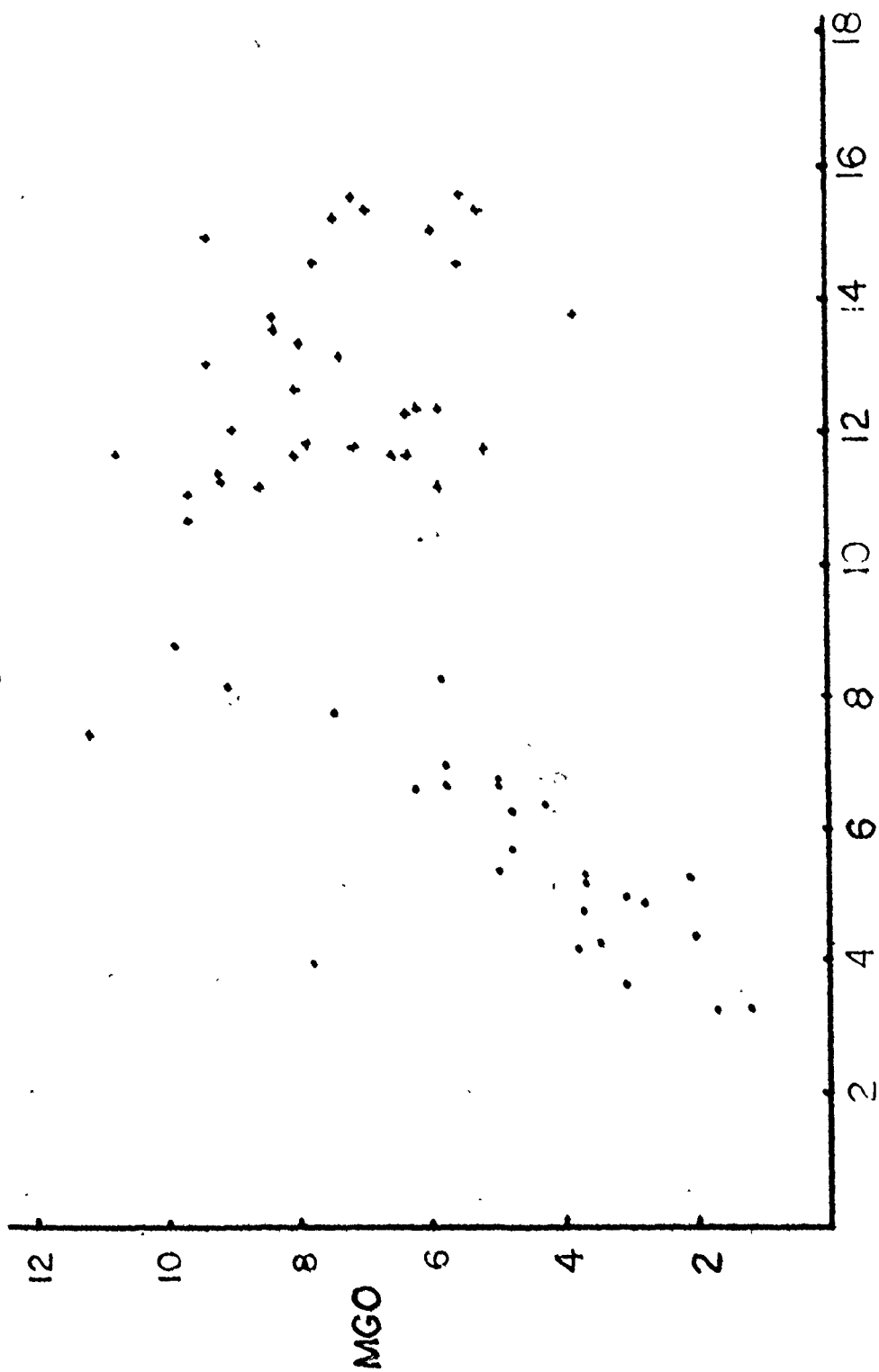
REGIONAL ASPECTS, SUMMARY AND CONCLUSIONS

In this chapter many of the conclusions reached in previous sections are repeated in brief. It is felt, however, that, since many of the observations applying to the Tallan Lake Sill, apply to most rocks in the Bancroft area, a certain "regionalisation" of these conclusions is warranted.

(1) The chemistry of the Tudor volcanic is, when spilitisation is accounted for, not distinctly different from modern flood basalts and only slightly so (higher Fe/Mg) from mid-ocean ridge basalt. A distinctive series of calc-alkaline, fragmental rocks is found on top of the sequence, and may be related to development of an island arc (Figure 5.1).

Present day equivalents of such a tectonic environment, with pene-contemporaneous development of tholeiitic plateau basalts and calc-alkaline rocks are found in the Columbia River Plateau (High Cascades) and in the Caribbean Basin (Lesser Antilles Arc; calc-alkaline series in both instances parenthesised) (e.g. Donnelly, 1973).

Figure 5.1 FeO_{tot} vs. MgO for Tudor metavolcanics
(Sethuraman, 1970). Compare with
Figure 3.1a.
Crosses - metabasalt flows
Dots - fragmentary volcanics



FE0 + 0.9 FE2O3

(2) The spilitisation of volcanic and intrusive rocks in the Bancroft area has not resulted in a significant increase in potash contents. Indeed, bona fide spilites (e.g. sample 1317, Appendix 2a) are very low in K_2O . Consequently, it is not likely that chemical alteration took place as a result of low temperature interaction with seawater (Thompson, 1973).

The low potash contents are more reconcilable with processes (ion-exchange on plagioclase, devitrification of glass and corresponding changes in chemistry), taking place during diagenesis and burial metamorphism, as demonstrated for the Keweenaw volcanics (Jolly and Smith, 1972). Since the fluid in the pore spaces would be expected to become saturated with respect to some components at a faster rate than would be the case with open seawater, the residence time will be considerably shorter in the former case. Redeposition of various elements will take place, and this may account for the occurrence of localised calcium-rich pockets in mafic volcanics observed by Jolly and Smith (op. cit.) and the redistribution of alkalis, so strikingly demonstrated in felsic volcanic terrains. The occurrence of "epidote-bombs" (Jennings, 1969; Evans, 1964) in mafic volcanics may be an expression of redistribution of calcium in mafic metavolcanics in the Bancroft area, and the variation of alkalis in the Silent Lake "pluton" has already been noted (Appendix 2a,c).

(3) The chemistry of the Tallan Lake suite is very similar to that of central volcanic complexes in flood basalt sequences. The former are distinctly higher in TiO_2 and lower in CaO than the latter, and give rise to a marked chemical discontinuity in the lavas of many plateau basalt series (Thompson, 1972). The origin of this "Thompson Gap" is believed to be due to protracted fractionation of clinopyroxene in deep seated magma chambers.

It may alternatively be proposed that many of these central volcanoes are the result of hot spot activity in the mantle (Morgan, 1971), and probably reflect the effects of relatively deep melting in the mantle, as opposed to the fairly shallow and extensive melting that must have given rise to the formation of the flood basalts. This would adequately account for the high titania contents in the former (e.g. McGregor, 1968) and the fact that alkalic rocks frequently occur side by side with tholeiitic magma (Yoder and Tilley, 1962; Kushiro, 1972). If it is proposed that the alkaline rocks of the Bancroft area are essentially coeval with the anorthositic gabbros and albite syenites, and if the difference in age (1250 ± 25 m.y. for albite syenites; 1285 ± 41 m.y. for Blue Mountain nepheline syenite; 1310 ± 15 m.y. for Tudor volcanics; Silver and Lumbers, 1966; Krogh, 1964) between the intrusive and extrusive epochs is considered, it is seen to be similar to that of modern situations (Columbia

River basalts/Snake River basalts; Eocene-Miocene/Recent; Icelandic Plateau basalt/East Iceland central volcanic zone; Miocene/Recent) in which the hot spot concept is invoked to explain the different chemistry of the central volcanoes.

(4) Petrographic and chemical considerations support the concept of consanguinity of the albite syenites with the Tallan Lake Sill, and by extension, with the gabbroic intrusives in the Bancroft area in general. The proposed differentiation mechanism involves separation of liquid from a layered magma chamber, quiescent crystallisation, subsequent disruption, roof collapse and relatively clean separation of the syenite liquid. The concentration of the syenite in a restricted volume within the sill might point to the formation of a volcanic conduit. The occurrence of parasitic cones, erupting only highly differentiated liquids, is a well known phenomenon in central volcanoes (e.g. McBirney and Williams, 1969).

On the assumption that the model presented here is generally applicable, we might expect the following relationship between extrusive and intrusive events in a plateau basalt series:

(a) extrusion of primitive olivine tholeiite along fissures on to the surface;

(b) intrusion and convective crystallisation of magma, due to hot spot activity, aggregation of residual magma

pockets or a combination of both;

(c) extrusion and strata-bound injection of highly evolved, iron-rich liquids;

(d) quiescent crystallisation of ferrogabbro;

(e) extrusion and injection of syenitic (trachytes) and possibly peralkaline (pantellerites) liquids.

The common presence of two distinct chemical discontinuities in anorogenic, volcanic suites, the low FeTi - high FeTi transition (Thompson, 1972) and the Daly Gap, separating basaltic and trachytic compositions (Chayes, 1963), might be so explained. It is to be noted that the silicic differentiates in both the Thingmuli suite (Carmichael, 1964) and the Snake River suite (Tilley and Thompson, 1970) have invariant liquidus temperatures (see Figure 3.1a), so that it must be presumed that they all were extruded at the same stage of differentiation, their differences in chemistry being due to variable proportions of the phenocryst materials.

(5) The recognition of recumbent folds of large amplitude evidently necessitates a revision of the stratigraphy, and long range stratigraphic correlations, such as made by Lumbers (1967), however praiseworthy, can no longer be unquestionably accepted. Chemical methods of stratigraphic correlation may be of use in future studies, since it would seem that Na/K ratios of silicic rocks are some indication of

the plagioclase contents of altered, and subsequently metamorphosed rhyolites.

(6) Although experimental data do not allow us to estimate the temperature maximum attained during metamorphism of the Tallan Lake Sill with sufficient precision, the minimum estimate of 625°C at 4 kb pressure is in harmony with that of 650°C and 5.5 kb by Jennings (1969). Metamorphism would therefore appear to be of the low pressure intermediate type of Miyashiro (1961), which accords with the pressure type recorded in other amphibolite terrains where assemblage garnet-cummingtonite-hornblende is present (Hietanen, 1973; Robinson and Jaffe, 1969).

The significance of the reaction cummingtonite + plagioclase \rightleftharpoons clinopyroxene + garnet and its hornblende equivalent cummingtonite + plagioclase \rightleftharpoons hornblende + garnet, in addition to the reaction orthopyroxene + plagioclase \rightleftharpoons clinopyroxene + garnet, as potential geobarometers in amphibolite and granulite terrains, is to be emphasised. In this respect we may note the absence of cummingtonite in garnet-bearing amphibolites of the Adirondack Lowlands (Engel and Engel, 1962) and the breakdown of orthopyroxene in granulites of the Adirondack Massif (de Waard, 1967), whereas cummingtonite and orthopyroxene (also: wollastonite in calc-silicate granulites) are stable in the amphibolite

and granulite terrain of the Hastings Basin and Frontenac Axis area, respectively (Wynne-Edwards, 1967). Such distinct pressure types may perhaps not constitute a classic paired metamorphic belt (Miyashiro, 1961) but that a severe tectonic disturbance separates both sides of the St. Lawrence River is indicated by the fact that the two stratigraphic successions, worked out for the Frontenac Axis by Wynne-Edwards (op. cit.), and for the Adirondack Lowlands by Engel and Engel (1953), although dipping in the same direction, are nearly exact mirror images (Wynne-Edwards, 1967).

(7) From the association of muscovite and calcite and the omnipresence of peristerite in leucosyenites, it is clear that retrogression has been prevalent and has extended the temperature range of metamorphism down to around 500°C.

The widespread occurrence of retrograde assemblages in the northern part of the Hastings Basin and adjacent portions of the Haliburton Highlands (Jennings, 1969; Lal and Moorhouse, 1969) contrasts sharply with their near-absence in central parts of the basin (Lumbers, 1967), and might reflect the slow cooling of the gneiss domes separating the Hastings Basin and the Haliburton Highlands. The retrogression of cordierite to chlorite, kyanite and andalusite described by Lal and Moorhouse (op. cit.) is of particular interest, since kyanite and sillimanite are usually formed

in prograde assemblages from the area (Carmichael, 1970; Sethuraman and Moore, 1973). A decline in pressure during metamorphism seems required, which might be due to uplift and unroofing of cover rocks after emplacement of the gneiss domes. The general occurrence of all three Al_2SiO_5 -polymorphs in this particular tectonic setting is of interest (Albee, 1968; Hietanen, 1966; Reesor and Moore, 1971).

It is also possible that the intersection of univariant reactions with steep P-T slopes, such as hornblende + garnet \rightleftharpoons cummingtonite + plagioclase and staurolite \rightleftharpoons cordierite + Al_2SiO_5 (Ganguly, 1972) which are of common occurrence in the Bancroft area, may be due to such uplift.

(8) Although the viscosity contrast between granitic basement and overlying volcanic sedimentary cover of the Grenville Group may have been sufficient to generate the gravitational instability, presumably required for initiation of diapiric doming (Ramberg, 1971), it has been convincingly argued by Rosenfeld (1968) and Fletcher (1972) that such doming will be greatly enhanced by intrastratal flow. That the latter possibility must be entertained for the Bancroft area, is shown by the prevalent boudinage of competent beds, the ubiquity of dragfolds in marble, the inferred presence of nappe structures on a regional scale, and the occurrence of isoclinal folds in outcrop (Carmichael, 1967; Evans, 1964),

notably in the gneiss domes themselves. The fact that minerals formed during the "main" metamorphic event frequently cross-cut foliation, the presence of triple points in plagioclase-rich rocks (Voll, 1960), the annealing of broken plagioclase and the intrusion of post-kinematic, unfoliated granitic dykes, are all arguments in favour of a relaxation of tectonic stresses prior to the thermal maximum.

As is clear from the foregoing the Tallan Lake Sill reflects in many ways the problems associated with many Grenville Province rocks, which cannot be settled by study of the Tallan Lake rocks alone. Persistent questioning of these rocks in the light of their regional setting, however, must eventually lead to a satisfactory solution of many Grenville problems.

The present author hopes to have made a contribution in this respect, but, failing this, can only wish to have raised more of the pertinent questions to be asked.

REFERENCES

- ADAMS, F.D. and BARLOW, A.E., 1910. Geology of the Haliburton and Bancroft areas, Province of Ontario. Geol. Surv. Can. Memoir 6, 419p.
- ALBEE, A.L., 1968. Metamorphic zones in Northern Vermont. In Studies of Appalachian Geology, Northern and Maritime (Editors Zen, White, Hadley and Thompson). Interscience Publ., N.Y., 329-341.
- ANDERSON, A.T. Jr., and MORIN, M., 1966. Two types of massif anorthosites and their implications regarding the thermal history of the crust. In Origin of Anorthosite and Related Rocks (Editor Y.W. Isachsen), N.Y. State Mus. Sci. Service Memoir 18, 57-70 (1969).
- ANDERSON, R.E., 1970. Ash-flow tuffs of Precambrian age in Southeast Missouri. Missouri Geol. Surv. and Water Resources, Rept. Invest., 46, 50p.
- APPLEYARD, E.C., 1969. Nepheline gneisses of the Wolfe Belt, Lyndoch Township, Ontario. II. Textures and mineral paragenesis. Can. Jour. Earth Sci., 6, 689-717.
- BONNICHSEN, W., 1969. Metamorphic pyroxenes and amphiboles in the Biwabik iron formation, Dunka River area, Minnesota. Mineral. Soc. Amer., Spec. Paper 2, 217-239.
- BREAKS, F.W., 1971. Origin of the Silent Lake pluton and its quartz-sillimanite nodules, near Bancroft, Ontario. Unpubl. M.Sc. thesis, McMaster Univ., Hamilton.
- BRYAN, W.B., 1970. Alkaline and peralkaline rocks of Socorro Island, Mexico. Ann. Rept. Dir. Geophys. Lab., Carnegie Inst. Year Book 1968, 194-200.
- BRYAN, W.B., FINGER, L.W. and CHAYES, F., 1969. Estimating proportions in petrographic mixing equations by least-squares approximation. Science, 163, 926-927.
- BURNHAM, C.W., HOLLOWAY, J.R. and DAVIS, N.F., 1969. Thermodynamic properties of water to 1000°C and 10,000 bars. Geol. Soc. Amer., Spec. Paper 132, 96p.
- CAMERON, K.L., 1971. Amphibole phase relations along the join $Mg_{3.5}Fe_{3.5}Si_8O_{22}(OH)_2 - Ca_2Mg_{2.5}Fe_{2.5}Si_8O_{22}(OH)_2$. Ann. Rept. Dir. Geophys. Lab., Carnegie Inst. Year Book 1970, 145-150.

- CARMICHAEL, D.M., 1967. Structure and metamorphism, Central Hastings County, Ontario. Geol. Surv. Can., Paper 67-1, 133-134.
- CARMICHAEL, D.M., 1970. Intersecting isograds in the Whetstone Lake area, Ontario. Jour. Petrol., 11, 147-181.
- CARMICHAEL, I.S.E., 1964. The petrology of Thingmuli, a Tertiary volcano in Eastern Iceland. Jour. Petrol., 5, 435-460.
- CHAYES, F., 1963. Relative abundance of intermediate members of the oceanic basalt-trachyte association; author's reply to preceding discussions. Jour. Geophys. Res., 68, 5108-5109.
- CLAISSE, F. and QUINTIN, M., 1967. Generalization of the Lachance-Traill method for the correction of the matrix effect in X-ray fluorescence analysis. Jour. Can. Spectroscopy, 12, 129-133.
- DEER, W.A., HOWIE, R.A. and ZUSSMAN, J., 1962. Rock-Forming Minerals. Longmans, London, 5 volumes.
- DONNELLY, T.W., 1973. Late Cretaceous basalts from the Caribbean: A possible flood basalt province of vast size. Trans. Amer. Geophys. Union, 54, 1004.
- DONNELLY, T.W., KAY, R. and ROGERS, J.J.W., 1973. Chemical petrology of Caribbean basalts and dolerites; Leg 15, Deep Sea Drilling Project. Trans. Amer. Geophys. Union, 54, 1002-1004.
- DOSTAL, J., 1973. Geochemistry and petrology of the Loon Lake pluton, Ontario. Unpubl. Ph.D. thesis, McMaster Univ., Hamilton.
- ENSLIE, R.F., 1966. Crystallization and differentiation of the Michikaman intrusion. In Origin of Anorthosite and Related Rocks (Editor Y.W. Isachsen), N.Y. State Mus. Sci. Service Memoir 18, 163-174 (1969).
- ENGEL, A.E.J. and ENGEL, C.G., 1953. Grenville series in the Northwest Adirondack Mountains. Geol. Soc. Amer., 64, 1013-1098.
- ENGEL, A.E.J. and ENGEL, C.G., 1962. Progressive metamorphism of amphibolite, Northwest Adirondack Mountains, N.Y. Geol. Soc. Amer. Bull., Buddington Volume, 37-82.
- ERNST, W.G., 1966. Synthesis and stability relations of ferrotremolite. Amer. Jour. Sci., 264, 37-65.

- ERNST, W.G., 1968. Amphiboles. Springer-Verlag, N.Y., 125p.
- EUGSTER, H.P. and WOMES, D.R., 1962. Stability relations of the ferruginous biotite, annite. *Jour. Petrol.*, 3, 82-125.
- EVANS, A.M., 1964. Geology of Ashby and Denbigh Townships. Ont. Dept. Mines Geol. Rept. 26, 39p.
- FLETCHER, R.C., 1972. Application of a mathematical model to the emplacement of mantled gneiss domes. *Amer. Jour. Sci.*, 272, 197-216.
- FYFE, W.S., TURNER, F.J. and VERHOOGEN, J., 1958. Metamorphic reactions and metamorphic facies. *Geol. Soc. Amer. Memoir* 73.
- GANGULY, J., 1972. Staurolite stability and related paragenesis: theory, experiments and application. *Jour. Petrol.*, 13, 335-365.
- GOROSHNIKOV, V.I. and YUR'YEV, L.D., 1965. Cordierite-polyamphibole and anthophyllite-cordierite rocks of the Krivoy Rog district. *Dokl. Akad. Nauk USSR. A.G.I. transl., Earth Science Section*, 163, 140-143.
- GROBLER, N.J. and WHITFIELD, G.G., 1970. The olivine-apatite magnetitites and related rocks in the Villa Nova occurrence of the Bushveld igneous complex. In *Symposium on the Bushveld Igneous Complex and Other Layered Intrusions* (Editors Visser and Von Gruenowaldt), *Geol. Soc. S. Afr. Spec. Publ.* 1, 208-227.
- GUNN, M., 1967. The incident attenuation factor in X-ray omission analysis and the determination of some heavy elements in standard rocks. *Can. Jour. Spectroscopy*, 12, 163-168.
- HEINRICH, K.F.J., 1966. X-ray absorption uncertainty. In *The Electron Microprobe* (Editors McKinley, Heinrich and Wittry), J. Wiley and Sons, 296-377.
- HEWITT, D.A., 1973. Stability of the assemblage muscovite-calcite-quartz. *Amer. Mineral.*, 58, 785-791.
- HEWITT, D.F. and JAMES, W., 1956. Geology of Dungannon and Mayo Townships. Ont. Dept. Mines Ann. Rept. 64, pt.8, 65p.

- HIETANEN, A., 1966. Metamorphic environment of anorthosite in the Boehls Butte area, Idaho. In *Origin of Anorthosites and Related Rocks* (Editor Y.W. Isachsen), N.Y. State Mus. Sci. Service Memoir 18, 371-386 (1969).
- HIETANEN, A., 1973. Coexisting cummingtonite and aluminous hornblende from garnet amphibolite, Boehls Butte area, Idaho, U.S.A. *Lithos*, 6, 261-264.
- HOLDAWAY, M.J., 1972. Thermal stability of Al-Fe epidote as a function of f_{O_2} and Fe content. *Contr. Mineral. and Petrol.*, 37, 307-340.
- HOSCHEK, G., 1973. Die Reaktion Phlogopit + Calcit + Quarz = Tremolit + Kalifeldspat + H_2O + CO_2 . *Contr. Mineral. and Petrol.*, 39, 231-238.
- HSU, L.C., 1968. Selected phase relationships in the system Al-Mn-Fe-Si-O-H: a model for garnet equilibria. *Jour. Petrol.*, 9, 40-83.
- HSU, L.C. and BURNHAM, C.W., 1969. Phase relationships in the system $Fe_3Al_2Si_3O_{12}$ - $Mg_3Al_2Si_3O_{12}$ - H_2O at 2.0 kilobars. *Geol. Soc. Amer. Bull.*, 80, 2393-2408.
- JAFFE, H.W., ROBINSON, P. and KLEIN, C. Jr., 1968. Exsolution lamellae and optic orientation of clin amphiboles. *Science*, 160, 776-778.
- JAMES, H.L., 1966. Chemistry of the iron-rich sedimentary rocks. U.S.G.S. Prof. Paper 440-W, 61p.
- JASMUND, K. and SCHAEFER, R., 1972. Experimentelle Bestimmung der P-T Stabilitätsbereiche in der Mischkristallreihe Tremolit-Tschermakit. *Contr. Mineral. and Petrol.*, 34, 101-115.
- JENNINGS, D.S., 1969. Origin and metamorphism of part of the Harmon Group near Bancroft, Ontario. Unpub. Ph.D. thesis, McMaster Univ., Hamilton.
- JOLLY, W.T. and SMITH, R.E., 1972. Degradation and metamorphic differentiation of the Keweenaw tholeiitic lavas of Northern Michigan, U.S.A. *Jour. Petrol.*, 13, 273-310.
- KLEIN, C. Jr., 1966. Mineralogy and petrology of the metamorphosed Wabush iron formation, Southwestern Labrador. *Jour. Petrol.*, 7, 246-305.

- KLEIN, C. Jr., 1968. Coexisting amphiboles. *Jour. Petrol.*, 9, 281-330.
- KRANCK, E.H., 1966. Anorthositic and rapakivi, magmas from the lower crust. In *Origin of Anorthositic and Related Rocks* (Editor Y.W. Tsachsen). N.Y. State Mus. Sci. Service Memoir 18, 93-98 (1969).
- KROGH, T.E., 1964. Strontium isotopic variation and whole-rock isochron studies in the Grenville Province of Ontario. M.I.T. 1381-12, Twelfth Ann. Progress Rept. for 1964, USAEC., 73-124.
- KUSHIRO, I., 1960. Si-Al relation in clinopyroxene from igneous rocks. *Amer. Jour. Sci.*, 258, 548-554.
- KUSHIRO, I., 1972. Partial melting of synthetic and natural peridotites at high pressures. *Ann. Rept. Director Geophys. Lab., Carnegie Inst. Year Book 1971*, 357-362.
- LAL, R.K. and MOORHOUSE, W.W., 1969. Cordierite-gedrite rocks and associated gneisses of Fishtail Lake, Harcourt Township, Ontario. *Can. Jour. Earth Sci.*, 6, 145-165.
- LEROUX, J., MAHMUD, M. and DAVEY, A.B.C., 1967. Fluorescence yield of a given element as a function of the spectral distribution of the exciting primary beam. *Can. Jour. Spectroscopy*, 12, 169-174.
- LINDSLEY, D.H., SMITH, D. and HAGGERTY, S.E., 1971. Petrography and mineral chemistry of a differentiated flow of Picture Gorge basalt near Spray, Oregon. *Ann. Rept. Dir. Geophys. Lab., Carnegie Inst. Year Book 1969*, 264-284.
- LIPMAN, P.W., 1965. Chemical comparison of glassy and crystalline volcanic rocks. *U.S.G.S. Bull.* 1201D, 23p.
- LUMBERS, S.B., 1967. Stratigraphy, plutonism and metamorphism in the Ottawa River remnant in the Bancroft-Madoc area of the Grenville Province of Southeastern Ontario, Canada. Unpubl. Ph.D. thesis, Princeton Univ.
- MACDONALD, G.A. and KATSURA, T., 1964. Chemical compositions of Hawaiian lavas. *Jour. Petrol.*, 5, 82-133.
- MACGREGOR, I.D., 1969. The system $MgO-SiO_2-TiO_2$ and its bearing on the distribution of TiO_2 in basalts. *Amer. Jour. Sci.*, 267A, Schairer Volume, 342-363.

- MCBIRNEY, A.R. and WILLIAMS, H., 1969. Geology and petrology of the Galapagos Islands. Geol. Soc. Amer. Memoir 118, 197p.
- MELSON, W.G., 1973. Basaltic glasses from the Deep Sea Drilling Project; chemical characteristics, compositions of alteration products, and fission track "ages". Trans. Amer. Geophys. Union, 54, 1011-1014.
- METZ, P., 1970. Experimentelle Untersuchung der Metamorphose von kieselig dolomitischen Sedimenten. II. Die Bildungsbedingungen des Diopsids. Contr. Mineral. and Petrol., 28, 221-250.
- MICHOT, P., 1966. Geological environments of the anorthosites of South Rogaland, Norway. In Origin of Anorthosites and Related Rocks (Editor Y.W. Isachsen). N.Y. State Mus. Sci. Service Memoir 18, 411-424 (1969).
- MIYASHIRO, A., 1961. Evolution of metamorphic belts. Jour. Petrol., 2, 277-311.
- MORGAN, W.J., 1971. Convection plumes in the lower mantle. Nature, 230, 42-48.
- MUIR, I.D., 1954. Crystallization of pyroxenes in an iron-rich diabase from Minnesota. Min. Mag., 30, 376-388.
- NORRISH, K. and HUTTON, J.T., 1969. An accurate X-ray spectrographic method for the analysis of a wide range of geological samples. Geochim. Cosmochim. Acta, 33, 431-453.
- ORVILLE, P.M., 1972. Plagioclase cation exchange equilibria with aqueous chloride solutions: results at 700°C and 2000 bars in the presence of quartz. Amer. Jour. Sci., 272, 234-272.
- OSBORN, E.F., 1959. Role of oxygen pressure in the crystallization of basaltic magma. Amer. Jour. Sci., 257, 609-647.
- PETTIJOHN, F.J., 1957. Sedimentary Rocks, 2nd Edition. Harper and Row, Publ., N.Y., 718p.
- RAMBERG, H., 1970. Model studies in relation to intrusion of plutonic bodies. In Mechanism of Igneous Intrusion (Editors Newall and Rast). Geol. Jour. Spec. Issue 2, 261-286.
- RANSAY, J.G., 1967. Folding and Fracturing of Rocks. McGraw-Hill, N.Y., 368p.

- REESOR, J.E. and MOORE, J.M. Jr., 1971. Petrology and structure of the Thor-Odin gneiss dome, Shuswap metamorphic complex, British Columbia. Geol. Surv. Can. Bull. 195, 149p.
- ROBIE, R.A., BETHKE, P.M. and BEARDSLEY, K.M., 1967. Selected X-ray crystallographic data, molar volumes, and densities of minerals and related substances. U.S.G.S. Bull. 1248, 87p.
- ROBIE, R.A. and WALDBAUM, D.R., 1968. Thermodynamic properties of minerals and related substances at 298.15°K (25°C) and one atmosphere (1.013 bars) pressure and at higher temperatures. U.S.G.S. Bull. 1259, 256p.
- ROBINSON, P. and JAFFE, H.W., 1969. Chemographic exploration of amphibole assemblages from Central Massachusetts and Southwestern New Hampshire. Mineral. Soc. Amer. Spec. Paper 2, 251-274.
- ROBINSON, P., JAFFE, H.W., KLEIN, C. Jr. and ROSS, M., 1969. Equilibrium coexistence of three amphiboles. Contr. Mineral. and Petrol., 22, 248-258.
- ROSENFELD, J.L., 1968. Garnet rotations due to the major paleozoic deformations in Southeast Vermont. In Studies of Appalachian Geology, Northern and Maritime (Editors Zan, White, Hadley and Thompson). Interscience Publ., N.Y., 185-202.
- ROSS, M., PAPIKE, J.J. and SHAW, K.W., 1969. Exsolution textures in amphiboles as indicators of subsolidus thermal histories. Mineral. Soc. Amer. Spec. Paper 2, 275-299.
- SCHREYER, W. and SEIFERT, F., 1969. Compatibility relations of the aluminosilicates in the systems $MgO-Al_2O_3-SiO_2-H_2O$ and $K_2O-MgO-Al_2O_3-SiO_2-H_2O$ at high pressures. Amer. Jour. Sci., 267A, Schairer Volume, 407-443.
- SETHURAMAN, K., 1970. Petrology of Grenville metavolcanic rocks in the Bishops Corners-Donaldson area, Ontario. Unpubl. Ph.D. thesis, Carleton Univ., Ottawa.
- SETHURAMAN, K. and MOORE, J.M. Jr., 1973. Petrology of meta-volcanic rocks in the Bishops Corners-Donaldson area, Grenville Province, Ontario. Can. Jour. Earth Sci., 10, 589-614.

- SHAW, D.M., 1962. Geology of Chandos Township. Ont. Dept. Mines Geol. Rept., 11, 1-28.
- SHAW, D.M., 1972. Origin of the Apsley gneiss. Can. Jour. Earth Sci., 9, 18-35.
- SHAW, D.M. and KUDO, A.M., 1965. A test of the discriminant function in the amphibolite problem. Min. Mag., 34, 423-435.
- SHIDO, F., 1958. Plutonic and metamorphic rocks of the Nokoso and Iritono districts in the Central Abukuma Plateau. Jour. Fac. Sci. Univ. Tokyo, 11, 131-217.
- SILVER, L.T. and LUMBERS, S.B., 1966. Geochronologic studies in the Bancroft-Madoc area of the Grenville Province, Ontario, Canada. Geol. Soc. Amer. Spec. Paper 87, 156 (Abstr.).
- SIMPSON, E.S.W., 1954. The Okonjoje igneous complex, South West Africa. Trans. Geol. Soc. S. Afr., 57, 125-172.
- STOUT, J.H., 1972. Phase petrology and mineral chemistry of coexisting amphiboles from Telemark, Norway. Jour. Petrol., 13, 99-145.
- THOMPSON, G., 1973. A geochemical study of the low-temperature interaction of sea-water and oceanic igneous rocks. Trans. Amer. Geophys. Union, 54, 1015-1019.
- THOMPSON, R.N., 1972. Evidence for a chemical discontinuity near the basalt-"andesite" transition in many anorogenic volcanic suites. Nature, 236, 106-110.
- TILLEY, C.E. and THOMPSON, R.N., 1970. Melting and crystallization relations of the Snake River basalts of Southern Idaho, U.S.A. Earth Planet. Sci. Lett., 8, 79-92.
- TILLEY, C.E., YODER, H.S. Jr. and SCHAIERER, J.F., 1968. Melting relations of igneous rock series. Ann. Rept. Dir. Geophys. Lab., Carnegie Inst. Year Book 1966, 450-457.
- TUOMINEN, H.V. and MIKKOLA, T., 1950. Metamorphic Mg-Fe enrichment in the Orijärvi region as related to folding. Bull. Comm. Geol. Finl., 150, 67-92.
- TUTTLE, O.F. and BOWEN, N.L., 1958. Origin of granite in the light of experimental studies in the system $\text{NaAlSi}_3\text{O}_8$ - KAlSi_3O_8 - SiO_2 . Geol. Soc. Amer. Memoir 74, 153p.

- VALLANCE, T.G., 1960. Concerning spilites. Proc. Linn. Soc. N.S.W., 85, 8-52.
- VALLANCE, T.G., 1967. Mafic rock alteration and isochemical development of some cordierite-anthophyllite rocks. Jour. Petrol., 8, 84-96.
- VAN DE KAMP, P.C., 1968. Geochemistry and origin of metasediments in the Haliburton-Madoc area, Southeastern Ontario. Can. Jour. Earth Sci., 5, 1337-1372.
- VISWANATHAN, K. and EBERHARD, E., 1968. The peristerite problem. Schweiz. Min. Petr. Mitt., 48, 803-814.
- VOLL, G., 1960. New work on petrofabrics. Lpool. Manch. Geol. Jour., 2, 503.
- DE WAARD, D., 1967. The occurrence of garnet in the granulite-facies terrane of the Adirondack Highlands and elsewhere, an amplification and a reply. Jour. Petrol., 8, 210-232.
- DE WAARD, D., 1970. The anorthosite-charnockite suite of rocks of Roaring Brook Valley in the Eastern Adirondacks (Marcy Massif). Amer. Mineral., 55, 2063-2075.
- WAGER, L.R. and BROWN, G.M., 1967. Layered Igneous Rocks. Oliver and Boyd, Edinburgh and London, 588p.
- WEISBROD, A., 1973. Refinements of the equilibrium conditions of the reaction Fe cordierite \rightarrow Almandine + Quartz + Sillimanite (+ H₂O). Ann. Rept. Dir. Geophys. Lab., Carnegie Inst., ²Year Book 1972, 518-521.
- WINKLER, H.G.F., 1967. Petrogenesis of metamorphic rocks. 2nd Edition. Springer-Verlag, N.Y., 237p.
- WYNNE-EDWARDS, H.R., 1967. Westport map-area, Ontario, with special emphasis on the Precambrian rocks. Geol. Surv. Can. Memoir 346, 142p.
- WYNNE-EDWARDS, H.R., 1972. The Grenville Province. In Variations in Tectonic Styles in Canada (Editors R.A. Price and R.J.W. Douglas). Geol. Assoc. Can. Spec. Paper 2, 264-334.
- YODER, H.S. Jr., 1967. Spilites and serpentinites. Ann. Rept. Dir. Geophys. Lab., Carnegie Inst. Year Book 1965, 269-279.

- YODER, H.S. Jr. and TILLEY, C.E., 1962. Origin of basalt magmas: an experimental study of natural and synthetic rock systems. Jour. Petrol., 3, 342-532.
- ZEN, E-an., 1966. Construction of pressure-temperature diagrams for multicomponent systems after the method of Schreinemakers - a geometric approach. U.S.G.S. Bull. 1225.
- ZEN, E-an., 1973. Thermochemical parameters of minerals from oxygen-buffered hydrothermal equilibrium data: method, application to annite and almandine. Contr. Mineral. and Petrol., 39, 65-80.

APPENDIX 1

CHEMICAL COMPARISON OF TALLAN LAKE ROCKS
WITH OTHER SERIES

	120	1	2	3
SiO ₂	48.48	48.44	48.13	47.99
TiO ₂	2.84	2.95	3.53	3.99
Al ₂ O ₃	12.87	13.15	13.29	13.24
Fe ₂ O ₃	3.36	3.78	4.72	1.61
FeO	10.45	9.92	9.53	13.60
MnO	0.23	0.24	0.22	0.20
MgO	5.68	5.62	5.63	5.32
CaO	9.36	10.79	10.11	9.56
Na ₂ O	4.55	2.57	3.10	2.64
K ₂ O	0.38	0.43	0.63	0.91
P ₂ O ₅	0.44	0.42	0.43	0.69
H ₂ O+	1.32	0.70	0.60	0.03
H ₂ O-	0.15	0.75	0.13	0.02
CO ₂	0.42	n.d.	n.d.	n.d.
Sum	100.53	99.76	100.05	99.83

	420	TL-61-45	4	5
SiO ₂	46.34	46.00	46.04	45.78
TiO ₂	3.52	4.36	3.11	3.24
Al ₂ O ₃	11.12	13.00	13.91	14.29
Fe ₂ O ₃	3.19	3.90	2.76	2.74
FeO	14.66	14.15	13.91	13.35
MnO	0.33	0.32	0.30	0.27
MgO	4.13	4.30	3.89	4.41
CaO	8.41	8.60	7.45	8.74
Na ₂ O	3.61	3.10	3.45	3.08
K ₂ O	0.54	0.50	1.88	1.66
P ₂ O ₅	2.28	2.33	2.28	2.22
H ₂ O+	1.07		0.74	0.37
H ₂ O-	0.09	1.20	0.13	0.08
CO ₂	0.15	0.04	n.d.	n.d.
Sum	99.44	101.80	100.02	100.23

	303	605A	69-29-5	6	7	8
SiO ₂	43.72	42.05	42.00	43.05	41.30	45.87
TiO ₂	4.08	4.12	4.88	2.54	6.10	4.65
Al ₂ O ₃	10.05	13.44	13.00	10.58	13.20	10.66
Fe ₂ O ₃	3.59	4.07	3.50	4.49	4.80	4.11
FeO	19.25	19.87	16.54	18.23	14.00	15.59
MnO	0.61	0.41	0.38	0.22	0.27	0.29
MgO	3.41	4.28	4.80	3.92	4.50	3.50
CaO	8.15	9.61	8.60	10.37	9.60	8.28
Na ₂ O	2.49	2.94	2.71	3.39	2.50	2.84
K ₂ O	0.42	0.42	0.52	0.30	0.20	0.96
P ₂ O ₅	1.83	1.64	2.43	2.95	0.92	1.70
H ₂ O ⁺	1.20	1.30		0.11		1.42
H ₂ O ⁻	0.11	0.15	1.53	0.16	0.70	0.47
CO ₂	0.59	0.27	0.96	n.d.	n.d.	n.d.
Sum	99.50	99.57	100.90	100.31	98.10	100.34
	Tl-61-35	69-28-2	309	9	10	11
SiO ₂	47.10	50.50	51.95	46.84	51.14	52.10
TiO ₂	2.75	3.03	1.84	2.75	2.41	2.80
Al ₂ O ₃	13.00	14.50	13.24	13.58	13.95	11.50
Fe ₂ O ₃	3.80	3.00	3.63	4.43	2.15	6.40
FeO	16.18	13.85	13.86	13.84	12.97	14.20
MnO	0.37	0.32	0.37	0.25	0.44	0.31
MgO	3.30	2.60	1.83	2.92	2.21	0.70
CaO	6.40	6.30	5.99	8.58	6.56	6.20
Na ₂ O	2.92	4.58	4.54	3.30	3.59	3.60
K ₂ O	1.43	0.44	0.45	2.00	2.33	1.70
P ₂ O ₅	1.52	1.31	0.66	1.03	1.59	0.91
H ₂ O ⁺	1.36		0.85	n.d.	0.22	
H ₂ O ⁻		0.88	0.06	n.d.	0.12	0.60
CO ₂	0.00	0.06	0.37	n.d.	n.d.	n.d.
Sum	100.10	101.50	99.64	99.52	100.26*	101.00

	69-30-2	207	606	12	13	14	15
SiO ₂	53.30	53.76	56.37	55.34	55.60	56.75	56.45
TiO ₂	1.92	1.31	1.20	1.93	1.59	1.29	1.50
Al ₂ O ₃	13.80	13.51	16.44	14.02	15.14	14.51	15.88
Fe ₂ O ₃	3.00	4.20	2.96	3.31	6.22	2.39	2.60
FoO	12.10	12.99	8.13	8.73	5.36	10.63	8.13
MnO	0.29	0.41	0.26	0.17	0.29	0.25	0.17
MgO	3.60	0.72	0.96	2.71	1.88	1.12	1.06
CaO	6.60	5.87	3.91	6.54	5.08	4.56	4.39
Na ₂ O	3.44	4.09	6.37	4.54	5.95	4.02	3.56
K ₂ O	0.40	0.98	1.09	1.33	1.36	3.32	5.50
P ₂ O ₅	0.43	0.26	0.28	0.65	0.66	0.63	0.38
H ₂ O+		0.75	0.83	0.64	0.38	0.15	n.d.
H ₂ O-	0.97	0.12	0.08	0.18	0.14	0.03	n.d.
CO ₂	0.74	0.30	1.49	n.d.	n.d.	n.d.	n.d.
Sum	100.60	99.27	100.37	100.09	99.65	99.65	99.62

	105	210	310	110	16	17	18
SiO ₂	62.13	64.30	68.31	69.73	59.27	61.90	62.12
TiO ₂	0.85	0.41	0.45	0.36	1.12	0.25	0.80
Al ₂ O ₃	13.10	17.06	13.73	13.23	13.68	16.75	18.16
Fe ₂ O ₃	2.38	1.50	2.69	1.05	5.33	2.27	2.01
FeO	7.59	4.05	3.86	4.00	5.10	4.83	3.50
MnO	0.17	0.07	0.10	0.06	0.28	0.30	0.08
MgO	0.56	0.17	0.11	0.21	1.07	0.57	0.82
CaO	3.05	1.66	2.00	1.85	4.76	2.30	3.17
Na ₂ O	5.01	8.01	5.95	5.66	4.51	7.20	6.45
K ₂ O	2.07	1.83	1.67	2.12	2.00	3.25	1.49
P ₂ O ₅	0.19	0.02	0.01	0.01	0.42	0.07	0.17
H ₂ O+	0.97	0.32	0.30	0.54	1.42	0.20	0.68
H ₂ O-	0.09	0.10	0.08	0.05	1.39	0.10	0.06
CO ₂	1.73	0.13	0.20	0.80	n.d.	n.d.	n.d.
Sum	99.89	99.63	99.44	99.67	100.35	100.07	99.51

	19	20	21
SiO ₂	62.70	66.18	69.80
TiO ₂	0.44	0.67	0.34
Al ₂ O ₃	18.41	14.55	12.90
Fe ₂ O ₃	0.63	5.55	0.70
FeO	2.37	1.59	2.40
MnO	0.05	0.11	0.08
MgO	0.40	0.38	0.21
CaO	2.49	1.07	1.70
Na ₂ O	3.85	5.91	4.80
K ₂ O	7.59	2.91	3.10
P ₂ O ₅	0.15	0.11	0.07
H ₂ O+	n.d.	0.96	3.40
H ₂ O-	n.d.	0.26	0.40
CO ₂	n.d.	n.d.	n.d.
Sum	99.08	100.20	99.90

- 1 Olivine tholeiite dyke. Thingmuli Volcano, Iceland (Carmichael, 1964)
- 2 Andesite-bearing olivine basalt. Galapagos Islands (McBirney and Williams, 1969)
- 3 Glass from McKinney basalt. Snake River Group, Idaho (Tilley and Thompson, 1970)
- 4 Basalt of Sunset Cone Flow. Craters of the Moon, Idaho (Tilley and Thompson, 1970)
- 5 Middle ferrogabbro. Okonjeje Complex, Namibia (Simpson, 1954)
- 6 Ferrodiorite, Uzb, Skaergaard Intrusion, E. Greenland (Wager and Brown, 1967)
- 7 Dyke in anorthosite. Michikamau anorthosite, Labrador (Emalie, 1966)
- 8 Ferrogabbro, Beaver Bay Complex, Minnesota (Muir, 1954)
- 9 Jotunite. Roaring Brook Valley, Adirondack Massif, New York (DeWaard, 1970)
- 10 Basalt. Cinder Buttes, Craters of the Moon, Idaho (Tilley and Thompson, 1970). Total includes 0.12% SrO ; 0.25% BaO ; 0.15% FeO and 0.10% F .
- 11 Large dyke cutting anorthosite and leucogabbro. Michikamau anorthosite, Labrador (Emalie, 1966)
- 12 Icelandite. Duncan Island, Galapagos Archipelago (McBirney and Williams, 1969)
- 13 Leucodiorite inclusion in cinder cone. Jarvis Island, Galapagos Archipelago (McBirney and Williams, 1969)
- 14 Tholeiitic andesite, Devil's Orchard Flow. Craters of the Moon, Idaho (Tilley and Thompson, 1970)
- 15 Charnockite. Roaring Brook Valley, Adirondack Massif, New York (DeWaard, 1970)
- 16 Andesite dyke. Thingmuli Volcano, Iceland (Carmichael, 1964)

- 17 Soda trachyte. James Island, Galapagos Islands
(McBirney and Williams, 1969)
- 18 Quartz-syenite. Inclusion in cinder cone. Jarvis
Island, Galapagos Archipelago (McBirney and
Williams, 1969)
- 19 Farsundite. Roaring Brook Valley, Adirondacks Massif,
New York (DeWaard, 1970)
- 20 Siliceous trachyte. Jarvis Island, Galapagos
Archipelago (McBirney and Williams, 1969)
- 21 Glassy margin of acid dyke. Thingmuli Volcano,
Iceland (Carmichael, 1964)

APPENDIX 2

ALTERATION OF IGNEOUS ROCKS, COMPARED
WITH THE CHEMISTRY OF ROCKS FROM THE DANCROFT AREA

(a) Na-Ca exchange in mafic rocks

	1	2	3	4	5	6	7
SiO ₂	48.48	48.44	49.58	49.66	47.90	49.63	51.69
TiO ₂	2.84	2.95	1.16	1.21	1.68	1.57	1.58
Al ₂ O ₃	12.87	13.13	14.74	14.77	15.18	15.18	15.47
Fe ₂ O ₃	3.36	3.78	-	-	3.94	3.85	-
FeO	10.45	9.92	12.70*	11.87*	8.80	6.08	11.05*
MnO	0.23	0.24	0.20	0.19	0.20	0.15	0.18
MgO	5.68	5.62	7.97	8.11	9.20	5.10	8.38
CaO	9.36	10.79	9.85	11.39	6.08	6.62	6.84
Na ₂ O	4.55	2.57	3.48	2.15	4.52	4.29	4.39
K ₂ O	0.38	0.43	0.21	0.44	0.08	1.28	0.22
P ₂ O ₅	0.44	0.42	0.12	0.21	0.29	-	0.20
H ₂ O+	1.92	0.70	-	-	1.60	3.49	-
H ₂ O-	0.15	0.75	-	-	-	-	-
CO ₂	0.42	n.d.	-	-	0.13	-	-
Sum	100.53	99.76	100.01	100.00	99.69	99.98	100.00

* Total Fe expressed as FeO

1 Sample 120, Tallan Lake Sill (this work)

2 Olivine tholeiite dyke, Thingmuli Volcano, Iceland (Sample Q101; Carmichael, 1964)

3 Tuder volcanics metabasalt; average of 32 analyses (Sethuraman, 1970)

4 Nicoya Peninsula tholeiite; average of 6 analyses (Dennolly et al., 1973)

5 Hornblende-godrito-cummingtonite rock. Sample 1317 (this work; K. Ramal, Univ. Manitoba, analyst)

6 Average spilite (Vallance, 1960)

7 Hydrated, albitised Kowonawan basalt; average of 14 analyses (Jolly and Smith, 1972)

(b) Alteration of volcanic glasses

	8	9	10	11	12
SiO ₂	50.92	42.22	43.24	59.26	61.20
TiO ₂	1.20	2.22	2.16	1.72	1.64
Al ₂ O ₃	16.29	17.72	16.36	11.59	12.11
Fe ₂ O ₃	9.91*	15.64*	4.99	4.93	3.54
FoO	-	-	17.10	9.24	10.78
MnO	n.d.	n.d.	0.11	0.23	0.06
MgO	8.17	1.99	4.63	5.81	2.36
CaO	12.09	0.62	1.56	1.61	1.52
Na ₂ O	2.72	2.43	3.09	1.34	4.22
K ₂ O	0.17	3.26	1.03	3.09	0.12
P ₂ O ₅	0.19	0.04	0.75	n.d.	0.41
H ₂ O+	n.d.	n.d.	4.81		1.74
H ₂ O-	n.d.	n.d.	0.13	1.31	0.10
Sum	101.74	86.14	99.96	100.13	99.88

* Total Fe expressed as Fe₂O₃

8 Fresh, basaltic glass. Defocused electron probe analysis (Nelson, 1973)

9 Palagonite, formed by hydration of 8. Defocused electron probe analysis (Nelson, 1973)

10 Cordierite-anthophyllite hornfels, formed from brecciated basalt (Vallance, 1967)

11 Garnet-plagioclase-biotite gneiss, adjacent to cordierite-cordierite gneiss, Haliburton Highlands, Ontario (Lal and Meerhouse, 1969)

12 Cordierite-anthophyllite-quartz hornfels, formed from amygdaloidal basalt (Vallance, 1967)

	13	14	15	16	17	18	19	20
SiO ₂	71.46	73.52	76.26	75.74	68.80	70.95	81.60	80.10
TiO ₂	0.21	0.19	0.13	0.08	0.47	0.61	0.11	0.13
Al ₂ O ₃	12.72	12.18	11.53	11.02	13.40	14.82	9.50	13.16
Fe ₂ O ₃	0.94	1.08	2.22	1.87	4.00	1.69	1.60	1.74
FeO	0.31	0.14	0.31	0.99	0.16	0.72	0.08	0.56
MnO	0.07	0.05	0.03	0.02	0.04	n.d.	0.02	n.d.
MgO	0.22	0.20	0.03	0.75	0.52	0.11	0.00	0.21
CaO	0.86	0.74	0.00	0.01	1.10	0.22	0.12	0.01
Na ₂ O	3.40	1.03	0.13	1.16	7.70	7.98	2.00	0.11
K ₂ O	4.72	7.97	8.52	7.10	0.38	0.44	3.60	0.95
P ₂ O ₅	0.03	0.02	0.01	0.02	0.13	n.d.	0.00	n.d.
H ₂ O+	3.67	1.42	0.46	0.59	0.72	n.d.	0.53	n.d.
H ₂ O-	0.98	1.12	0.03	0.06	0.04	n.d.	0.03	n.d.
CO ₂	0.02	0.01	n.d.	n.d.	0.19	n.d.	n.d.	n.d.
Sum	99.61	99.69	99.66	99.41	99.80	97.54	99.66	98.97

- 13 Rhyolitic welded tuff, unaltered. Klendyko quadrangle, Arizona (Lipman, 1965)
- 14 Rhyolitic welded tuff, devitrified. Klendyko quadrangle, Arizona (Lipman, 1965)
- 15 Intrusive rhyolite. St. Francois Mountains, Missouri (Anderson, 1970)
- 16 Quartz-monzonite. Silent Lake Pluton, Hastings Co., Ontario (Sample J2; Brooks, 1971)
- 17 Felsite with albitised plagioclase. St. Francois Mountains, Missouri (Anderson, 1970)
- 18 Trondhjemite. Silent Lake Pluton, Hastings Co., Ontario (Sample PW27; Brooks, 1971)
- 19 Welded tuff, with silicified lithophyase. St. Francois Mountains, Missouri (Anderson, 1970)
- 20 Quartz-sillimanite nodulo. Silent Lake Pluton, Hastings Co., Ontario (Sample J24N; Brooks, 1971)

APPENDIX 3

PLAGIOCLASE COMPOSITIONS

Sample	Ant*	Remarks
117	25+31+24	Diopside marble
217	34+26	-do-
317	26	Scapolite marble
417	34+24	Amphibolite
517	33+24	-do-
617	33+37+25	-do-
717	35+31	Marble
817	34	Scapolite marble
917	29+32+24	Feather amphibolite
1017	28+22	-do-
1117	28+22	-do-; cummingtonite-hornblende
1217	10	-do-; cummingtonite-hornblende
1317	20+22	-do-; cumm.-hornblende-gedrite
1417	21+26	-do-; hornblende-gedrite
1517	19+25	Hornblende hornfels
<u>Tallan Lake Gill</u>		
1617	24+20	Assemblage 1
1917	30	-do-
2017	43+38	-do-
2117	24	Scapolite-biotite rock
2217	22+18	Assemblage 1
2317	26+22	-do-
2417	30+26+20	-do-
2517	26/17	-do-
2617	16+19/13	Leucosyenite dyke
2917	17	Assemblage 1
3017	22/16	-do-

*From univocal stage measurements on sections LX (Doer, Howie and Sugerman, 1962). Numbers refer to Ant from core of plagioclase outward.

+Denotes diffuse zoning; /denotes discontinuous zoning

Sample	Age	Remarks
3217	16+19+16	Assemblage 2
3317	17	-do-
3517	19+26+22	Amphibolite xenolith
3717	17	Assemblage 2
3917	20+24+22	-do-
4017	20/13/0	-do-
4017B	16/13	-do-
4117	20+16/13	-do-
4317	19/13	-do-
4417	22+25+18	-do-
4517	22/14+11	-do-
4617	21/14+11	-do-
4717	15+17/11	-do-
4917	15+19/20	-do-
120	26/21+15	Assemblage 1
220	21+23/18	-do-
320	20+16/13	Assemblage 2
420	15+19/13	-do-
520	15+19/13	-do-
106	16+19	-do-
206	18+20/13	-do-
306	16+19	-do-
606	15+17/13/0	-do-
905	22+26/16	Assemblage 1
805	22+26/18	-do-
705	20+16/13	Assemblage 2
605D	20+26/19+16	-do-
505	17+19/13	-do-
405	16/13	-do-
305	16/13+10	-do-
205	13+8/0	-do-
105	10+8/0	Assemblage 4

Sample	Age	Remarks
1419	19+23	Feather amphibolite
1219	21+26	Assemblage 1
1019	23/18	-do-
919	16+19	Assemblage 2
819	13+10/0	-do-
719A	10/0	Assemblage 4
619	9/0	-do-
519	9/0	-do-
419	9/0	-do-
319	9/0	-do-
219	9/0	-do-
119	9/0	-do-
609	19+22	Assemblage 1
509	16/13+8/0	Assemblage 2
409	10+15/8	-do-
309	16/12+9	-do-
209	13+10/0	Assemblage 3
109	16/12	Assemblage 4
103	22+26	Assemblage 1
203	29+24/17	-do-
303	17/13	Assemblage 2
403	21+17	-do-
108	28+30+26	Assemblage 1
208	45+36+28	-do-
308	28+30/18	-do-
408	18+20/14+11	Assemblage 2
508	17+20	-do-
708	16+19/14	Assemblage 3
207	16/13+8	-do-
107	11+8	Assemblage 4

Sample	Age	Remarks
310	5/0	Assemblage 4
210	5/0	-do-
110	5/0	-do-
111	16+20	Assemblage 2

APPENDIX 4

THERMODYNAMIC DATA FOR UNIVARIANT REACTIONS INVOLVING THE
PHASES HORNBLENDE-CUMMINGTONITE-HEDENBERGITE-ALMANDINE-
ANORTHITE-QUARTZ-CALCITE-WATER-CARBON DIOXIDE AT AN
ASSUMED PRESSURE AND TEMPERATURE OF 5 Kb AND 627°C

(a) Basic data*

$\bar{v}^{900,5kb}$ (cal bar ⁻¹)	$\bar{g}^{900,5kb}$ (cal deg ⁻¹)	Formula	Symbol
6.7526	392.84	Ca ₂ Fe ₅ Si ₈ O ₂₂ (OH) ₂	hb ₁
6.6920	385.57	Ca ₂ Fe ₄ Al ₂ Si ₇ O ₂₂ (OH) ₂	hb ₂
6.6315	378.30	Ca ₂ Fe ₃ Al ₄ Si ₆ O ₂₂ (OH) ₂	hb ₃
6.6434	402.64	Fe ₇ Si ₈ O ₂₂ (OH) ₂	cm
1.6324	97.70	CaFeSi ₂ O ₆	cpx
2.7551	183.17 [†]	Fe ₃ Al ₂ Si ₃ O ₁₂	gnt
2.4090	119.35	CaAl ₂ Si ₂ O ₈	an
0.5423	26.09	SiO ₂	qtz
0.8827	49.76	CaCO ₃	cc
0.5441	33.76	H ₂ O	w
0.3577	62.90	CO ₂	CO ₂

* Entropy data for all minerals computed from Robie and Waldbaum (1968), using assumptions outlined in Chapter 4, section 3.2. Volume data from Robie et al. (1967). No pressure correction applied.

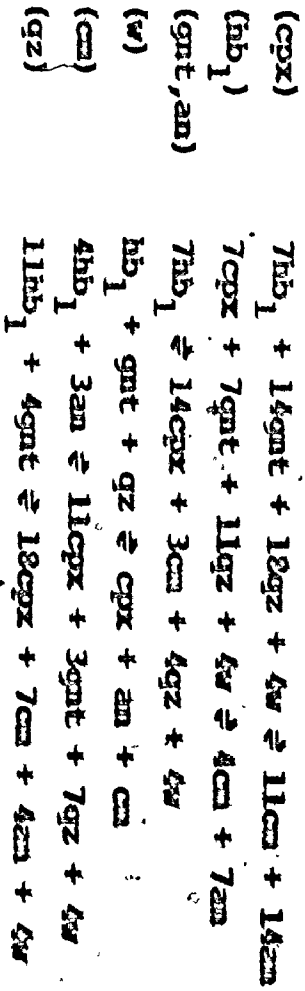
Data for H₂O from Burnham et al. (1969).

Data for CO₂ computed assuming ideality.

† Compare value of $\bar{g}_{\text{almandine}}^{298.15, \text{lbar}} = 67.68 \pm 1.70$ cal deg⁻¹ using assumptions in this work with $\bar{g}_{\text{almandine}}^{298.15, \text{lbar}} = 68.3 \pm 3.0$ cal deg⁻¹ computed from experimental work (Zon, 1973).

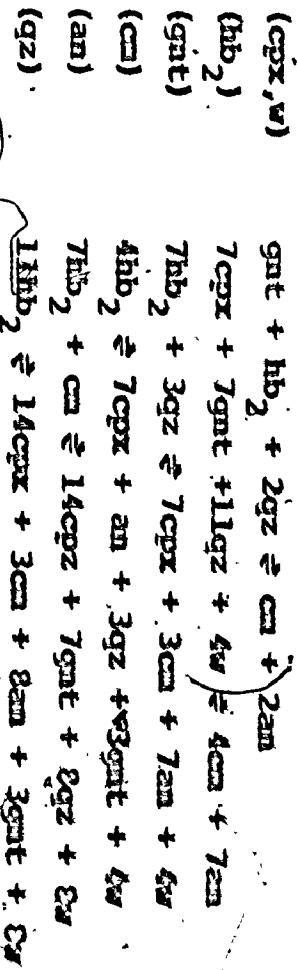
(b) Reactions

1. Invariant Point (hb₂, hb₃, cc, CO₂)



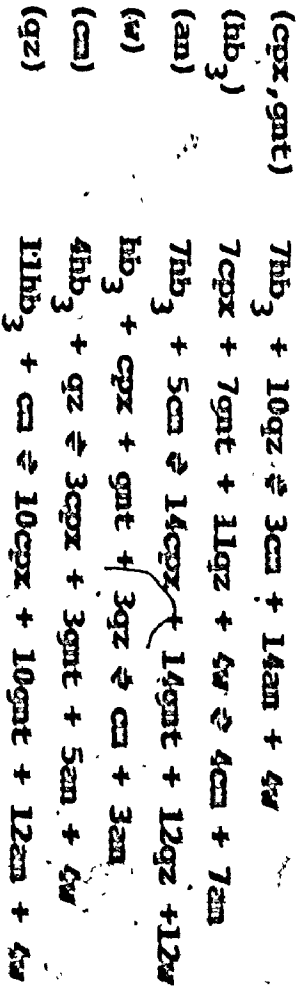
	DE/DT = kS/kV	DT/DE x 1000
	20.05 bar deg ⁻¹	49.85 deg kb ⁻¹
	12.63	79.16
	-470.03	-2.13
	21.71	36.09
	-6.10	-163.85
	5.79	17.70

2. Invariant Point (hb₁, hb₃, cc, CO₂)



	DE/DT = kS/kV	DT/DE x 1000
	21.95 bar deg ⁻¹	45.54 deg kb ⁻¹
	12.63	79.16
	44.17	22.64
	-27.55	-36.39
	-10.21	-97.90
	102.50	9.76

3. Invariant Point (hb₁, hb₂, cc, CO₂)



	DE/DT = kS/kV	DT/DE x 1000
	26.29 bar deg ⁻¹	30.04 deg kb ⁻¹
	12.63	79.16
	2.11	473.97
	18.99	52.67
	11.25	8.99
	-295.57	-3.38

	4. Invariant Point (hb ₂ , hb ₃ , cpx)	dP/dT = ΔS/ΔV 20.05 bar deg ⁻¹	dT/dP x 1000 49.86 deg kb ⁻¹
(cc, CO ₂)	7hb ₁ + 14gnt + 18gz + 4w ⇌ 11cm + 14an	-142.57	-7.01
(gnt, an)	7hb ₁ + 14CO ₂ ⇌ 5cm + 16gz + 14cc + 2w	103.63	9.65
(hb ₁)	7gnt + 17gz + 7cc + 3w ⇌ 3cm + 7an + 7CO ₂	499.63	2.00
(cm)	3hb ₁ + 5an + 11CO ₂ ⇌ 5gnt + 19gz + 11cc + 3w	-45.70	-21.88
(w)	3hb ₁ + 2gnt + 4CO ₂ ⇌ 3cm + 2an + 2gz + 4cc	-24.90	-40.17
(gz)	17hb ₁ + 16gnt + 18CO ₂ + 2w ⇌ 19cm + 16an + 18cc		

APPENDIX 5

CRYSTALLOGRAPHY OF SOME AMPHIBOLES
AND ONE CLINOPYROXENE

309	Ferrohastingsite	Cumingtonite (exsolved phase)
a	9.90 Å ⁰	9.59
b	18.24	18.24
c	5.35	5.35
β	104°54'	101°45'
V	934.4 Å ³	916.3

1317	Hornblende	Cumingtonite	Godrite
a	9.84 Å ⁰	9.50	18.67
b	18.11	18.11	17.90
c	5.32	5.32	5.29
β	105°1'	101°56'	90°
V	915.2 Å ³	895.4	1767.9

210	Ferrohastingsite	2617	Clinopyroxene
a	9.97 Å ⁰	a	9.80 Å ⁰
b	18.25	b	8.96
c	5.35	c	5.27
β	105°3'	β	105°40'
V	939.5 Å ³	V	445.2 Å ³

Values computed from Buerger precession photographs, calibrated with amphiboles of known crystallographic dimensions (collection Hawthorne)

APPENDIX 6**SAMPLE PREPARATION AND CHEMICAL
ANALYTICAL PROCEDURE**

For each sample approximately 1 kg of rock was split in a jaw crusher and then ground to pass a 150 mesh sieve.

Samples 120, 420, 303, 606 and 105 were analysed for all major elements and Rb by Mr. J.R. Muysson, whereas determination of FeO, MgO, Na₂O, P₂O₅, H₂O⁺, H₂O⁻ and CO₂ for all remaining samples (605A, 309, 207, 310, 210, 110) was performed by the same analyst, and SiO₂, TiO₂, Al₂O₃, FeO_{tot}, MnO, CaO, K₂O were determined by the author using X-ray fluorescence spectrography.

Details concerning procedure, precision and accuracy of analysis by J.R. Muysson can be found in Shaw (1972).

Sample preparation for X-ray fluorescence analysis involved regrinding of rock powder to at least 300 mesh and fusion with a light element flux to a glass pellet.

The flux consisted of lithium tetraborate and lithium carbonate (in weight proportions of 19.0:14.8) which were fused and then ground, as recommended by Norrish and Hutton (1969), but no heavy absorber was added to the flux. Of this flux 1.50 grams was added to 0.28 grams of rock powder and 0.02 grams of NaNO₃, the latter to ensure oxidation of transition elements.

Fluorescence analysis was performed on a Philips PW1540 X-ray spectroscopy unit, equipped with a gasflow counter using a methane-argon mixture.

All samples were run in sets of four, using U.S.G.S.

standard W-1 as an external standard in each set. In addition, U.S.G.S. standard rocks G-2, GSP-1, BCR-1 and AGV-1 and the previously analysed samples 120, 420, 303, 606 and 105 were run against W-1 and the samples to be analysed.

Counts were accumulated for at least 200 seconds, in separate runs of 20 seconds, for each sample in order to achieve a precision of better than 1%. Deadtime corrections were made for all count rates exceeding 5000 cps, using a deadtime of 1.52 μ sec.




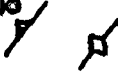




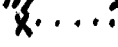



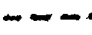

Initial reduction of data was achieved by expressing count rates into abundance of the elements without taking differences in mass absorption effects into consideration. Next, the mass absorption coefficients were calculated using values given by Heinrich (1966) and corrections for inter-element effects, using α -coefficients (Claisse and Quintin, 1967), and incident radiation (Gunn, 1967; Leroux et al., 1967) were applied, with due regard for the contributions of Li, B and O. New values for element abundances so derived were substituted for the ones previously obtained and the process was reiterated once more for all elements and at least twice for light elements as Al and Si.

Although it is difficult to estimate the accuracy of the method, it was seen from working curves relating concentrations to corrected count rate that values for samples of known chemistry do not deviate by more than 0.20% of their

true value, except for Al_2O_3 where deviations up to 0.50% were observed. As there is no stringent requirement for the analyses to total 100%, the fact that all analyses sum up to between 99% and 100% should also inspire some confidence in the method of analysis and data reduction.

GEOLOGY OF THE TALLAN LAKE SILL

Legend

-  Motagabbro
-  Motasyonito, loucosyonito and albite granite
-  Marble
-  Strike and dip of inclined, vertical gneissosity
-  Generalised strike and dip of metasediments
-  Axial trace of Chandos syncline
-  Axial trace of Rose Island dome
-  Pratt's Creek fault (largely inferred)
-  Sampling traverse
-  Generalised outcrop area
-  Lithological contact (observed, inferred)
-  Paved road
-  Gravel road, bush trail
-  Swamp, muskeg

Foot 2500 1000 0 0.5

Meters 1000 500 0 0.5 1.0

Scale 1:15,840 or 1 inch to 1/4 mile

Geology by D.M. Shaw (1958)



ranito

noissosity

monts

od)

10 Miles

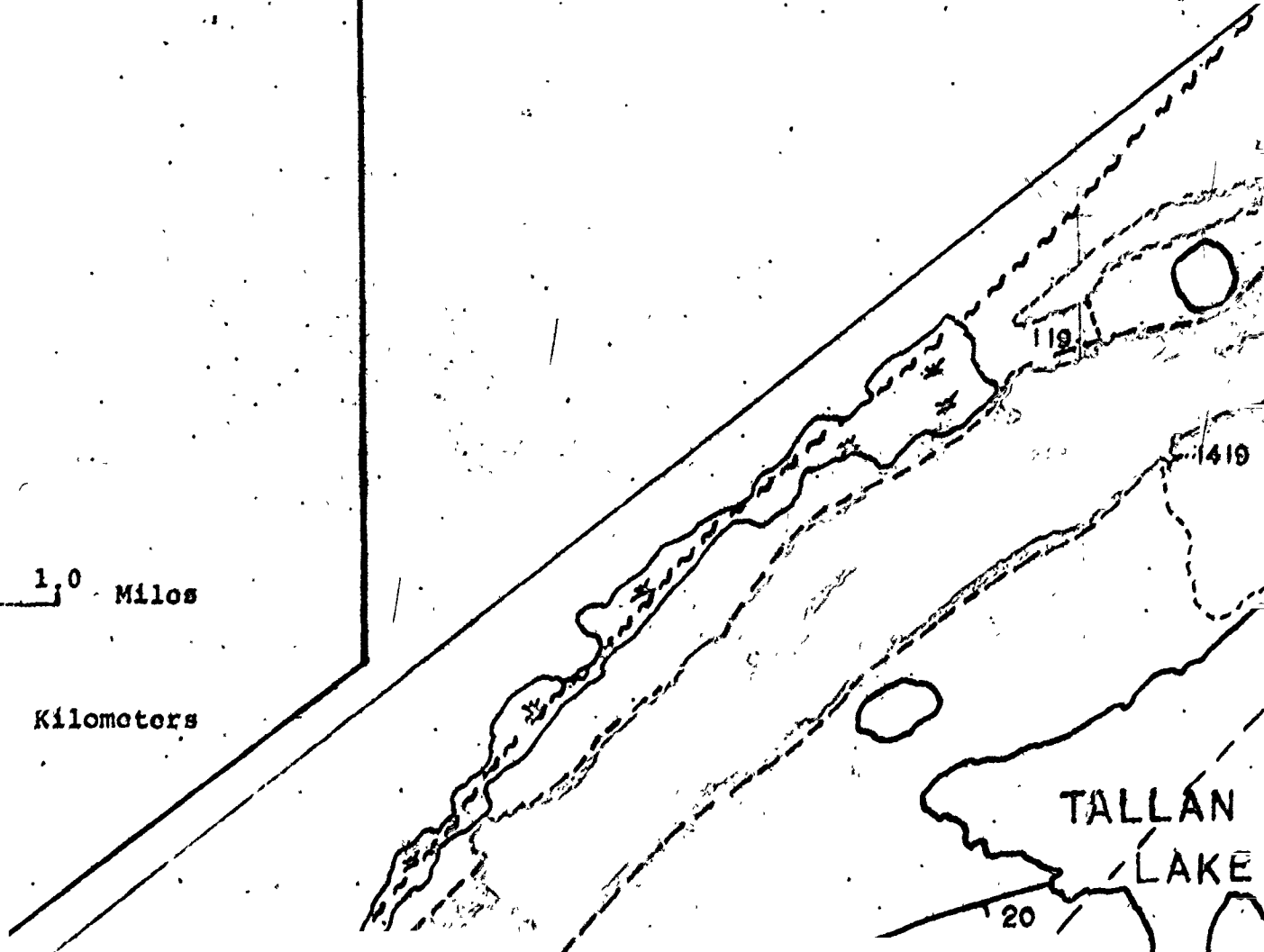
100 Kilometers

TALLAN LAKE

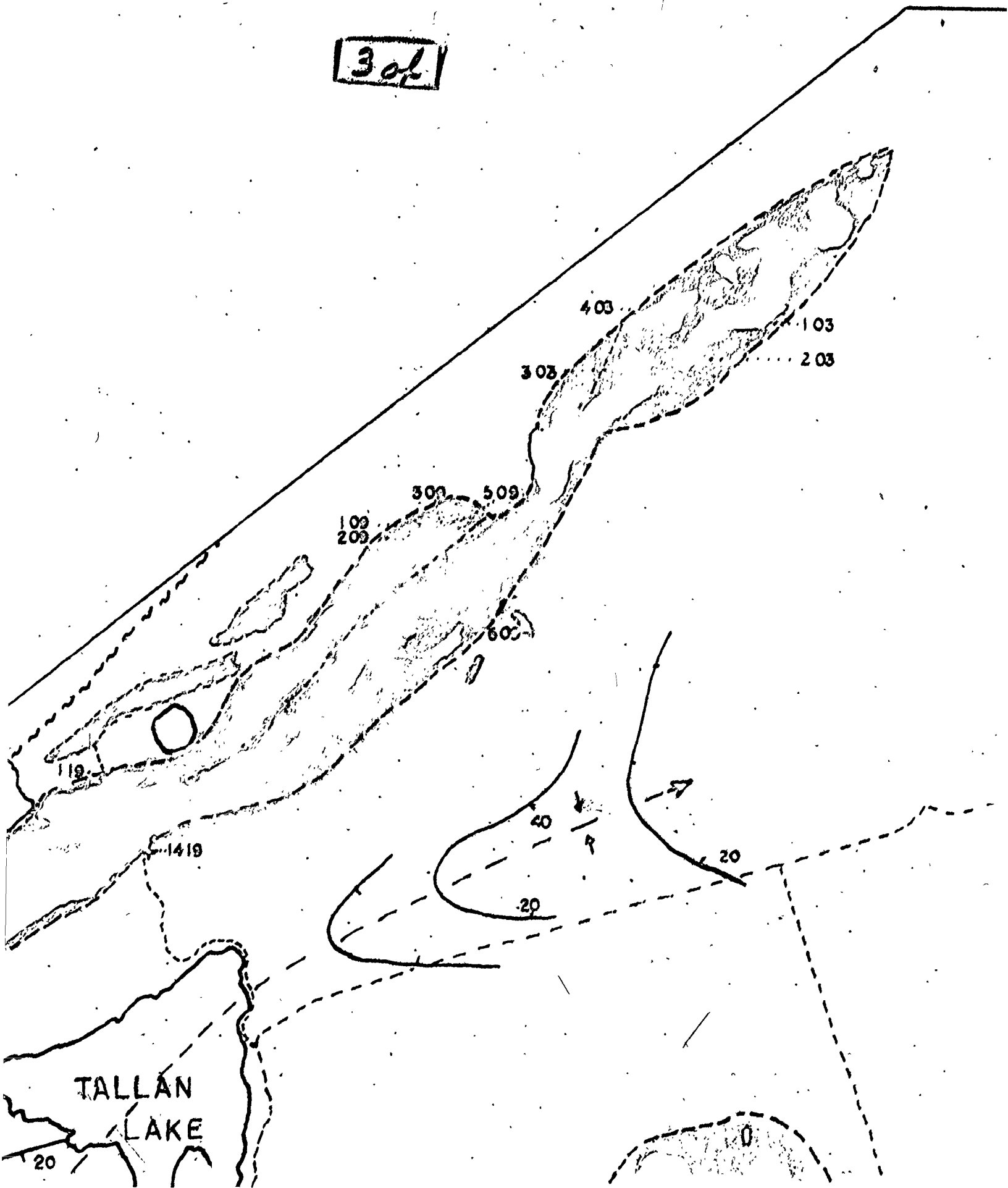
20

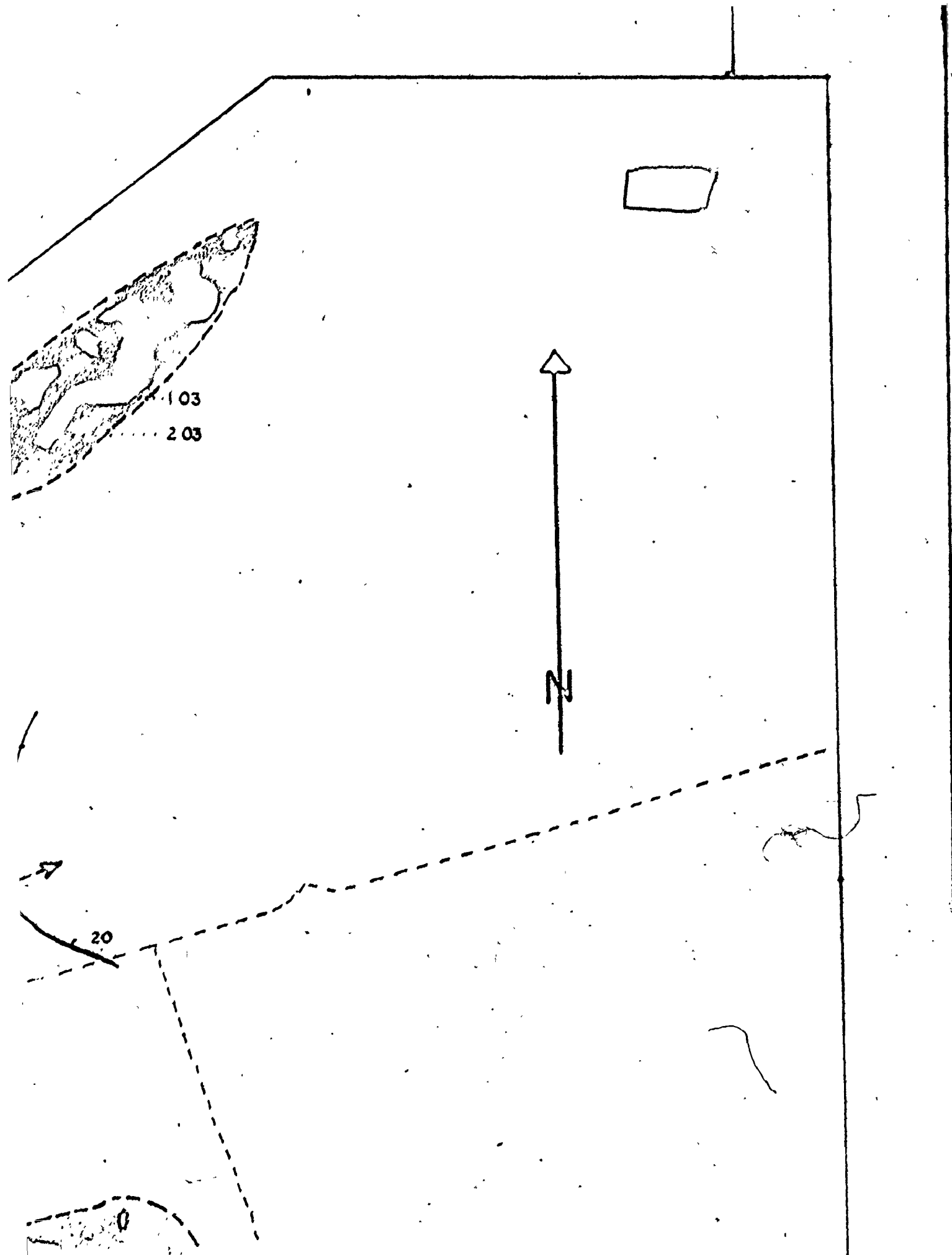
410

19



30f





Meters

1000

500

0

0.5

1.0

Scale 1:15,840 or 1 inch to 1/4 mile

Geology by D.M. Shaw (1958)
D.S. Jennings (1966)
J.L. Griep (1968)



44°50' N

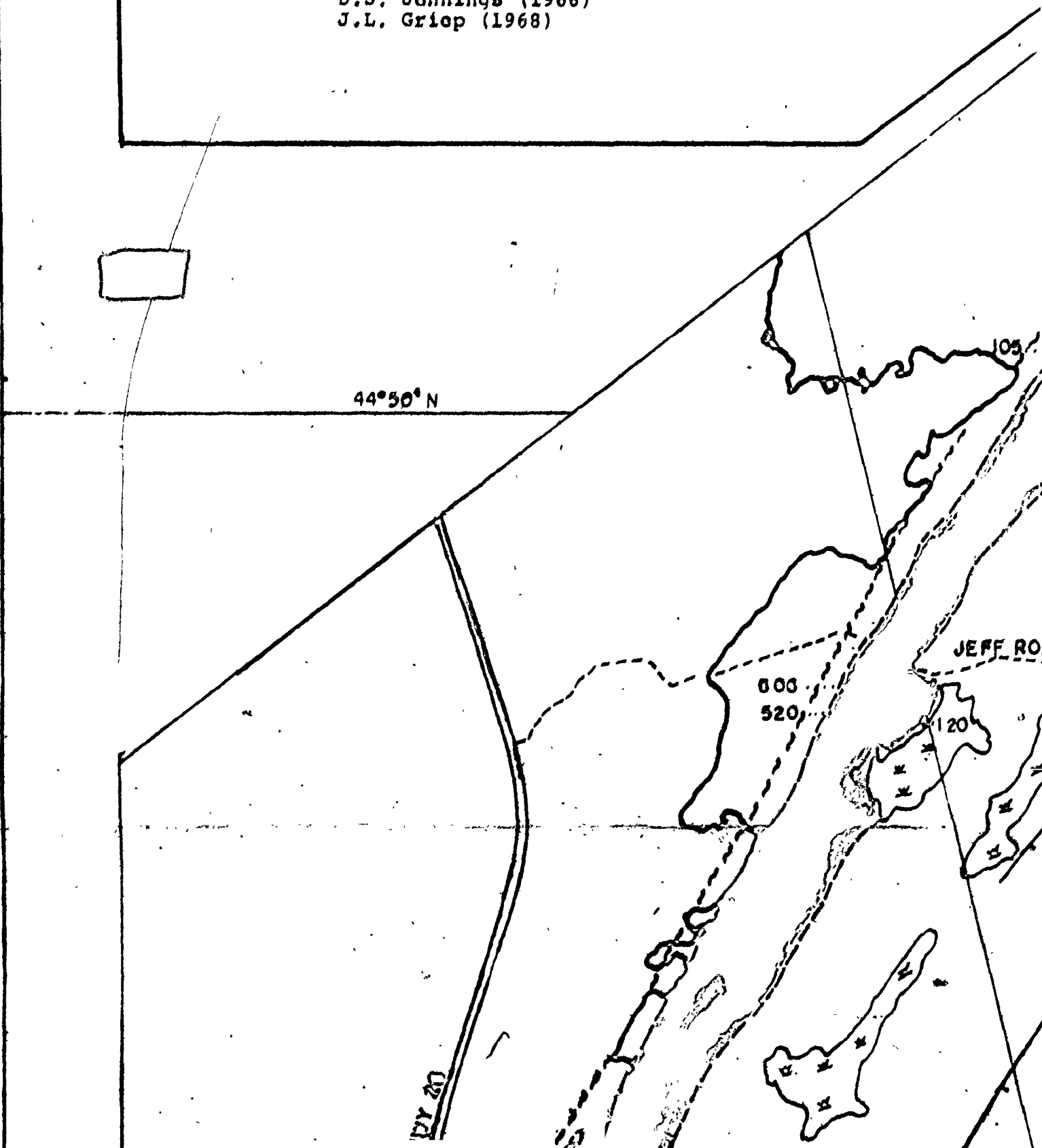
JEFF ROA

800

520

120

BY 20



1.0 Miles

1.0 Kilometers



TALLAN LAKE

20

45

30

15

CLYDESDALE ROAD

50

JEFF ROAD

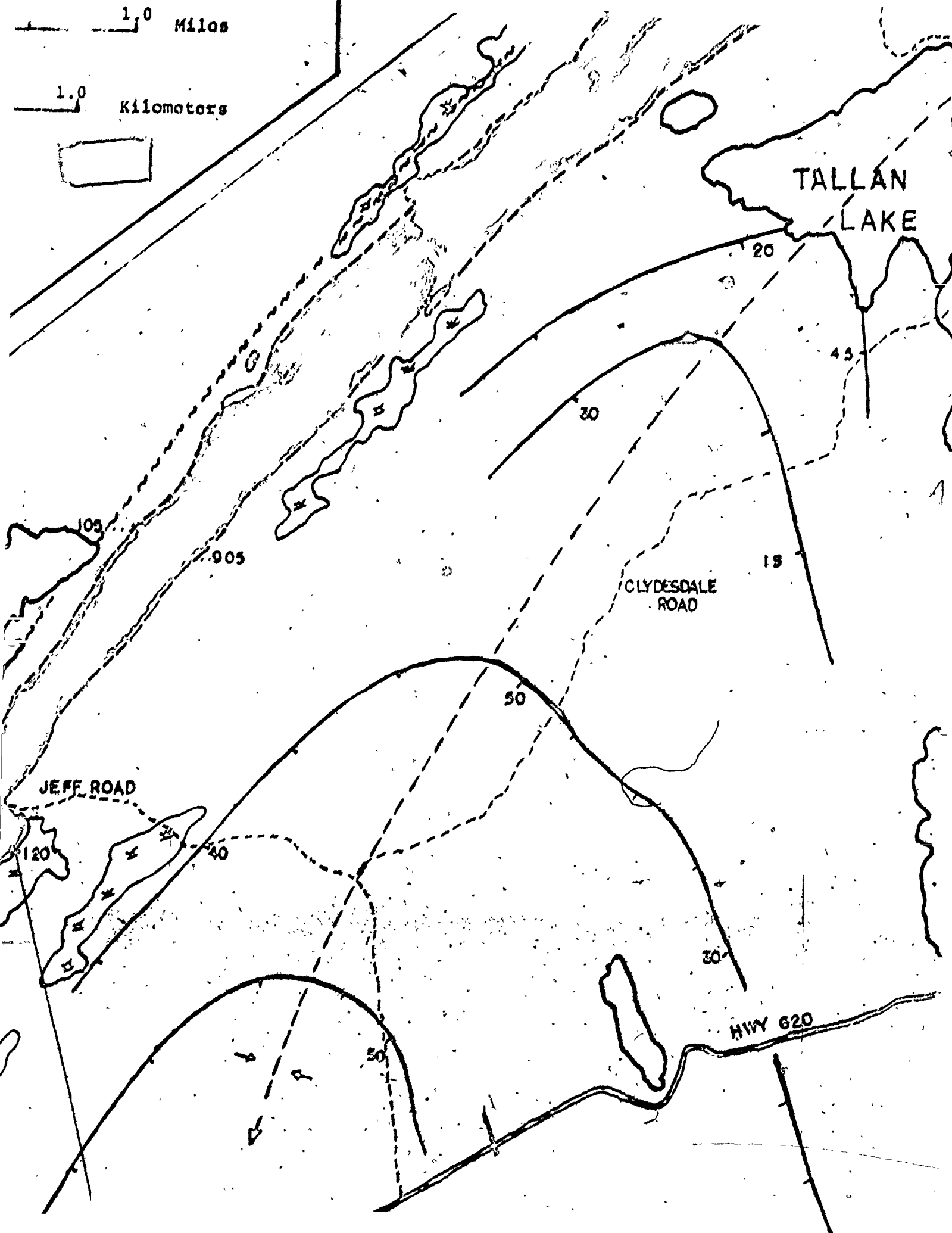
120

40

30

HWY 620

50



ALLAN
LAKE

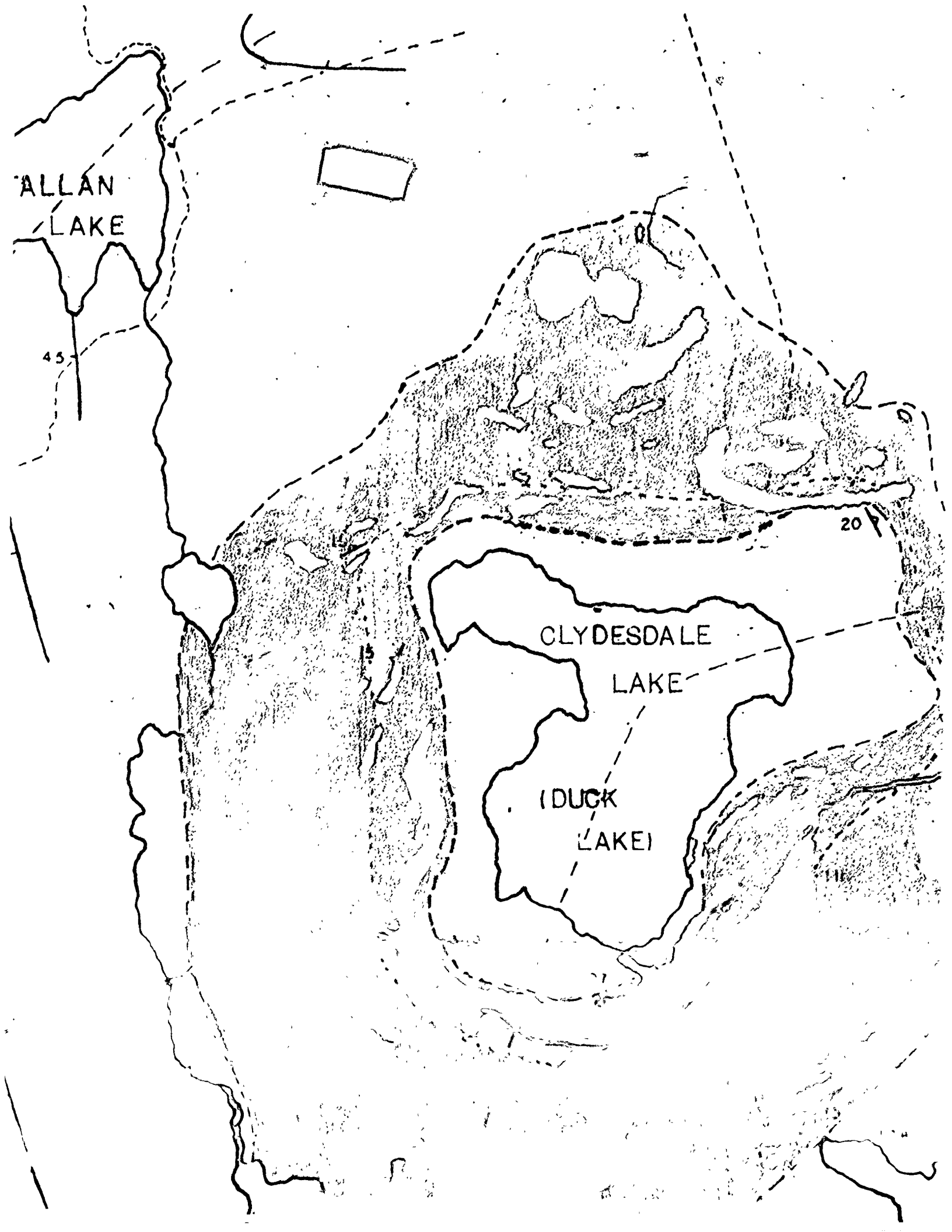
45

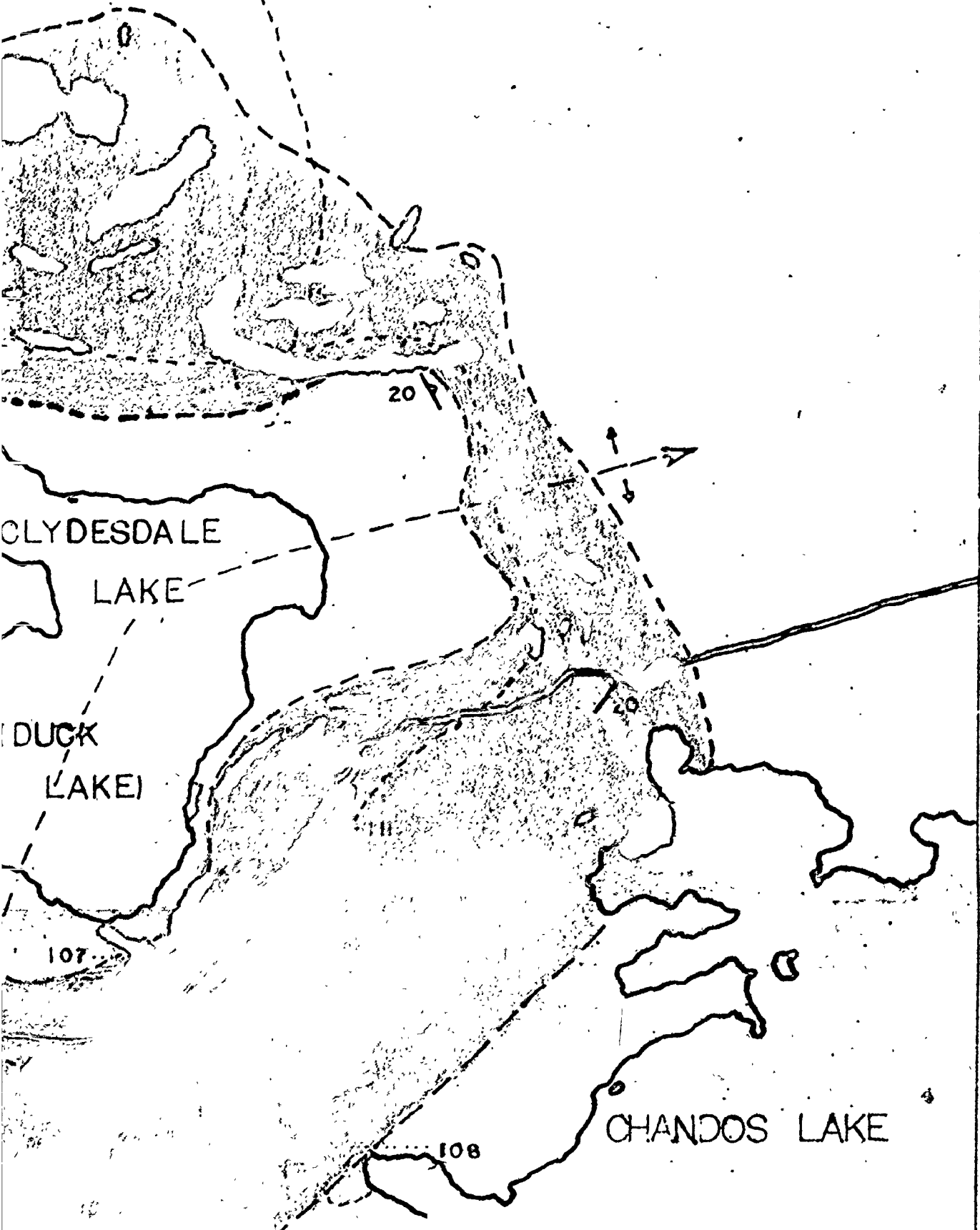


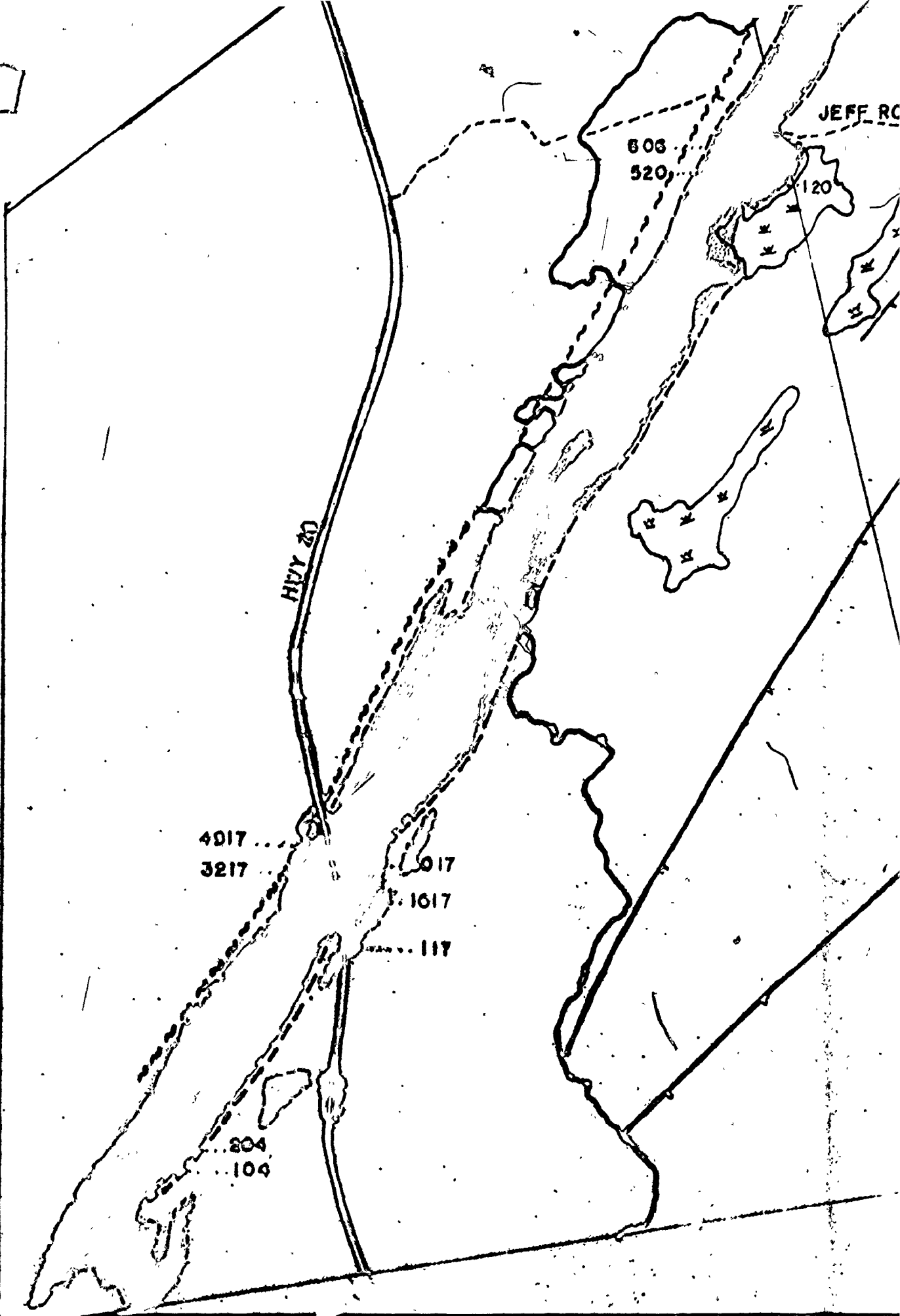
20

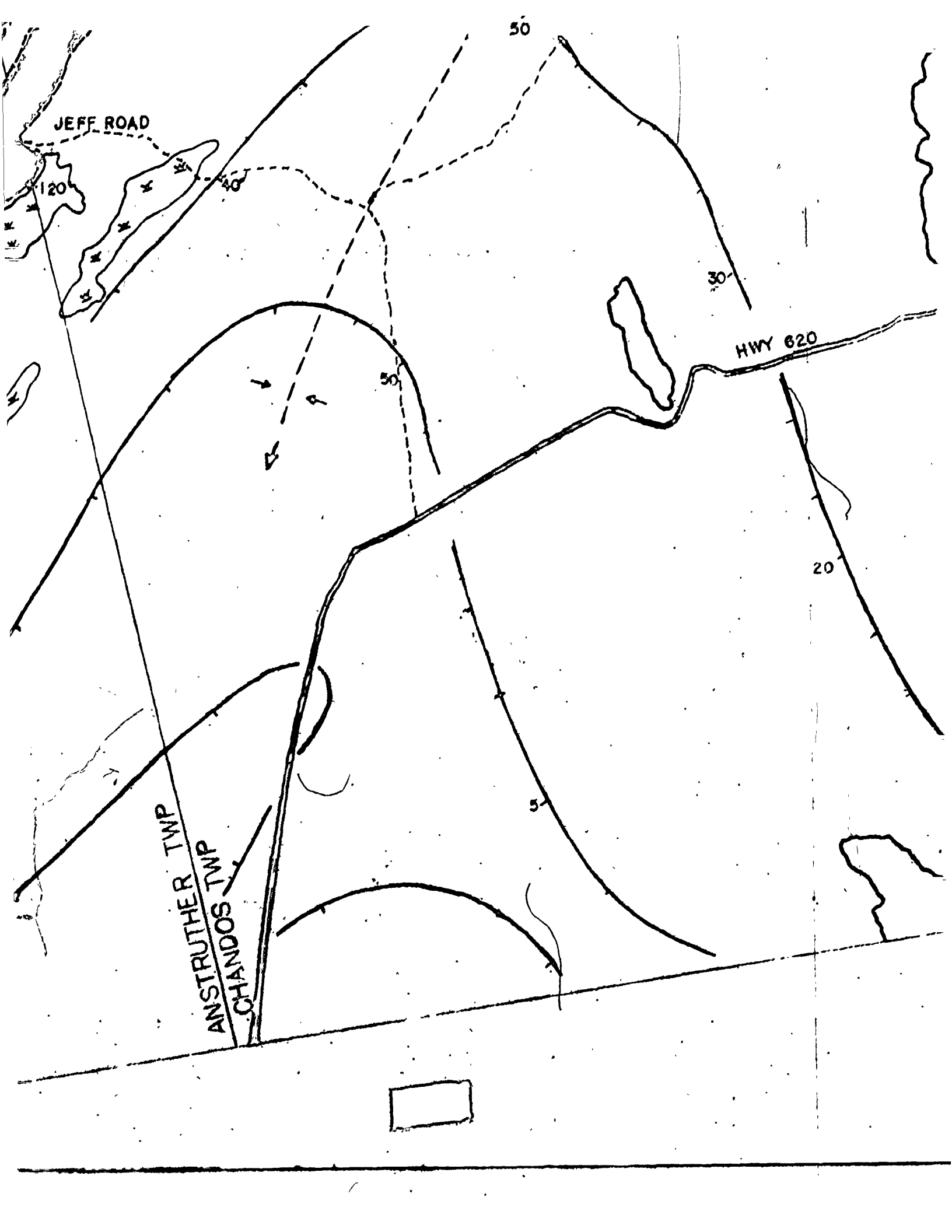
CLYDESDALE
LAKE

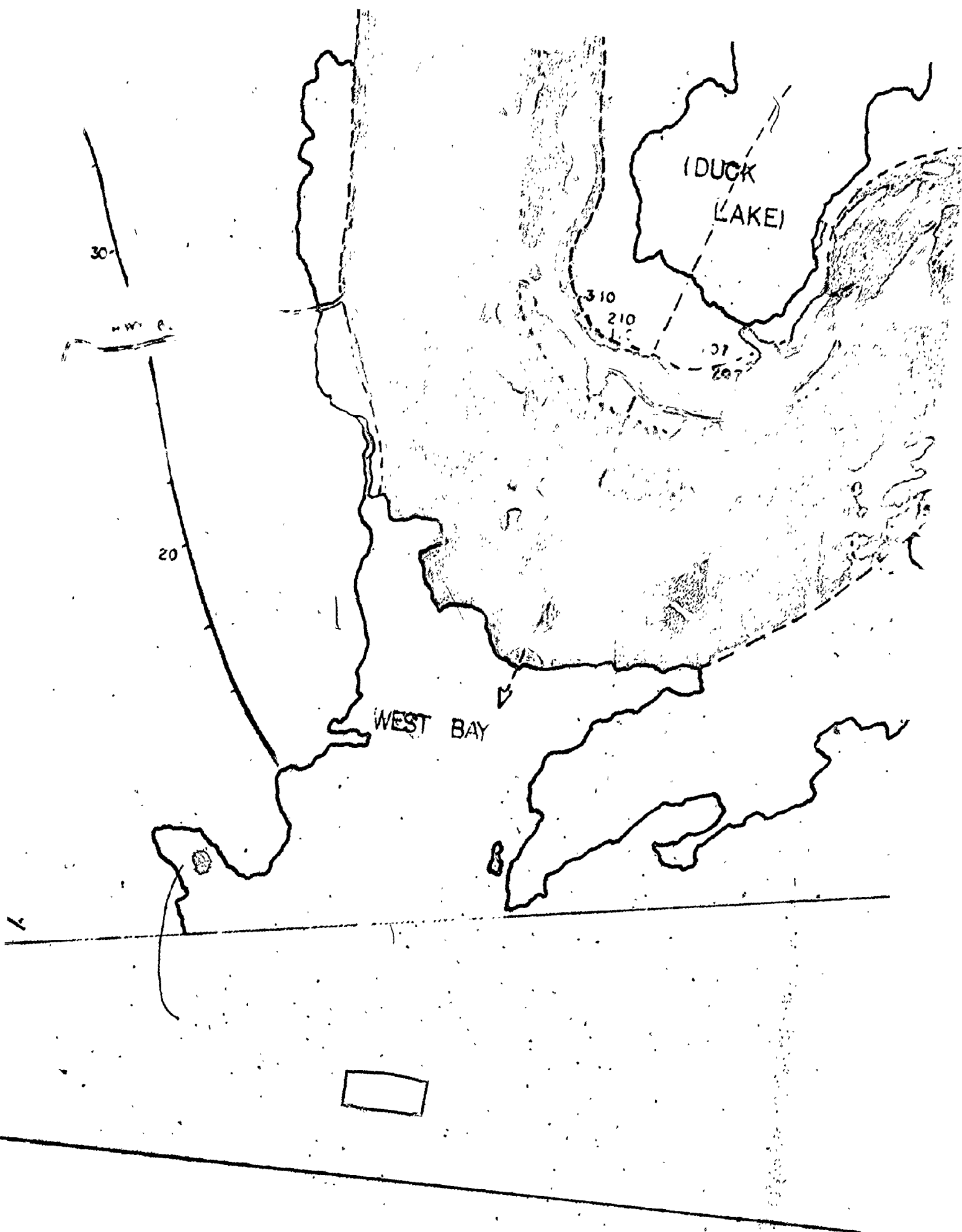
(DUCK
LAKE)











30-

M.W.P.

20

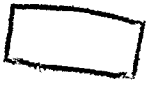
WEST BAY

(DUCK LAKE)

310

210

107



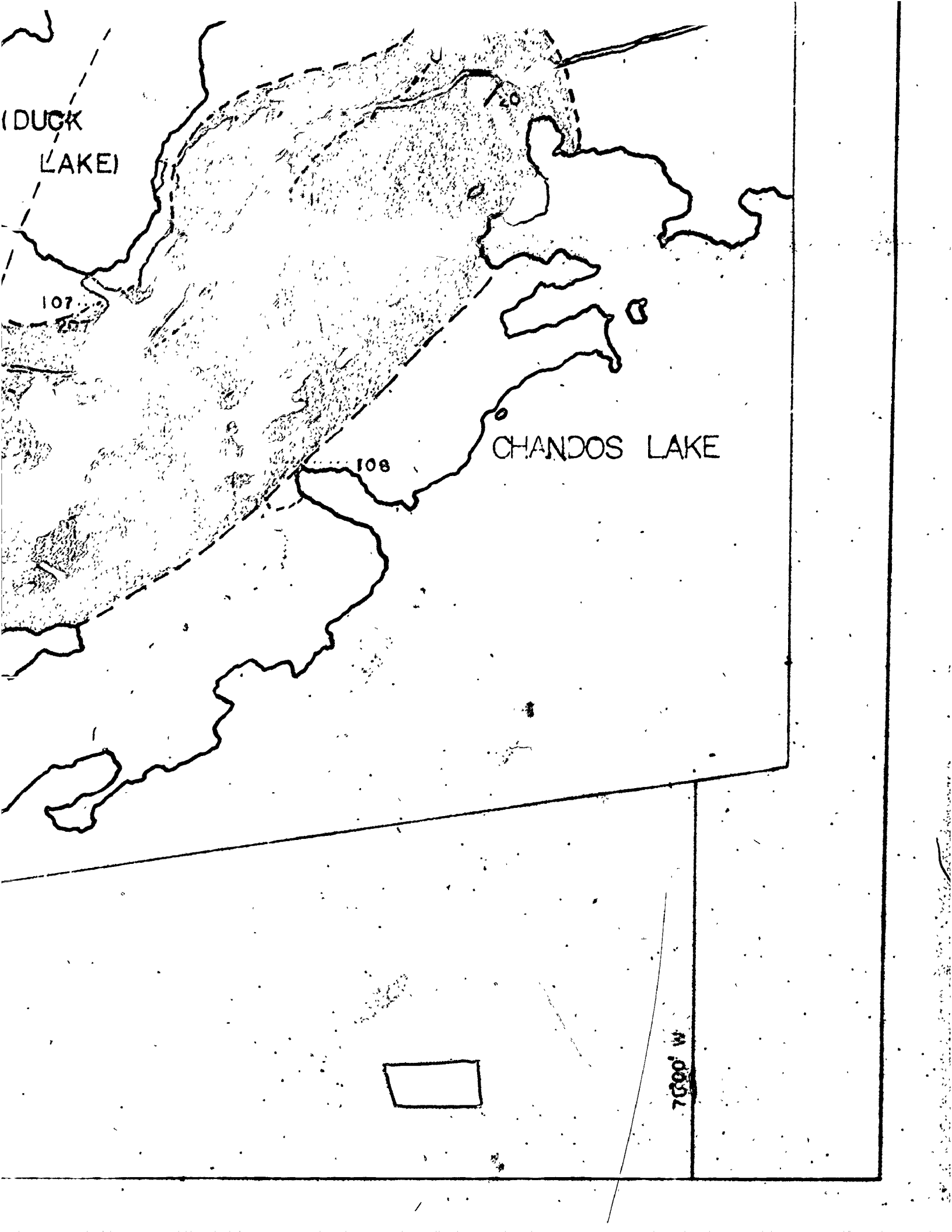
(DUCK
LAKE)

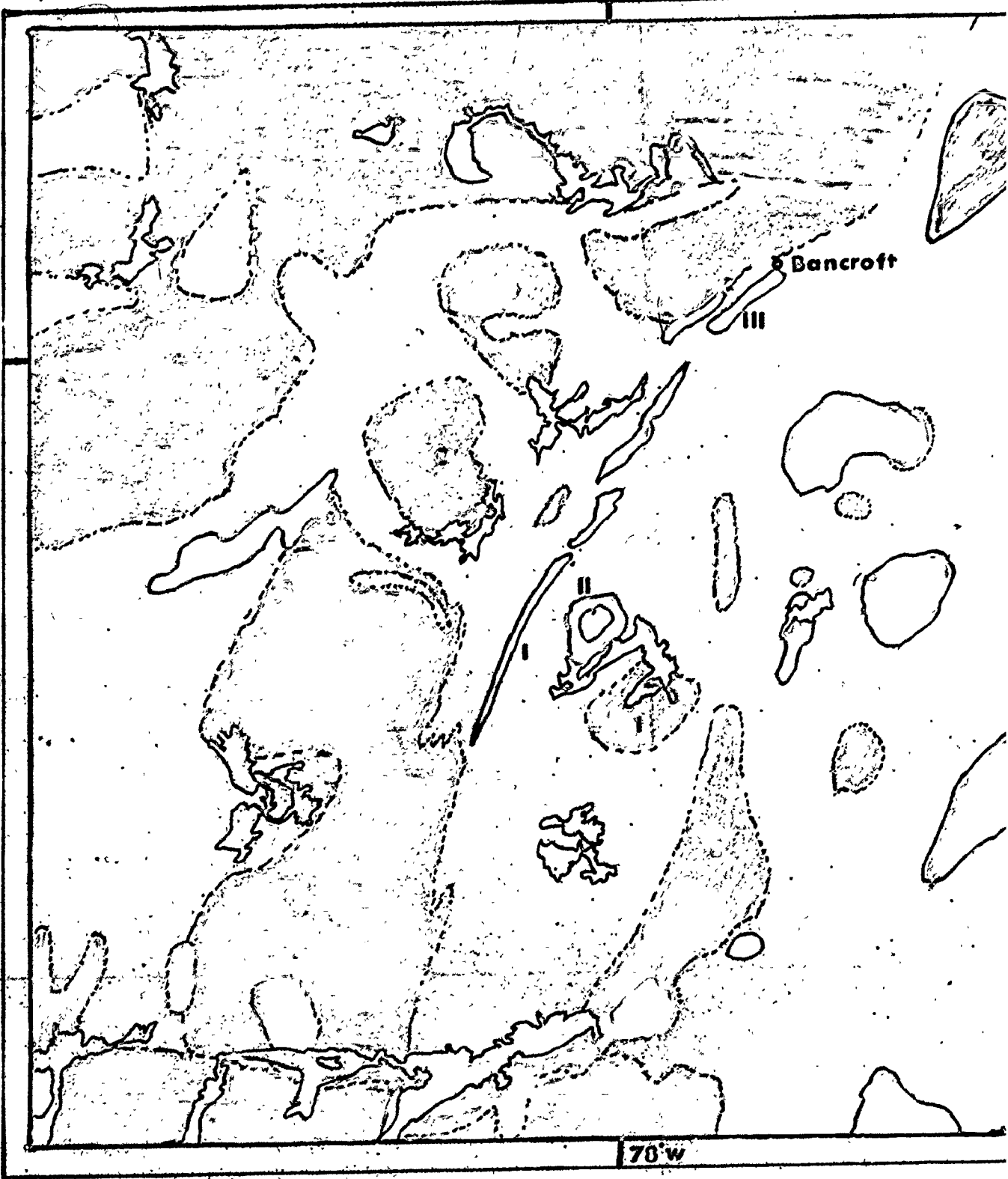
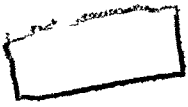
107

CHANDOS LAKE

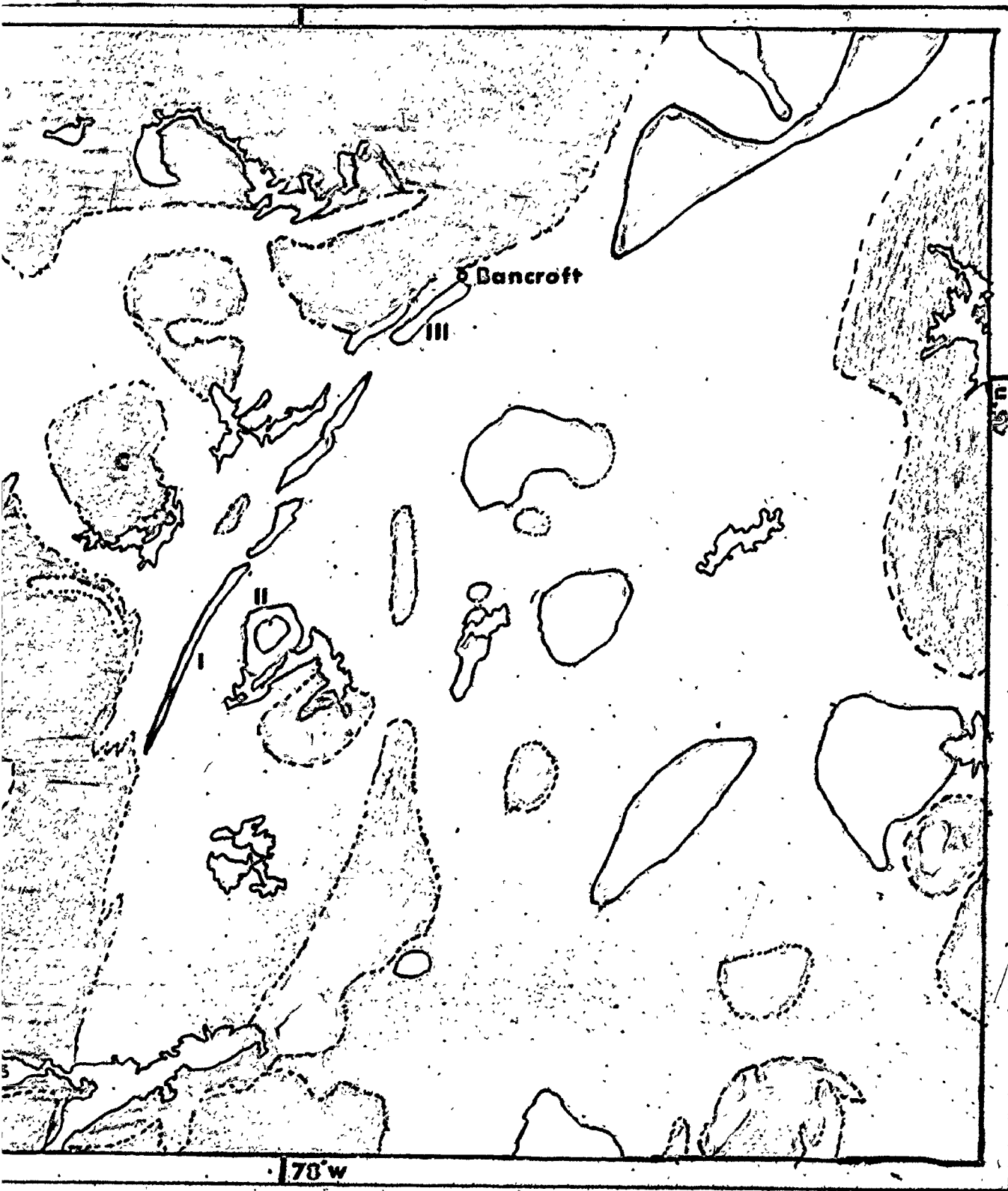
108

7000' W

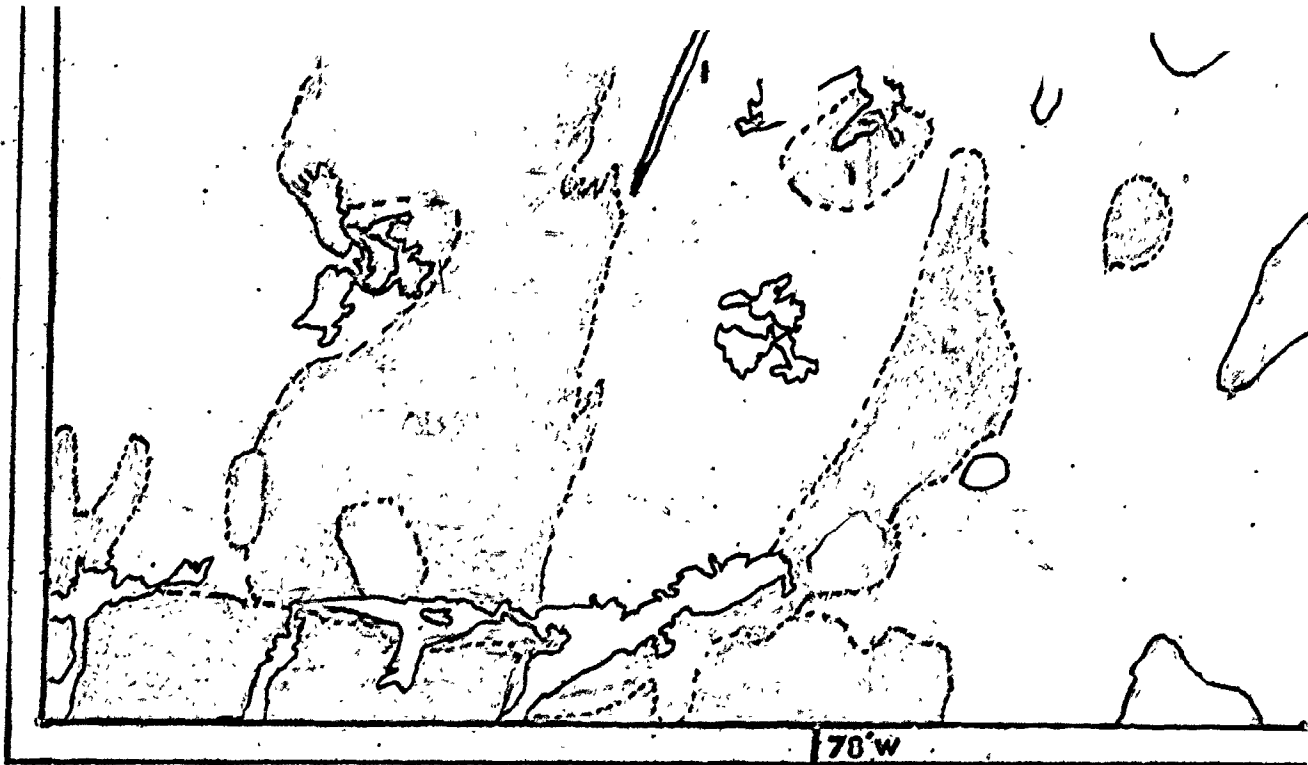




LEGEND





LEGEND




L E G E N D

Pre-kinematic

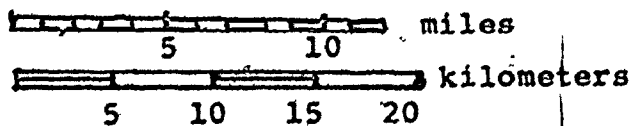
-  Grenville Supergroup Sequence
-  Gabbroic Intrusives
- I Tallan Lake Sill
- II Duck Lake Sill
- III Faraday Metagabbro
- IV Mallard Lake-Raglan Hills Gabbro
- V Umfraville Gabbro
- VI Thanet Gabbro
- VII Tudor Gabbro
- VIII Lingham Lake Complex
- IX Glamorgan Gabbro

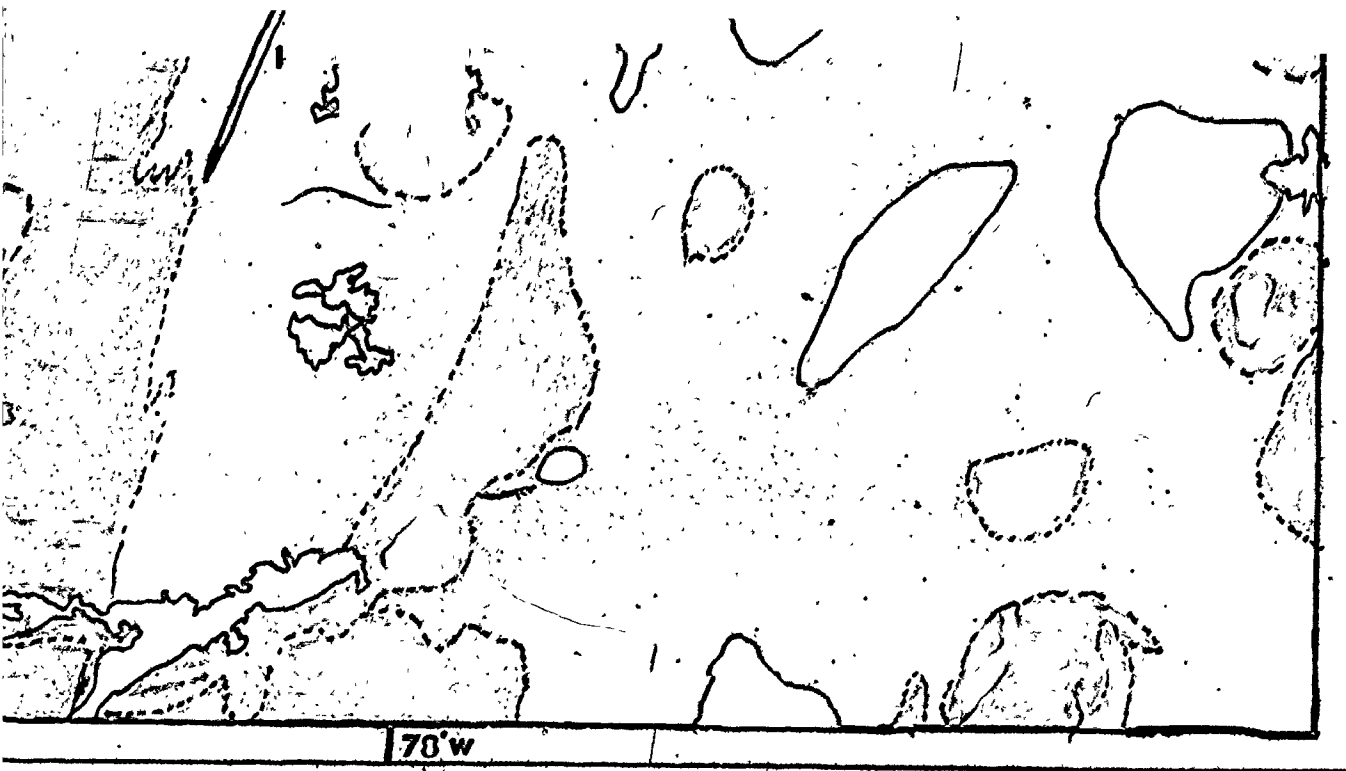
Synkinematic

-  Intrusives
- AB Anstruther-Burleigh gneiss dome
- C Cheddar gneiss dome
- D Deer Lake gneiss dome
- E Methuen granite
- F Weslemkoon granodiorite


 Paleo


Scale: 1:380,160





L E G E N D

 Synkinematic
Intrusives

 Post-kinematic
Intrusives

- AB Anstruther-Burleigh gneiss dome
- C Cheddar gneiss dome
- D Deer Lake gneiss dome
- E Methuen granite
- F Weslemkoon granodiorite

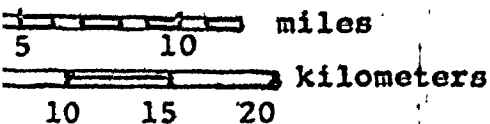
- 1 Loon Lake pluton
- 2 Gawley Creek syenite
- 3 Deloro granite
- 4 Mount Moriah syenite

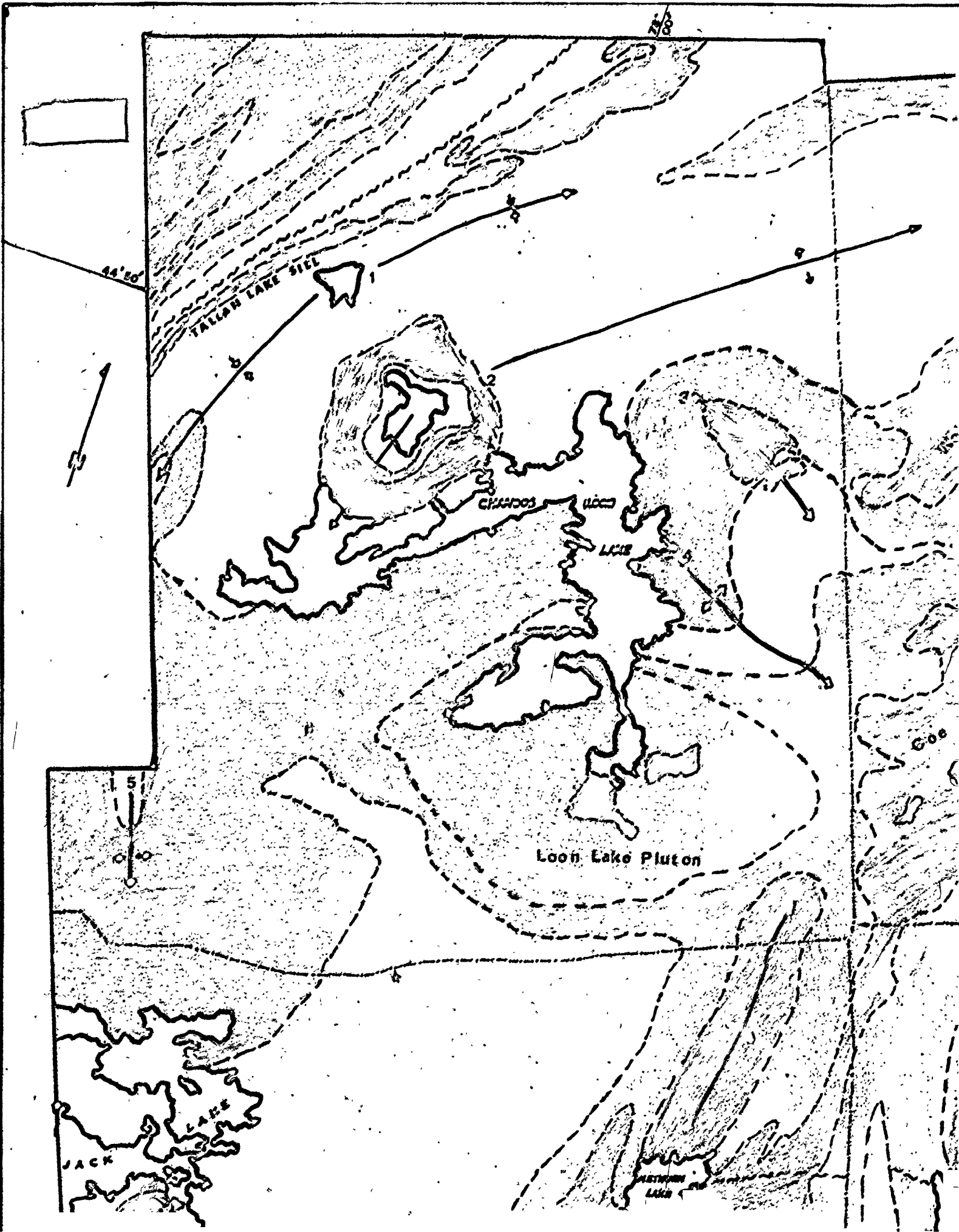


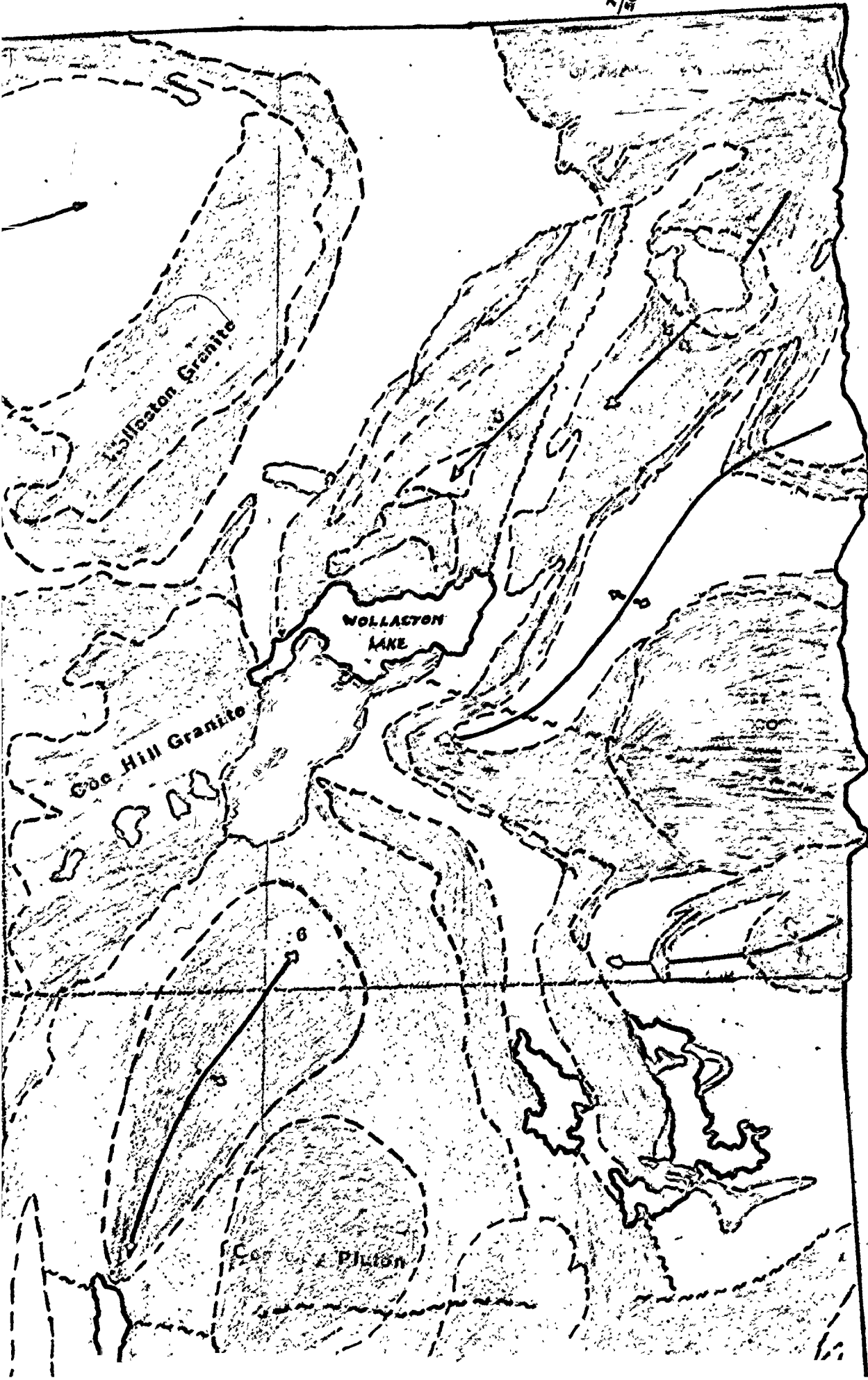
Paleozoic limestone



1:380,160







3 of 1

L E G E N D

a Pre-kinematic

- Metavolcanics
- Quartzo-feldspathic paragneiss, meta-arkose
- Paragneiss, amphibolite
- Marble
- Gabbro
- Trondhjemite, albite syenite, albite granite
- Nepheline syenite

b Synkinematic

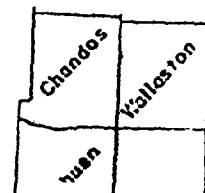
- Quartz-monzonite, hybrid granite gneiss

c Post-kinematic

- Potassic monzonite, syenite, granite

Structural features

1. Chandos Syncline
2. Rose Island Dome
3. Glen Alda Syncline
- 4.



Loon Lake Pluton



44°40'

BLUE DOUSTAIN
SERPENTINE
SYENITE

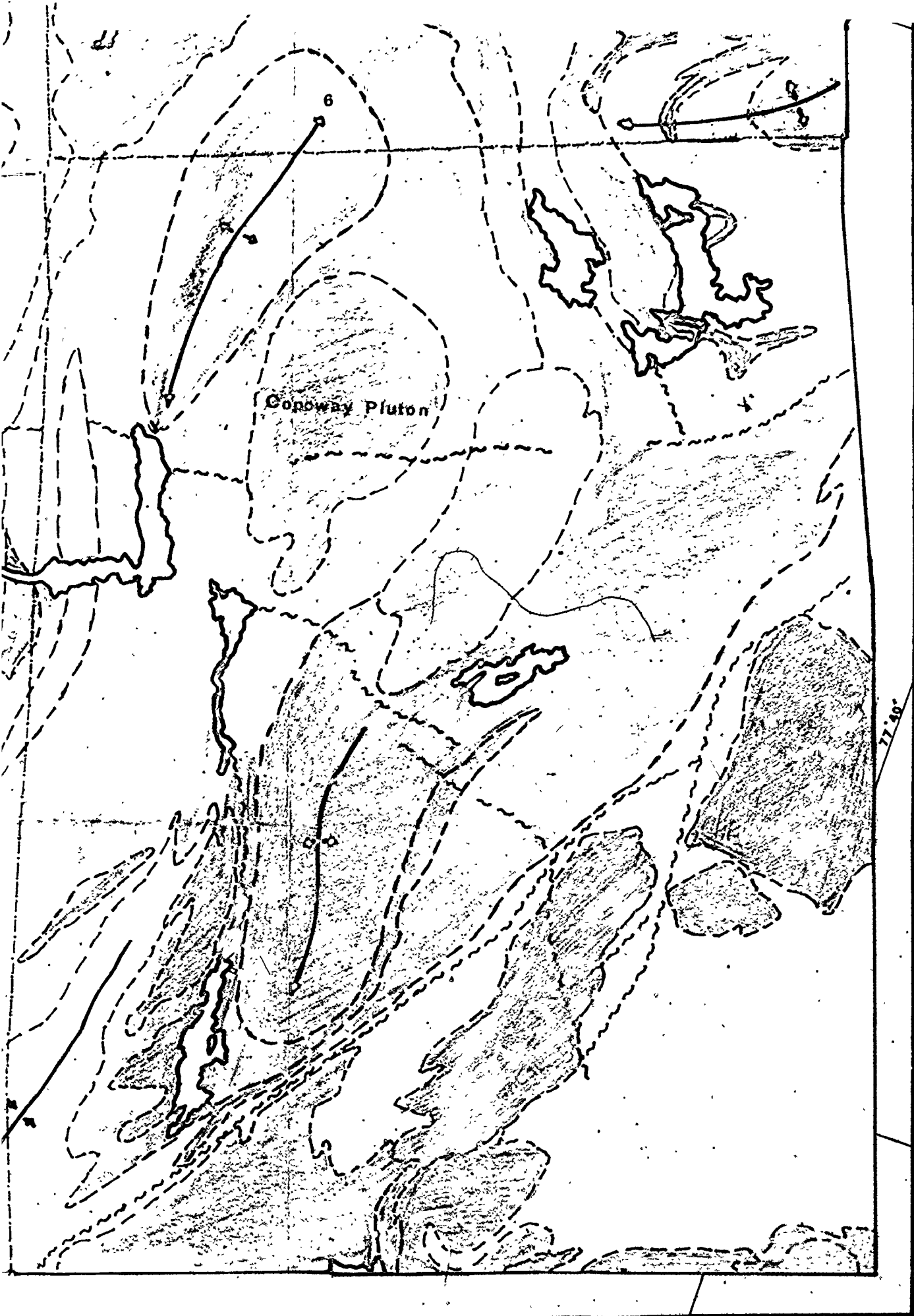
Mothuon Granite

KASSINOK
LAKE

GAN LAKE

MITHUN
LAKE







Copoway Pluton

77°40'


fe




 Trondhjemite, albite syenite, albite granite

 Nepheline syenite

b Synkinematic

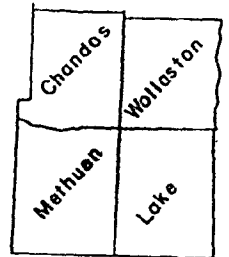
 Quartz-monzonite, hybrid granite gneiss

c Post-kinematic

 Potassic monzonite, syenite, granite

Structural features

1. Chandos Syncline
2. Rose Island Dome
3. Glen Alda Syncline
4. Owenbrook Anticline
5. Wolfe Hill Anticline
6. The Ridge Dome



Scale: 1:83,760

Modified from
Lumbers (1967)

